THE REACTIONS
OF CHLORINE ATOMS
IN AQUEOUS SOLUTION

by

Mark Bydder

Submitted in accordance with the requirements for
the degree of Doctor of Philosophy.

The University of Leeds
Cookridge Radiation Research Centre

August 1999

The candidate confirms that the work submitted is his own
and that appropriate credit has been given where reference has been made to
the work of others.

Acknowledgements

The work described in this thesis was carried out during the period October 1995 to September 1998 at Cookridge Radiation Research Centre, The University of Leeds. Financial support was provided by the Natural Environment Research Council under research grant GST/02/1258. I acknowledge the contribution to this project made by my supervisor, Dr. G. A. Salmon, and the academic staff at C.R.R.C., Drs. G. V. Buxton and F. Wilkinson. The administrative and technical support of G. Coultate, C. Kilner and S. Watkins, and the friendship of J. Wang and particularly Dr. J. E. Williams, who performed some of the experiments described in Chapter 5, were much appreciated. Thanks also to my sister, Dr. M. Bydder, for proof-reading the entire thesis.

THE REACTIONS OF CHLORINE ATOMS IN AQUEOUS SOLUTION

Mark Bydder

Doctor of Philosophy

August 1999

Abstract

In this study the techniques of pulse radiolysis and laser flash photolysis have been used to investigate the reactions of the chlorine atom with organic and inorganic solutes in aqueous solution. The aim was to assess for the first time its contribution to the chemistry within cloud droplets.

A number of rate constants and activation energies have been measured for the reactions of Cl· with species thought to be present in cloud water. In the special case of chloride, the reaction proceeds to an equilibrium with the less reactive $Cl_2\cdot^-$ radical, $Cl\cdot + Cl^- \leftrightarrow Cl_2\cdot^-$. However, variation in the literature of the equilibrium constant ranges over four orders of magnitude. Further investigation of this equilibrium has been undertaken, showing agreement with the highest reported value. Other special cases investigated were the reactions of Cl· with SO_4^{2-} and NO_3^-, which are also equilibria. The kinetic scheme for these reactions in the presence of chloride, comprising a double equilibrium mechanism, was investigated, giving values for the equilibrium constants. The consistency of these results was confirmed by measuring the equilibrium constant for the reaction $SO_4\cdot^- + NO_3^- \leftrightarrow SO_4^{2-} + NO_3\cdot$. Previous atmospheric modelling studies have included the reactions of the OH·, $SO_4\cdot^-$, $NO_3\cdot$ and $Cl_2\cdot^-$ radicals but not those of the Cl· atom, perhaps as a result of the high stability constant of $Cl_2\cdot^-$ and the scarcity of available data. This study has found the Cl· atom to be an extremely reactive species, whose reactions occur frequently at the diffusion controlled rate. Therefore despite its low concentration in comparison to $Cl_2\cdot^-$, the Cl· atom is likely to be the more active form of radical chlorine in the atmospheric aqueous phase.

List of Figures

List of Tables

List of Equations

$$K_H(S) = \frac{[S]}{p(S)} \quad [1.1]$$

$$H^* = \frac{[HCHO\,(aq)] + [CH_2(OH)_2]}{p(HCHO\,(g))} \quad [1.2]$$

$$-\frac{dE}{dx} = \frac{2\pi e^4 NZ}{m_o v^2}\left\{\ln\frac{m_o v^2 E}{2I^2(1-\beta^2)} - \left(2\sqrt{1-\beta^2} - 1 + \beta^2\right)\ln 2 + 1 - \beta^2 + \frac{1}{8}\left(1-\sqrt{1-\beta^2}\right)^2\right\} \quad .....[1.3]$$

$$\phi = \frac{\text{No. of species formed}}{\text{No. of photons absorbed}} \quad [1.4]$$

$$\text{Sensitivity / Gy V}^{-1} = \frac{(OD / V)_{dosimeter}}{(G\varepsilon)_{dosimeter} \times l} \quad [2.1]$$

$$(G\varepsilon)_{sample} = \frac{(OD / V)_{sample} \times (G\varepsilon)_{dosimeter}}{(OD / V)_{dosimeter}} \quad [2.2]$$

$$k_{obs} = \frac{k_{3.7} + k_{3.8}K_{3.1}[Cl^-]}{1 + K_{3.1}[Cl^-]} + \left[\frac{k_{3.5} + k_6 K_{3.1}[Cl^-]}{1 + K_{3.1}[Cl^-]}\right][t\text{-}BuOH] \quad [3.1]$$

$$k_{obs} = \frac{k_{-3.1}(k_{3.5}[t\text{-}BuOH] + k_{3.7}) + (k_{3.1}[Cl^-] + k_{3.5}[t-BuOH] + k_{3.7})(k_{3.6}[t\text{-}BuOH] + k_{3.8})}{k_{3.1}[Cl^-] + k_{-3.1} + (k_{3.5} + k_{3.6})[t-BuOH] + k_{3.7} + k_{3.8}} \quad .....[3.2]$$

$$I = \frac{k_{3.7} + k_{3.8}K_{3.1}[Cl^-]}{1 + K_{3.1}[Cl^-]} \quad [3.3a]$$

$$G = \frac{k_{3.5} + k_{3.6}K_{3.1}[Cl^-]}{1 + K_{3.1}[Cl^-]} \quad [3.3b]$$

$$I = \frac{k_{3.7}}{K_{3.1}[Cl^-]} + k_{3.8} \quad [3.4a]$$

$$G = \frac{k_{3.5}}{K_{3.1}[Cl^-]} + k_{3.6} \quad [3.4b]$$

$$k_{3.5} = (3.9 \pm 0.35) \times 10^{13} / k_{-3.1} \quad dm^3\ mol^{-1}\ s^{-1} \quad [3.5]$$

$$k_{3.7} = (1.5 \pm 0.15) \times 10^{10} / k_{-3.1} \quad s^{-1} \quad [3.6]$$

$$k_{eff} = -\frac{d[R^\cdot]}{dt} = \frac{k_{3.5}[t\text{-}BuOH]}{1 + Q_{3.1}(t)[Cl^-]} \quad [3.7]$$

$$\frac{1}{G\varepsilon_{corr}} = \frac{1}{(G\varepsilon)_o} + \frac{1}{(G\varepsilon)_o}.\frac{k_{3.5}[t-BuOH]}{k_{3.1}[Cl^-]} \quad [3.8]$$

$$[Cl_2^{\cdot-}] = C_1 e^{\lambda(1)t} + C_2 e^{\lambda(2)t} + C_3 e^{\lambda(3)t} \quad [4.1]$$

$$[Cl_2^{\cdot-}] = C_2 e^{\lambda(2)t} + C_3 e^{\lambda(3)t} \quad [4.2]$$

$$[SO_4^{\cdot -}] = C_4\, e^{\lambda(2)t} + C_5\, e^{\lambda(3)t} \qquad [4.3]$$

$$\Delta E^{\circ} = \frac{RT \ln K}{F} \qquad [4.4]$$

$$k_{eff} = -\frac{d[R^{\cdot}]}{dt} = \frac{k_{3.5}[t-BuOH]}{Q_{3.1}(t)[Cl^-] + 1 + ([SO_4^{2-}]/Q_{4.1}(t)[Cl^-])} \qquad [4.5]$$

$$k_{obs} = \frac{k[S]}{1 + K_{3.1}[Cl^-]} = \frac{8{\cdot}5 \times 10^9 [S]}{1{\cdot}4 \times 10^5} \approx 6 \times 10^4 [S]\ s^{-1} \qquad [5.1]$$

$$\frac{1}{k_{obs}} = \frac{1}{k_{diff}} + \frac{1}{k_{react}} \qquad [5.2]$$

$$\log k_{obs} = \log k_{diff} + \log\left(\frac{1}{1 + e^{-x}}\right) \qquad [5.3]$$

$$x = \frac{\Delta G^{\neq}}{RT} \qquad [5.4]$$

$$\Delta G^{\neq} = \frac{\lambda}{4}\left(1 + \frac{\Delta G^{o}}{\lambda}\right)^2 \qquad [5.5]$$

$$\left(\frac{[Cl^{\cdot}][SO_4^{2-}]}{[Cl^-][SO_4^{\cdot -}]}\right)_{eq} \cdot \left(\frac{[Cl^-][NO_3^{\cdot}]}{[Cl^{\cdot}][NO_3^-]}\right)_{eq} = \left(\frac{[SO_4^{2-}][NO_3^{\cdot}]}{[SO_4^{\cdot -}][NO_3^-]}\right)_{eq} \qquad [6.1]$$

$$K_{4.1} \cdot K_{4.5} = K_{6.1} \qquad [6.2]$$

$$[NO_3^{\cdot}] = C_1 \exp\lambda(1) + C_2 \exp\lambda(2) \qquad [6.3]$$

$$-\lambda(1) \approx k_{6.1}[NO_3^-] + k_{-6.1}[SO_4^{2-}] + (k_{4.2} + k_{6.3})[t\text{-}BuOH] + k_{4.3} + k_{6.4} \qquad [6.4]$$

$$k_{obs} = k_f + k_b \qquad [6.5]$$

$$k_{obs} = k_f + k_b + k_{loss} \qquad [6.6]$$

$$-\lambda(2) \approx \frac{k_{4.2}[t\text{-}BuOH] + k_{4.3} + K_{6.1}([NO_3^-]/[SO_4^{2-}])(k_{6.3}[t\text{-}BuOH] + k_{6.4})}{K_{6.1}([NO_3^-]/[SO_4^{2-}]) + 1} \qquad [6.7]$$

$$\left[\frac{A(450)}{A(630)}\right]_{t\to\infty} = \frac{\varepsilon_2}{\varepsilon_1} + \frac{\varepsilon_3}{\varepsilon_1}\left(\frac{[SO_4^{\cdot -}]}{[NO_3^{\cdot}]}\right)_{eq} = \frac{\varepsilon_2}{\varepsilon_1} + \frac{\varepsilon_3}{K_{6.1}\varepsilon_1} \cdot \frac{[SO_4^{2-}]}{[NO_3^-]} \qquad [6.8]$$

$$\frac{d[Cl^{\cdot}]}{dt} = k_{-3.1}[Cl_2^{\cdot -}] - (k_{3.1}[Cl^-] + k_{3.5}[t\text{-}BuOH] + k_{3.7})[Cl^{\cdot}] \qquad [A1.1]$$

$$\frac{d[Cl_2^{\cdot -}]}{dt} = k_{3.1}[Cl^-][Cl^{\cdot}] - (k_{-3.1} + k_{3.6}[t\text{-}BuOH] + k_{3.8})[Cl_2^{\cdot -}] \qquad [A1.2]$$

$$\frac{d^2[Cl_2^{\cdot -}]}{dt^2} + A\frac{d[Cl_2^{\cdot -}]}{dt} + B[Cl_2^{\cdot -}] = 0 \qquad [A1.3]$$

$$[Cl_2^{\cdot -}] = C_1\, e^{\lambda(1)t} + C_2\, e^{\lambda(2)t} \qquad [A1.4]$$

$$\lambda(1,2) = \frac{-A \pm \sqrt{A^2 - 4B}}{2} \qquad [A1.5]$$

$$\lambda(1,2) \approx \frac{-A \pm \left(A - \frac{2B}{A}\right)}{2} \approx -A\ ,\ -\frac{B}{A} \qquad [A1.6]$$

$$-\lambda(1) \approx A = k_{3.1}[Cl^-] + k_{-3.1} + k_{3.7} + k_{3.8} \qquad [A1.7]$$

$$[Cl_2\cdot^-] = C_1 e^{\lambda(2)t},\ \lambda(2) = -\frac{B}{A} \qquad [A1.8]$$

$$[Cl\cdot] = \frac{k_{-3.1} C_1 e^{\lambda(2)t}}{k_{3.1}[Cl^-] + k_{3.5}[t\text{-}BuOH] + k_{3.7} + \lambda(2)} + C_3 e^{\beta t} \qquad [A1.9]$$

$$[Cl\cdot] = C_4 C_1 e^{\lambda(2)t},\ C_4 = \frac{k_{-3.1}}{k_{3.1}[Cl^-] + k_{3.5}[t\text{-}BuOH] + k_{3.7} + \lambda(2)} \qquad [A1.10]$$

$$Q_{3.1} = \frac{[Cl_2^{\cdot-}]}{[Cl^-][Cl\cdot]} = \frac{1}{[Cl^-]C_4} \approx \frac{k_{3.1}}{k_{-3.1}} + \frac{k_{3.5}[t\text{-}BuOH]}{k_{-3.1}[Cl^-]} \qquad [A1.11]$$

$$[t\text{-}BuOH] \le [Cl^-] \qquad [A1.12]$$

$$\frac{d^2[Cl_2^{\cdot-}]}{dt^2} + A\frac{d[Cl_2^{\cdot-}]}{dt} + B[Cl_2^{\cdot-}] = k_{3.1}k_{3.4}[Cl^-]^2[SO_4^{\cdot-}] \qquad [A1.13]$$

$$[Cl_2\cdot^-] = C_1 (e^{\lambda(1)t} + C_5 e^{\lambda(2)t} + C_6 e^{\alpha t}) \qquad [A1.14]$$

$$[Cl\cdot] = C_4 C_1 (e^{\lambda(1)t} + C_7 e^{\lambda(2)t} + C_8 e^{\alpha t} + C_9 e^{\beta t}) \qquad [A1.15]$$

$$Q_{3.1}(t) = \frac{e^{\lambda(1)t} + C_5 e^{\lambda(2)t} + C_6 e^{\alpha t}}{[Cl^-]C_4 (e^{\lambda(1)t} + C_7 e^{\lambda(2)t} + C_8 e^{\alpha t} + C_9 e^{\beta t})} \qquad [A1.16]$$

$$\frac{d[Cl_2^{\cdot-}]}{dt} = a[Cl\cdot] - b[Cl_2^{\cdot-}] \qquad [A2.1]$$

$$\frac{d[Cl\cdot]}{dt} = b[Cl_2^{\cdot-}] - a[Cl\cdot] + c[SO_4^{\cdot-}] - e[Cl\cdot] - f[Cl\cdot] \qquad [A2.2]$$

$$\frac{d[SO_4^{\cdot-}]}{dt} = e[Cl\cdot] - c[SO_4^{\cdot-}] \qquad [A2.3]$$

$$\frac{d^3[Cl_2^{\cdot-}]}{dt^3} + M\frac{d^2[Cl_2^{\cdot-}]}{dt^2} + N\frac{d[Cl_2^{\cdot-}]}{dt} + P[Cl_2^{\cdot-}] = 0 \qquad [A2.4]$$

$$[Cl_2\cdot^-] = C_1 e^{\lambda(1)t} + C_2 e^{\lambda(2)t} + C_3 e^{\lambda(3)t} \qquad [A2.5]$$

$$\lambda^3 + M\lambda^2 + N\lambda + P = 0 \qquad [A2.6]$$

$$\lambda^3 + M\lambda^2 + N\lambda \approx 0 \qquad [A2.7]$$

$$\lambda(1,2) \approx \frac{-M \pm \sqrt{M^2 - 4N}}{2}. \qquad [A2.8]$$

$$M \gg |\lambda(3)| \qquad [A2.9]$$

$$N \gg |M\lambda(3)| \qquad [A2.10]$$

$$N\lambda(3) \approx -P \qquad [A2.11]$$

$$\lambda(1) \approx -M \qquad [A2.12]$$

$$\lambda(2) \approx -\frac{N}{M} \qquad [A2.13]$$

$$\lambda(3) \approx -\frac{P}{N} \qquad [A2.14a]$$

$$-\lambda(3) \approx \frac{f}{K_{3.1}[Cl^-] + 1 + ([SO_4^{2-}]/K_{4.1}[Cl^-]) + f(1/c + 1/b)} \qquad [A2.14b]$$

$$K_{3.1} \approx \frac{[Cl_2^-]}{[Cl^-][Cl\cdot]} \qquad [A2.15]$$

$$K_{4.1} \approx \frac{[Cl\cdot][SO_4^{2-}]}{[SO_4^{\cdot-}][Cl^-]} \qquad [A2.16]$$

$$-\frac{d\ln[Cl_2^-]}{dt} = k_{obs} \approx \frac{f}{K_{3.1}[Cl^-] + 1 + ([SO_4^{2-}]/K_{4.1}[Cl^-])} \qquad [A2.17]$$

$$k_{obs} = \frac{f + gK_{3.1}[Cl^-] + h([SO_4^{2-}]/K_{4.1}[Cl^-])}{K_{3.1}[Cl^-] + 1 + ([SO_4^{2-}]/K_{4.1}[Cl^-])} \qquad [A2.18]$$

$$\frac{1}{k_{obs}} = \frac{1}{k_{A3.1}} + \frac{1}{K_{A3.1}k_{A3.1a}} \qquad [A3.1]$$

$$\frac{1}{k_{obs}} = \frac{1}{k_{A3.1a}} + \frac{1}{K_{A3.1}k_{A3.1a}} \qquad [A3.2]$$

$$\frac{1}{k_{obs}} = \frac{1}{k_{A3.1}} + \frac{1}{k_{A3.1a}} + \frac{1}{K_{A3.1}k_{A3.1a}} \qquad [A3.3]$$

$$\gamma^3 + n\gamma + p = 0 \qquad [A4.1]$$

$$\lambda(2) = -\frac{\gamma(1)}{2} + \sqrt{\frac{\gamma(1)^2}{4} + \frac{p}{\gamma(1)}} - \frac{M}{3} \qquad [A4.2]$$

List of Reactions

$O_2 + h\nu \rightarrow O(^3P) + O(^1D)$ (1.1)

$O(^3P) + O_2 + M \rightarrow O_3 + M$ (1.2)

$O_3 + h\nu \rightarrow O_2 + O(^1D)$ (1.3)

$O_3 + O(^3P) \rightarrow 2\,O_2$ (1.4)

$HCHO\,(g) \leftrightarrow HCHO\,(aq) \leftrightarrow CH_2(OH)_2$ (1.5)

$HSO_3^- + H_2C(OH)_2 \leftrightarrow H_2C(OH)SO_3^- + H_2O$ (1.6)

$SO_2\,(g) + H_2O \leftrightarrow SO_2\,(aq)$ [also written as $SO_2 \cdot H_2O$] (1.7)

$SO_2 \cdot H_2O \leftrightarrow H^+ + HSO_3^-$ $pK_a = 1.8$ (1.8)

$HSO_3^- \leftrightarrow H^+ + SO_3^{2-}$ $pK_a = 7.2$ (1.9)

$HSO_3^- + H_2O_2 \leftrightarrow H_2O + A^- \rightarrow H_2SO_4$ (1.10)

$Fe(III) + HSO_3^- + H_2O + O_2 \rightarrow Fe(III) + H_2O_2 + HSO_4^-$ (1.11)

$\cdot OH + HSO_3^- \rightarrow H_2O + SO_3\cdot^-$ (1.12)

$SO_3\cdot^- + O_2 \rightarrow SO_5\cdot^-$ (1.13)

$SO_5\cdot^- + HSO_3^- \rightarrow HSO_5^- + SO_3\cdot^-$ (1.14)

$SO_5\cdot^- + HSO_3^- \rightarrow SO_4\cdot^- + SO_4^{2-} + H^+$ (1.15)

$SO_4\cdot^- + HSO_3^- \rightarrow SO_4^{2-} + H^+ + SO_3\cdot^-$ (1.16)

$SO_5\cdot^- + SO_5\cdot^- \rightarrow 2\,SO_4\cdot^- + O_2$ (1.17)

$SO_3\cdot^- + SO_3\cdot^- \rightarrow S_2O_6^{2-}$ (1.18)

$SO_4\cdot^- + SO_4\cdot^- \rightarrow S_2O_8^{2-}$ (1.19)

$SO_5\cdot^- + SO_5\cdot^- \rightarrow S_2O_8^{2-} + O_2$ (1.20)

$NO_3\cdot + HSO_3^- \rightarrow NO_3^- + SO_3\cdot^- + H^+$ (1.21)

$H_2O_2 + h\nu \rightarrow 2\,\cdot OH$ (1.22)

$HO_2\cdot + HO_2\cdot \rightarrow H_2O_2 + O_2$ (1.23)

$HO_2\cdot \leftrightarrow H^+ + O_2\cdot^-$ $pK = 4.8$ (1.24)

$O_3 + O_2\cdot^- + H_2O \rightarrow \cdot OH + OH^- + 2O_2$ (1.25)

$FeOH^{2+} + h\nu \rightarrow Fe^{2+} + \cdot OH$ (1.26)

$Fe^{2+} + H_2O_2 \rightarrow Fe^{3+} + \cdot OH + OH^-$ (1.27)

$H_2O \xrightarrow{\sim\sim} e^-_{aq},\ H\cdot,\ \cdot OH,\ H_2O_2,\ H_2,\ H^+$ (1.28)

$e^-_{aq} + S^n \rightarrow S^{n-1}$ (1.29)

$\cdot OH + S^n \rightarrow S^{n+1} + OH^-$ (1.30)

$e^-_{aq} + H_3O^+ \rightarrow H\cdot + H_2O$ (1.31)

$\cdot OH + \text{t-BuOH} \rightarrow H_2O + \cdot CH_2(CH_3)_2COH$ (1.32)

$e^-_{aq} + N_2O \rightarrow N_2 + O\cdot^-$ (1.33)

$O\cdot^- + H_2O \leftrightarrow \cdot OH + OH^-$ (1.34)

$e^-_{aq} + S_2O_8^{2-} \rightarrow SO_4\cdot^- + SO_4^{2-}$ (1.35)

$F_2 \xrightarrow{\sim\sim} 2\,F^*$ (1.36)

$F^* + Kr \longrightarrow KrF^*$ (1.37)

$KrF^* \longrightarrow Kr + F + h\nu$ (1.38)

$S_2O_8^{2-} + h\nu \rightarrow \phi\, SO_4\cdot^-$ (1.39)

$\cdot OH + 2\,SCN^- \rightarrow (SCN)_2\cdot^- + OH^-$ (2.1)

$Cl\cdot + Cl^- \leftrightarrow Cl_2\cdot^-$ (3.1)

$Cl\cdot + Cl\cdot \rightarrow Cl_2$ (3.2a)

$Cl\cdot + Cl_2\cdot^- \rightarrow Cl_2 + Cl^-$ (3.2b)

$Cl_2\cdot^- + Cl_2\cdot^- \rightarrow Cl_2 + 2Cl^-$ (3.2c)

$Cl^- + h\nu \rightarrow Cl\cdot + e^-_{aq}$ (3.3)

$SO_4\cdot^- + Cl^- \rightarrow SO_4^{2-} + Cl\cdot$ (3.4)

$Cl\cdot + \text{t-BuOH} \rightarrow \text{products}$ (3.5)

$Cl_2\cdot^- + \text{t-BuOH} \rightarrow \text{products}$ (3.6)

$Cl\cdot + H_2O \rightarrow \text{products}$ [*cf.* reaction (3.9)] (3.7)

$Cl_2\cdot^- + H_2O \rightarrow \text{products}$ [*cf.* reaction (3.9)] (3.8)

$Cl\cdot/Cl_2\cdot^- + H_2O \leftrightarrow HOClH\cdot \leftrightarrow H^+ + HOCl\cdot^- \leftrightarrow Cl^- + \cdot OH + H^+$ (3.9)

$SO_4\cdot^- + Cl^- \leftrightarrow Cl\cdot + SO_4^{2-}$ (4.1)

$SO_4\cdot^- + \text{t-BuOH} \rightarrow \text{products}$ (4.2)

$SO_4\cdot^- + H_2O \rightarrow SO_4^{2-} + H^+ + \cdot OH$ (4.3)

$SO_4\cdot^- + S_2O_8^{2-} \rightarrow SO_4^{2-} + S_2O_8\cdot^-$ (4.4)

$$NO_3\cdot + Cl^- \leftrightarrow Cl\cdot + NO_3^- \quad (4.5)$$

$$CH_3COCH_2Cl + H_2O \rightarrow CH_3COCH_2OH + Cl^- + H^+ \quad (5.1)$$

$$2\ CH_3COCH_2Cl \rightarrow \text{aldol} \rightarrow H_2O + \text{prod.} \quad (5.2)$$

$$CH_3COCH_2Cl + h\nu \rightarrow {}^1[CH_3COCH_2Cl]^* \quad (5.3)$$

$${}^1[CH_3COCH_2Cl]^* \rightarrow \cdot CH_2COCH_3 + Cl\cdot \quad (5.4)$$

$$Cl\cdot + CH_3COCH_2Cl \rightarrow Cl^- + \text{products} \quad (5.5)$$

$${}^1[CH_3COCH_2Cl]^* \rightarrow {}^3[CH_3COCH_2Cl]^* \quad (5.6)$$

$$Cl\cdot\,(aq) \overset{K_A}{\leftrightarrow} HOCl\cdot^- + H^+ \overset{K_B}{\leftrightarrow} \cdot OH + Cl^- + H^+ \quad (5.7)$$

$$SO_4\cdot^- + NO_3^- \leftrightarrow SO_4^{2-} + NO_3\cdot \quad (6.1)$$

$$e^-_{aq} + NO_3^- \rightarrow NO_3\cdot^{2-} \overset{H_2O}{\rightarrow} NO_2\cdot + 2OH^- \quad (6.2)$$

$$NO_3\cdot + \text{t-BuOH} \rightarrow NO_3^- + H^+ + \text{products} \quad (6.3)$$

$$NO_3\cdot + \text{water} \rightarrow NO_3^- + \cdot OH + H^+ \quad (6.4)$$

$$A + B \overset{K_{A3.1}}{\leftrightarrow} AB \overset{k_{A3.1a}}{\rightarrow} C \quad (A3.1)$$

Chapter 1

Atmospheric and Radiation Chemistry

1.1.1 Introduction

The combustion of sulfur-containing fossil fuels has almost entirely met Man's increasing energy needs since the Industrial Revolution. However, concomitant with the generation of electricity by burning coal and oil is the emission of gaseous sulfur dioxide into the atmosphere. The subsequent deposition of sulfuric acid by acid rain is the result of the oxidation of sulfur dioxide in the atmosphere via physical and chemical processes.

The term "acid rain" was first used by R. A. Smith to denote precipitation with a pH below 5.6 (the pH of water in equilibrium with carbon dioxide),[1] although natural emissions of sulfur dioxide make the pH of rain closer to 5. It is more correct to speak of "acid deposition" since this encompasses the different forms including fog and rain. Acid deposition is currently recognised to be a major problem throughout the world,[2,3] yet the problems associated with atmospheric air pollution are not recent. Indeed, the deleterious effects of emissions have been known since ancient times.[4] These problems intensified during the 19th century with the escalating use of coal in fuelling the Industrial Revolution, and in 1872 it was recognised that the damage to plants and buildings was caused by the acidification of rainwater due to the formation of sulfuric acid.[5] Scientists had long been aware of the sulfurous content of coal smoke, but sulfur dioxide was overlooked because sulfur emissions were thought to be too small to be important.[6]

Since the 1950s a network of *ca*. 160 sites forming the European Atmospheric Chemistry Network have been analysing the pH of rainwater throughout Europe. Samples are analysed for pH, $[SO_4^{2-}]$, $[Cl^-]$, $[NO_3^-]$ and $[NH_4^+]$ as well as $[Na^+]$, $[K^+]$, $[Mg^{2+}]$ and $[Ca^{2+}]$. From these data attention was drawn to the increase in $[SO_4^{2-}]$ with decreasing pH.[7] A more recent study has found that out of 120 sites 29 show a significant trend of increasing annual average precipitation acidity and 5 show a decrease.[8] This increase in the acidity of precipitation has led to increasing concern, instigating scientific collaboration and European legislation on emissions.

Figure 1.1 *Temperature variation with height in the atmosphere.*

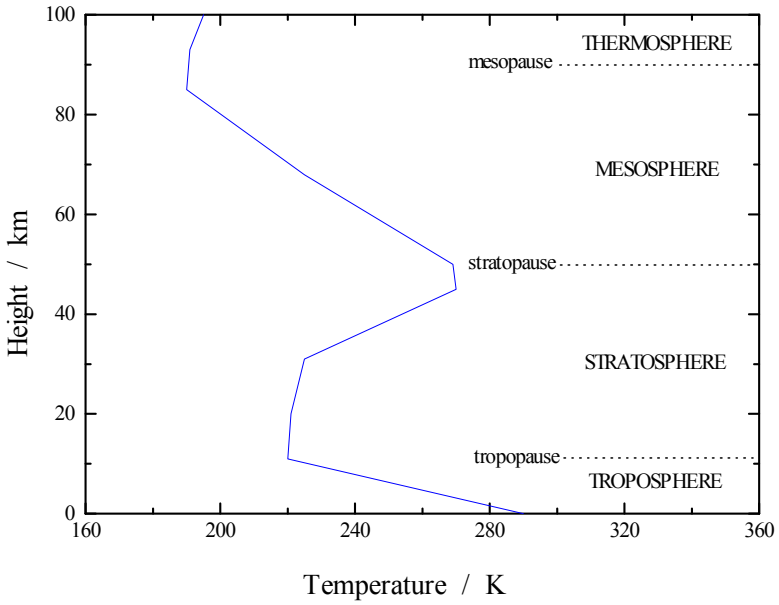

1.1.2. The Atmosphere

There are several well-defined regions in the atmosphere, identified by the temperature gradients existing at various heights, see Figure 1.1.[9,10] The variation in temperature is explained by the physical and chemical processes occurring in the atmosphere, which are driven by the Sun.

Energy radiated from the Sun has a maximum in the visible region of the electromagnetic spectrum, most of which passes through the atmosphere and is absorbed by the ground.[10] The ground temperature increases and conducts heat to the lower layers of the atmosphere, warming the troposphere from below. The warm air moves upwards due to its lower density, however since this involves an adiabatic expansion, thermal energy is expended and the temperature of the air decreases (see Section 1.1.3). In addition, the optically active species which are present in the atmosphere, such as H_2O and CO_2, can emit and absorb infra-red light through their vibrations. Therefore warm air, containing thermally excited molecules, radiates away energy. These processes account for the decrease in temperature with height up to *ca.* 11 km.

At altitudes above 20 km, the temperature increases again. This is attributed to the absorption of short wavelength light (< 290 nm) by O_2 and O_3, the net process being a conversion of light energy to thermal energy of the products. This mechanism is known as the Chapman model.[11]

$$O_2 + h\nu \rightarrow O(^3P) + O(^1D) \quad (1.1)$$

$$O(^3P) + O_2 + M \rightarrow O_3 + M \quad (1.2)$$

$$O_3 + h\nu \rightarrow O_2 + O(^1D) \quad (1.3)$$

$$O_3 + O(^3P) \rightarrow 2\,O_2 \quad (1.4)$$

The temperature in this region is determined by the photon intensity, I, and the O_2 density. At high altitudes, I is high but $[O_2]$ is low due to thinning of the atmosphere whilst at lesser altitudes $[O_2]$ may be high but I low due to the attenuation by the atmosphere above. At roughly 25 to 30 km the photon intensity and $[O_2]$ are at an optimum level so that the ozone density reaches a maximum. This region is known as the ozone layer.[10]

Above 50 km the heat gain by UV-absorption is too weak to compete with the radiative loss by vibration of optically active molecules and the temperature decreases. Above 80 km the temperature rises once more. However, at these altitudes the mean free path of particles is of the order of metres and consequently the energy distribution between translational, rotational and vibrational states may not be equilibrated. Typically, molecules will have high translational kinetic energy but not high vibrational and rotational energies, the collisions which help to transfer energy to these modes being so infrequent.

1.1.3 Tropospheric Mixing

A parcel of warm air at ground level will rise to a higher altitude, as it has a lower density than the colder air around it. At this higher altitude the pressure is less and therefore the parcel will expand, effectively doing work, pdV, against the surrounding atmosphere. Assuming that heat transfer from this parcel is negligible, i.e. it behaves adiabatically, the work done will be compensated for

by a decrease in temperature. However the new temperature of the parcel may still be higher than that of the surrounding air, in which case it will rise and expand as before, causing an upward movement of air. This situation, known as convective instability, occurs when the temperature gradient of the atmosphere is high in relation to the pressure gradient. It accounts for the mixing of gases and the chemical transport in the troposphere. Above a certain height (*ca*. 11 km) the temperature gradient is sufficiently low to prevent convective instability hence the atmosphere above this region is more stable. This marks the difference between the turbulently mixed troposphere and the layered stratosphere.

1.1.4. Cloud Formation

As warm, moist air rises and cools down it becomes thermodynamically unstable due to its saturation with water vapour, and condensation may be expected to occur. Homogeneous nucleation is the process whereby clusters consisting of several water molecules collide and coalesce into small droplets. However the vapour pressure of these small droplets, which is inversely proportional to the radius, means that they evaporate as fast as they are formed.[9] Calculations have shown that it is thermodynamically unfavourable for droplets to condense from water vapour except under conditions of extremely high supersaturation rarely encountered in the atmosphere.[12] However, droplets do form in the atmosphere and therefore an additional process to homogeneous nucleation must occur. The way that droplets arise in the atmosphere can be explained by taking into account the presence of aerosol particles, e.g. dust and soil, which result in heterogeneous nucleation. Water molecules condense on the surface of these particles, effectively producing droplets with a larger radius, and hence a tendency to continue growing rather than to evaporate.[10]

1.1.5. Aerosol Particles and Droplet Formation

Aerosol particles have two purposes in the formation of clouds. They serve as condensation nuclei, enabling clouds to form at fairly low degrees of supersaturation, and they contain water soluble material such as inorganic salts,

which contribute to the composition and chemistry of cloud water. If the aerosol particles are water soluble then droplets may form even when the air is not fully saturated, due to the lower vapour pressure of solutions than pure liquids.[13] Atmospheric aerosols are generally considered to be the particles that range in size from a few nanometres to tens of micrometres in diameter. They originate from sea spray, wind erosion of soils and industrial releases. Particles that are emitted directly are known as primary aerosols, and particles formed in the atmosphere by gas-to-particle conversion processes are known as secondary aerosols.

A minimum size of droplet must be reached for it to survive the fall to the ground without undergoing complete evaporation. For example, from an altitude of 2 km only droplets with an initial radius greater than 500 μm will reach the surface.[10] Thus most clouds do not lead to precipitation and will eventually dissipate. This is because, beyond a critical size, the rate of growth of a droplet is inversely proportional to its radius,[14] making condensation too inefficient to produce large droplets in the lifetime of the cloud. Larger drops must be formed by collisions and coalescence of smaller droplets.

Evidence has been presented that the nuclei set free by dissipating clouds are subject to renewed condensation and eventually pass through a series of condensation-evaporation cycles before being irretrievably removed by precipitation. Cloud condensation nuclei are estimated to undergo about 10 condensation-evaporation cycles on average during their residence time in the troposphere.[15]

1.1.6. Uptake/scavenging of Gases into Cloud Water

Once the droplets are formed atmospheric gases may dissolve into them.[16] The direct transfer of gas phase species into the aqueous phase is kinetically described in terms of the mass accommodation coefficient, α. It is defined as the fraction of molecules of a compound incorporated into the liquid phase per number of collisions between the gas-liquid interface and the compound. Values of α range between 0 and 1. Gases that do not dissolve well have values

less than 0.01, whereas soluble gases have values between 0.01 and 1.00.[17] The value of α for SO_2 lies between 0.02 and 0.05.[18,19]

The thermodynamic solubility of a species S in a given solvent (the fraction that stays in the droplet after transfer from the gas phase) is described for dilute solutions by the Henry's Law coefficient, $K_H(S)$, equation [1.1]

$$K_H(S) = \frac{[S]}{p(S)} \qquad [1.1]$$

where p(S) is the partial pressure of S in the gas phase in atmospheres and [S] is the concentration of S in solution in mol dm^{-3}. Some recent measurements of Henry's law coefficients for atmospherically relevant species are given in Table 1.1. The Henry's Law coefficients should be regarded as a first approximation only. This is because Henry's Law assumes a thermodynamically equilibrated distribution of a species S between the gas phase and the aqueous phase.

Table 1.1 *Henry's Law coefficients for some atmospheric gases.*

Species, S	**K_H at 298 K / mol dm^{-3} atm^{-1}**	**Reference**
H_2O_2	2.42×10^5	20
HCHO	1.44×10^4	21
·OH	2×10^2 to 10^5	22, 23
HO_2·	1.0×10^3	10
SO_2	1.23	44
CO_2	4.44×10^{-2}	9
O_3	1.80×10^{-2}	24
O_2	1.68×10^{-3}	10

In real atmospheric systems this requirement is not usually met due to highly rate controlled physical and chemical processes. E.g. if S undergoes chemical reaction once dissolved this will affect the concentration of S, and therefore the

fraction of S in solution will be higher than expected from the Henry's Law coefficient. In these cases the increased solubility can be expressed in terms of an effective Henry's Law constant, H^*.[10] Formaldehyde displays this behaviour due to its dissolution and subsequent hydration, reaction (1.5). The formation of the more soluble gem-diol upon solvation greatly increases the effective solubility of formaldehyde in water, see equation [1.2].

$$HCHO\,(g) \overset{H_2O}{\leftrightarrow} HCHO\,(aq) \overset{H_2O}{\leftrightarrow} CH_2(OH)_2 \qquad (1.5)$$

$$H^* = \frac{[HCHO\,(aq)] + [CH_2(OH)_2]}{p(HCHO\,(g))} \qquad [1.2]$$

1.1.7. The Acidity of Rainwater

The acidity of rainwater is governed by the concentrations of both strong and weak acids and also the presence of any neutralising basic species, in particular NH_3 from soil emissions and domestic animals.

The two methods for measuring the pH of rainwater are bulk sampling and individual droplet sampling. Bulk sampling techniques are more common, but have the drawback that the droplet compositions are averaged by mixing. A narrow pH range is observed with this technique, centred on pH 4.0 ± 0.2.[25,26] Since the drop size and ion concentration are inversely related,[27] it would seem that the extremes of concentration in the smaller drops are diluted upon mixing with the larger ones. Individual droplet sampling reveals a range of acidity from pH 2 to 8, with maxima at pH 2.5 to 3.0 and 4 to 5.[28]

1.1.8. Constituents of Cloud Water

Cloud water is composed of water, inorganic salts, transition metal ions and low molecular weight organic compounds, see Table 1.2. Inorganic salts include sulfates, nitrates and chlorides which originate from sea spray and gas-phase scavenging of ammonium sulfate and nitric and hydrochloric acids. The predominant metal is iron, with manganese and copper also present in much lower concentrations. Weathering and erosion of the earth's crust are the main

sources of transition metals. Organic compounds include carboxylic acids, aldehydes and ketones. There are many sources of aldehydes, both biogenic and anthropogenic. Direct emissions occur from the combustion of fuels by vehicles, furnaces and industries. The burning of biomass and the release of volatile compounds from plants also contribute.[29] In the presence of S(IV) these aldehydes form adducts, for example formaldehyde and HSO_3^- exist in equilibrium with hydroxomethansulfonate, HMS, reaction (1.6).

$$HSO_3^- + H_2C(OH)_2 \leftrightarrow H_2C(OH)SO_3^- + H_2O \qquad (1.6)$$

As $K_{1.6} = 3.6 \times 10^6$, a significant fraction of the HSO_3^- will be present in the form of HMS,[30] and since HMS is less reactive than its constituents it may hinder the oxidation of S(IV).[31,32]

Table 1.2 *Typical concentrations of some species in pH 4.5 cloud water.*

Species	Concentration / mol dm^{-3}	Reference
SO_4^{2-}	3×10^{-4}	33
Cl^-	5×10^{-5}	33
NO_3^-	2×10^{-5}	10
S(IV) [a]	10^{-7} to 5×10^{-5}	34
HCHO [a]	5×10^{-4}	35,36
O_3	6×10^{-10}	33
H_2O_2	3×10^{-5}	33
Fe(II)	*ca.* 10^{-6}	33
Mn(II)	*ca.* 10^{-7}	33

[a] Present in equilibrium with the HCHO-S(IV) adduct, HMS, see text.

Figure 1.2 *Speciation of S(IV) in the aqueous phase.*

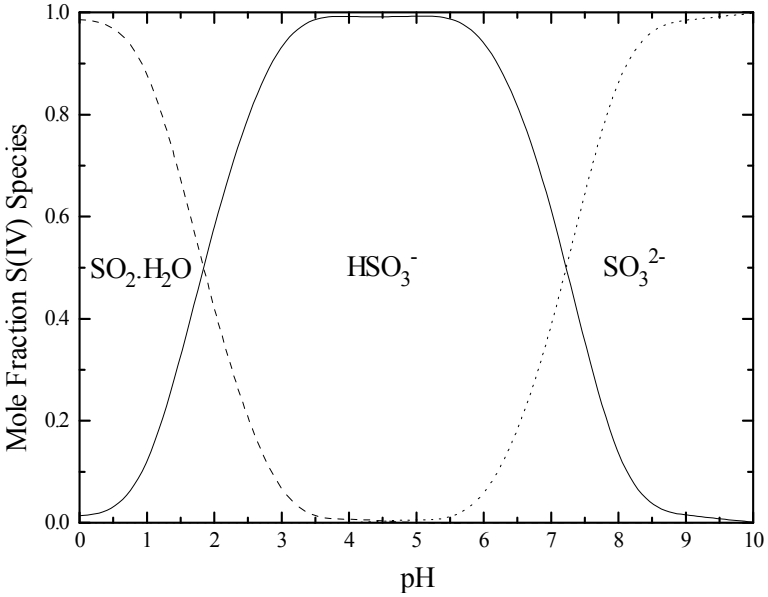

Sulfates are also formed within the cloud droplet from the oxidation of S(IV), see Section 1.2.1. S(IV) enters into the aqueous phase by scavenging of SO_2(g) by the droplet, and equilibrates with sulfite and hydrogen sulfite depending on the pH, reactions (1.7) to (1.9), see Figure 1.2.

$$SO_2\,(g) + H_2O \leftrightarrow SO_2\,(aq) \quad [\text{also written as } SO_2 \,.\, H_2O] \tag{1.7}$$

$$SO_2 \,.\, H_2O \leftrightarrow H^+ + HSO_3^- \qquad pK_a = 1.8 \tag{1.8}$$

$$HSO_3^- \leftrightarrow H^+ + SO_3^{2-} \qquad pK_a = 7.2 \tag{1.9}$$

1.1.9. Natural/biogenic Sources of SO_2

The only natural source of sulfur dioxide emission is from volcanoes. Volcanic eruptions produce enough sulfur dioxide to affect surrounding areas, whereas volcanic emissions not associated with eruption have very localised effects. Reduced sulfur compounds can be oxidised in the atmosphere to produce sulfur dioxide. These reduced sulfur compounds are emitted by terrestrial and marine biota as well as by volcanoes. Volcanic eruptions produce H_2S and marine emissions produce dimethylsulfide (DMS) and COS. Land emissions are in several forms including H_2S, DMS, methanethiol, CS_2 and COS. H_2S is also

produced from plant and animal decay.[37] In the atmosphere, the reduced sulfur compounds may be oxidised to SO_2 by ·OH, O_2 and O_3.[38,39,40,41]

1.1.10. Anthropogenic Sources

Although there are many pathways for its natural production, the dominant source of sulfur dioxide is anthropogenic emission. Anthropogenic sources are wide-ranging and include many industrial processes. The combustion of fossil fuels, refining of petroleum, burning of rubbish and smelting of sulfur-containing ores all emit sulfur dioxide as a by-product. There is also emission from low level pollution sources including exhaust gases from both diesel and petroleum combustion. The rise in fossil fuel consumption has caused a steady increase in man-made sulfur emissions. The total emission of SO_2 in 1976 was 103 Tg S/yr, which is around ten times greater than natural emissions on all continents.[10]

1.2.1. Oxidation of Sulfur Dioxide in Aqueous Solution

Four main pathways have been proposed for the oxidation of SO_2 in the aqueous phase of clouds. These are oxidation by ozone, oxidation by H_2O_2, transition metal ion catalysed oxidation by O_2 and the free-radical initiated oxidation by ·OH. These mechanisms are discussed in more detail below.

1.2.2. Oxidation by Ozone

Ozone is an important oxidant in clouds,[42] which reacts with S(IV) to form sulfate and oxygen, liberating H^+ ions. The rate is inversely related to $[H^+]$ due to the reactivity of O_3 towards the different forms of S(IV), which follows the pattern $SO_3^{2-} >> HSO_3^- >> SO_2.H_2O$.[32,34,43,44]

1.2.3. Oxidation by Hydrogen Peroxide

H_2O_2 is also an important oxidant in the atmosphere.[43] It is thought that the reaction proceeds with bisulfite in two steps, reaction (1.10).[45]

$$HSO_3^- + H_2O_2 \leftrightarrow H_2O + A^- \xrightarrow{H^+} H_2SO_4 \qquad (1.10)$$

The intermediate A^- is presumably the peroxymonosulfurous anion and its rearrangement by acid catalysis is rate limiting.[10] The mechanism leads to a rate law exhibiting an increasing rate with $[H^+]$, which is opposite to that for the reaction of S(IV) with ozone.[24,43,46,47]

1.2.4. Transition Metal Catalysed Oxidation by Oxygen

The direct oxidation of S(IV) by oxygen proceeds slowly, if at all, however it is catalysed by transition metal ions so that it represents an important pathway for S(IV) oxidation under the conditions relevant to cloud water.[48,49] Radical and non-radical mechanisms have been invoked. The non-radical mechanism is summarised by reaction (1.11).

$$Fe(III) + HSO_3^- + H_2O + O_2 \rightarrow Fe(III) + H_2O_2 + HSO_4^- \qquad (1.11)$$

The radical mechanism is more complicated and involves a number of consecutive steps. The initiation step is the formation of metal-sulfito complexes such as $Fe(SO_3)^+$, $Fe(SO_3)_2^-$ and $Fe(SO_3)_3^{2-}$.[50] The decomposition of these complexes by photolysis or a redox process results in the production of the reduced metal form and the $SO_3\cdot^-$ radical. The $SO_3\cdot^-$ radical becomes involved in the free radical mechanism outlined below, leading to $SO_4\cdot^-$ and $SO_5\cdot^-$ which oxidise Fe(II) back to Fe(III), thus completing the catalysis cycle.

1.2.5. Free-radical Initiated Oxidation

The mechanism of the free radical oxidation of S(IV) at pH 4.5 is summarised by reactions (1.12) to (1.20).[51,52] At different pH, S(IV) will exist in forms other than HSO_3^-, however the mechanism remains essentially the same.

Initiation

$$\cdot OH + HSO_3^- \rightarrow H_2O + SO_3\cdot^- \qquad (1.12)$$

Propagation

$$SO_3\cdot^- + O_2 \rightarrow SO_5\cdot^- \qquad (1.13)$$

$$SO_5\cdot^- + HSO_3^- \rightarrow HSO_5^- + SO_3\cdot^- \qquad (1.14)$$

$$SO_5\cdot^- + HSO_3^- \rightarrow SO_4\cdot^- + SO_4^{2-} + H^+ \qquad (1.15)$$

$$SO_4^{\cdot -} + HSO_3^- \rightarrow SO_4^{2-} + H^+ + SO_3^{\cdot -} \quad (1.16)$$

$$SO_5^{\cdot -} + SO_5^{\cdot -} \rightarrow 2\,SO_4^{\cdot -} + O_2 \quad (1.17)$$

Termination

$$SO_3^{\cdot -} + SO_3^{\cdot -} \rightarrow S_2O_6^{2-} \quad (1.18)$$

$$SO_4^{\cdot -} + SO_4^{\cdot -} \rightarrow S_2O_8^{2-} \quad (1.19)$$

$$SO_5^{\cdot -} + SO_5^{\cdot -} \rightarrow S_2O_8^{2-} + O_2 \quad (1.20)$$

At night-time, initiation of the chain is possible by reaction (1.21).

$$NO_3\cdot + HSO_3^- \rightarrow NO_3^- + SO_3^{\cdot -} + H^+ \quad (1.21)$$

The rate coefficients are summarised in Table 1.3. A recent study has reported that the simple free-radical-chain oxidation of S(IV) may be of less significance in the oxidation of S(IV) in cloud droplets than previously estimated.[52]

Table 1.3 *Rate constants for the reactions involved in the free radical initiated oxidation of S(IV).*

Reaction	Number	Rate constant / $dm^3\ mol^{-1}\ s^{-1}$	Reference
$\cdot OH + HSO_3^- \rightarrow H_2O + SO_3^{\cdot -}$	1.12	2.7×10^9	52
$SO_3^{\cdot -} + O_2 \rightarrow SO_5^{\cdot -}$	1.13	2.5×10^9	52
$SO_5^{\cdot -} + HSO_3^- \rightarrow HSO_5^- + SO_3^{\cdot -}$	1.14	8.6×10^3	52
$SO_5^{\cdot -} + HSO_3^- \rightarrow SO_4^{\cdot -} + SO_4^{2-} + H^+$	1.15	3.6×10^2	51,52,53
$SO_4^{\cdot -} + HSO_3^- \rightarrow SO_3^{\cdot -} + SO_4^{2-} + H^+$	1.16	6.8×10^8	52
$SO_5^{\cdot -} + SO_5^{\cdot -} \rightarrow 2\,SO_4^{\cdot -} + O_2$	1.17	$\sim 2.2 \times 10^8$	52
$SO_4^{\cdot -} + SO_4^{\cdot -} \rightarrow S_2O_8^{2-}$	1.18	4.5×10^8	52
$SO_3^{\cdot -} + SO_3^{\cdot -} \rightarrow S_2O_6^{2-}$	1.19	3.1×10^8	52
$SO_5^{\cdot -} + SO_5^{\cdot -} \rightarrow S_2O_8^{2-} + O_2$	1.20	4.8×10^7	52
$NO_3\cdot + HSO_3^- \rightarrow NO_3^- + SO_3^{\cdot -} + H^+$	1.21	1.4×10^9	54

1.2.6. Sources of Hydroxyl Radicals

A major source of hydroxyl radicals in the aqueous phase of clouds is the heterogeneous scavenging from the gas phase. There are also homogenous

aqueous phase processes that contribute significantly to their formation in cloud droplets. For example the photolysis of aqueous H_2O_2, reaction (1.22), is a direct source of ·OH radicals. Hydrogen peroxide is present in cloud water by heterogeneous scavenging from the gas phase and by the aqueous-phase disproportionation reaction of HO_2· radicals, reaction (1.23).[55]

$$H_2O_2 + h\nu \rightarrow 2\ \cdot OH \qquad (1.22)$$

$$HO_2\cdot + HO_2\cdot \rightarrow H_2O_2 + O_2 \qquad (1.23)$$

The HO_2· radical is produced by a number of reactions in both the aqueous- and the gas-phase, e.g. ·OH + O_3. Its incorporation into the aqueous phase is enhanced by a high solubility and the dissociation reaction (1.24).[56,57]

$$HO_2\cdot \leftrightarrow H^+ + O_2\cdot^- \qquad pK = 4.8 \qquad (1.24)$$

Aqueous phase processes result in the reconversion of HO_2· and $O_2\cdot^-$ to ·OH by reactions (1.22) and (1.23), or by the reaction of $O_2\cdot^-$ with ozone, reaction (1.25).

$$O_3 + O_2\cdot^- + H_2O \rightarrow \cdot OH + OH^- + 2\ O_2 \qquad (1.25)$$

Another important source of ·OH has been proposed to be the photolysis of Fe(III), reaction (1.26).[58,59] This photolytic conversion of Fe(III) to Fe(II) provides a source of Fe(II), which can generate further ·OH by the Fenton reaction, reaction (1.27).[55]

$$FeOH^{2+} + h\nu \rightarrow Fe^{2+} + \cdot OH \qquad (1.26)$$

$$Fe^{2+} + H_2O_2 \rightarrow Fe^{3+} + \cdot OH + OH^- \qquad (1.27)$$

1.3.1. Radiation Chemistry of Aqueous Solutions

Pulse radiolysis and laser flash photolysis are suitable tools for studying a wide range of free-radical reactions. These techniques coupled with absorption

detection methods make possible the study of very fast reactions involving aquated species.

1.3.2. Pulse Radiolysis

Pulse radiolysis involves the use of an electron accelerator to deliver ionising radiation in intense single pulses each lasting *ca*. 1 μs or less. A single pulse can produce concentrations of intermediates high enough to be studied by methods such as ultraviolet or visible spectroscopy or by electrical conductivity. Details of the apparatus used in this study can be found in Chapter 2. A Van de Graaff accelerator has been used to introduce fast electrons directly into the sample. At energies lower than 10 MeV the electrons interact with the medium through inelastic collision causing ionisation and excitation. Linear energy transfer, LET, also known as the stopping power, is given by the average amount of energy lost by a fast charged particle per unit length in a medium. This study is concerned with radiation of low LET; a more detailed explanation of the effects of LET on ionisation events and spur reactions can be found elsewhere.[60] The LET of electrons with energy less than 10 MeV is given by the Bethe formula, equation [1.3].[61]

$$-\frac{dE}{dx}=\frac{2\pi e^4 NZ}{m_o v^2}\left\{\ln\frac{m_o v^2 E}{2I^2\left(1-\beta^2\right)}-\left(2\sqrt{1-\beta^2}-1+\beta^2\right)\ln 2+1-\beta^2+\frac{1}{8}\left(1-\sqrt{1-\beta^2}\right)^2\right\} \qquad \text{.....[1.3]}$$

where *e* is the charge on the electron

N is the number of atoms per m^3 in the medium

m_o is the rest mass of the electron

v is the velocity of the bombarding electrons

I is the mean excitation potential of the electrons in the stopping material

z is the atomic number of the stopping material

and β is the ratio of v to the speed of light, $\beta=\frac{v}{c}$.

Fast electrons with energy in the range 10 to 1000 MeV lose energy by the emission of an x-ray following deceleration by the coulombic field of a nucleus (radiative collision). These x-rays are known as Bremsstrahlung. This provides a mechanism whereby energy can escape from the medium without effecting a

chemical change. Electrons can also be deflected by the coulombic field of a nucleus in an elastic collision. No energy is lost in the scattering (known as Rutherford scattering), but a wide distribution of the lowest energy electrons is caused. This is of importance in the irradiation of solids. Electrons can also interact with matter to produce low energy electromagnetic waves known as Cerenkov radiation. When electrons with velocity greater than the velocity of light in the medium enter the medium they emit light as they slow down. This light is Cerenkov radiation.

1.3.3. Ionisation Events

When ionising particles pass through a medium they cause excitation and ionisation of molecules along their path. Secondary electrons are generated in the ionisation process. Each of these events is known as a spur and within this isolated volume a series of reactions occurs immediately following the ionisation event. Occasionally the secondary electrons may be formed with sufficient energy to form tracks of their own. These electrons are called are δ-rays, see Figure 1.3.

It is generally accepted that the spurs are in thermal equilibrium with the bulk solution after 10^{-12} s when the chemical stage begins. This spur expansion stage is thought to last up to 10^{-7} s. It is here that the molecular products of water radiolysis are formed and diffuse out of the spurs and into the bulk solution, as indicated in Figure 1.4.[62] A full description of the spur and other early processes in radiation chemistry can be found elsewhere.[63,64,65]

Figure 1.3 *Track of fast electron.*

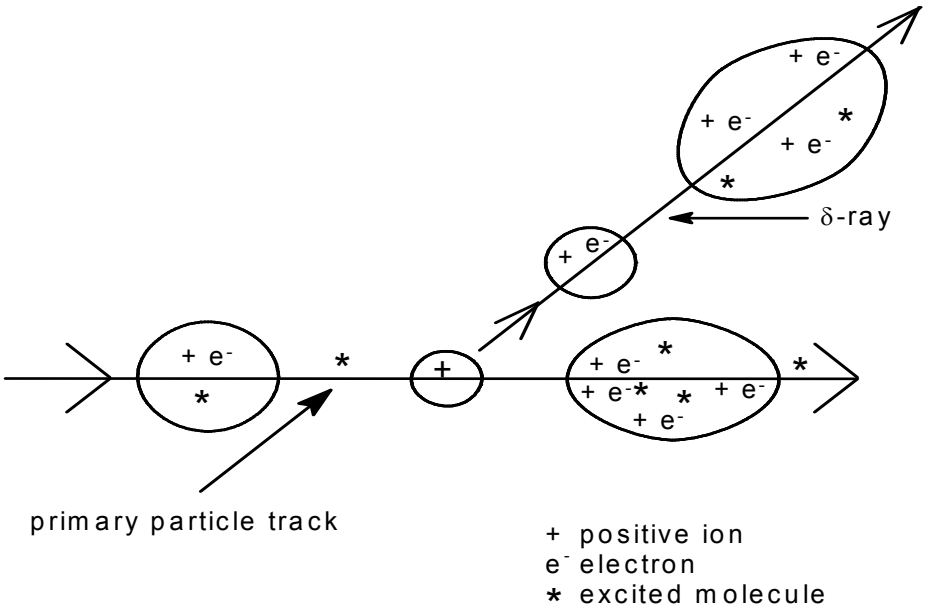

Figure 1.4. *Radiolysis of water.*

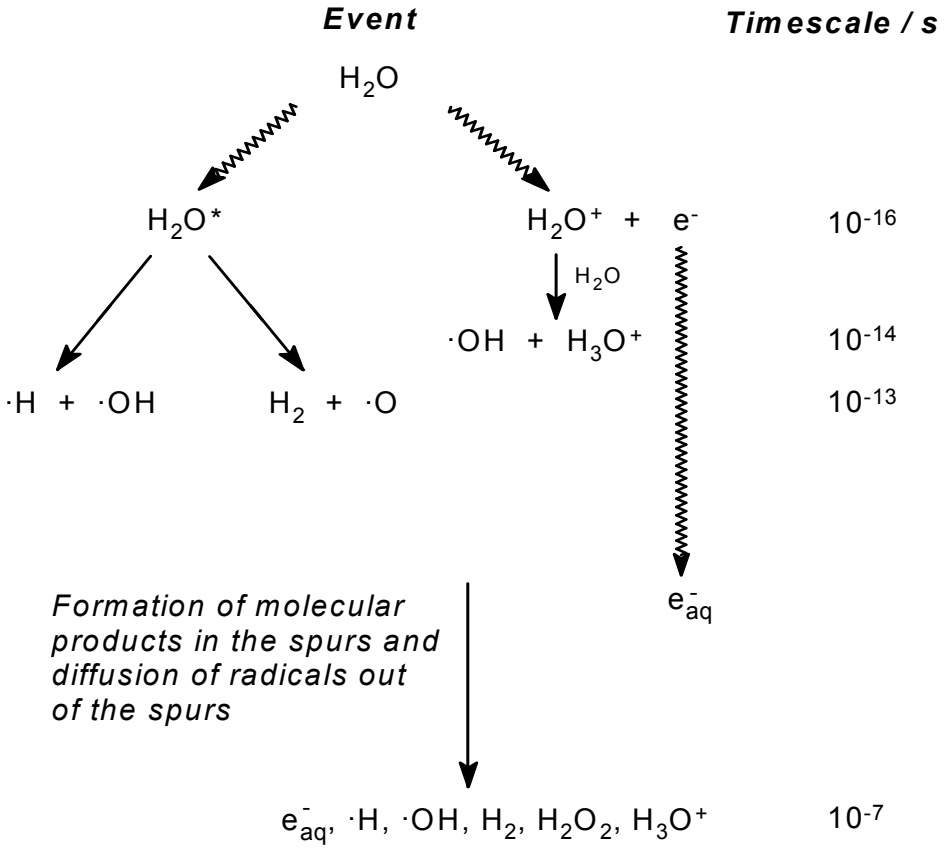

Table 1.4 *Radical and molecular product yields (G-values).*

Species, S	G(S) / 10^{-9} mol J^{-1}	Species, S	G(S) / 10^{-9} mol J^{-1}
e_{aq}^-	272	H^+	272
·OH	282	H·	57
H_2O_2	71	H_2	47

1.3.4. Radiolysis of Water

After completion of the spur processes, the result of radiolysis of water by fast electrons is the formation of radical and non-radical products, reaction (1.28).

$$H_2O \rightsquigarrow e_{aq}^-,\ H\cdot,\ \cdot OH,\ H_2O_2,\ H_2,\ H^+ \qquad (1.28)$$

The yields of these species are given by their G-values in mol J^{-1}. The G-value is dependent on the nature of the ionising radiation. In Table 1.4 is shown typical values for irradiation of water by fast electrons taken from Ref. 62.

1.3.5. The Hydrated Electron

This species is a powerful reductant, $E^o = -2.9$ V,[66] which has a strong optical absorption in the red region of the spectrum. It reacts as a nucleophile in electron transfer processes, reaction (1.29), and also by dissociative electron capture, e.g. $e_{aq}^- + N_2O$ in reaction (1.33).

$$e_{aq}^- + S^n \rightarrow S^{n-1} \qquad (1.29)$$

1.3.6. The Hydroxyl Radical

This is a strong oxidant, $E^o = 2.72$ V in acidic solution,[66] which readily oxidises inorganic ions. The reaction is often written as an electron transfer process, reaction (1.30), although this is an over simplification in many cases. The ·OH radical undergoes reaction with organic species primarily by H-abstraction from C-H, or addition to unsaturated carbon bonds.

$$\cdot OH + S^n \rightarrow S^{n+1} + OH^- \qquad (1.30)$$

1.3.7. The Hydrogen Atom

The H· atom is a slightly less powerful reductant than e^-_{aq}, $E^o = -2.3$ V.[66] In its reactions with organic molecules H· behaves like the hydroxyl radical, reacting by H-abstraction and addition to unsaturated carbon bonds. At low pH, H· becomes the predominant reducing radical due to reaction (1.31), $k_{1.31} = 2.3 \times 10^{10}$ dm^3 mol^{-1} s^{-1}.[67]

$$e^-_{aq} + H_3O^+ \rightarrow H\cdot + H_2O \qquad (1.31)$$

1.3.8. Interconversion/removal of Primary Radicals

When reducing conditions are required ·OH can be converted into an unreactive radical by the addition of 2-methyl-propan-2-ol (t-BuOH), reaction (1.32), for which $k_{1.32} = 6.0 \times 10^8$ dm^3 mol^{-1} s^{-1},[67] leaving e^-_{aq} and H· as the only reactive radicals in the solution.

$$\cdot OH + \text{t-BuOH} \rightarrow H_2O + \cdot CH_2(CH_3)_2COH \qquad (1.32)$$

When oxidising conditions are required, the hydrated electrons can be converted into hydroxyl radicals by saturating the solution with nitrous oxide, reactions (1.33) and (1.34). The rate constants for these reactions are very high ($k_{1.33} = 9.1 \times 10^9$ dm^3 mol^{-1} s^{-1}, $k_{1.34} = 9.3 \times 10^7$ s^{-1} and $k_{-1.34} = 1.2 \times 10^{10}$ dm^3 mol^{-1} s^{-1}).[67]

$$e^-_{aq} + N_2O \rightarrow N_2 + O\cdot^- \qquad (1.33)$$

$$O\cdot^- + H_2O \leftrightarrow \cdot OH + OH^- \qquad (1.34)$$

Another widely used one electron oxidant is the sulfate radical, which is converted from e^-_{aq} by reaction with $S_2O_8^{2-}$ by reaction (1.35). This is a fast reaction with rate constant $k_{1.35} = 1.2 \times 10^{10}$ dm^3 mol^{-1} s^{-1}.[67] The $SO_4\cdot^-$ radical has a reduction potential of $E^o = 2.43$ V.[66]

$$e^-_{aq} + S_2O_8^{2-} \rightarrow SO_4\cdot^- + SO_4^{2-} \qquad (1.35)$$

1.3.9. Photochemistry

Photochemistry is the initiation of chemical processes by the excitation of specific atomic/molecular orbitals using electromagnetic radiation. Absorption of radiation gives rise to electronic transitions between discrete energy levels which can proceed to form high energy products, e.g. free radicals.[9,68]

1.3.10. Excimer Laser

The laser flash photolysis apparatus used in this study involves an excimer laser operated with the gases argon, krypton and fluorine. An electrical discharge is passed through a dilute mixture of these gases (ArF or KrF) in a buffer gas, helium. This results in the formation of an unstable molecule with the property that its ground state is dissociative and therefore it only exists in an excited state, an excimer, reactions (1.36) to (1.38).[9]

$$F_2 \xrightarrow{h\nu} 2\,F^* \qquad (1.36)$$

$$F^* + Kr \longrightarrow KrF^* \qquad (1.37)$$

$$KrF^* \longrightarrow Kr + F + h\nu \qquad (1.38)$$

The life-time of the KrF^* excimer is of the order of nanoseconds, followed by its spontaneous relaxation to the ground state and the concomitant emission of a photon. The Kr and F atoms separate due to the repulsive potential that is the ground-state of the molecule, which ensures the population inversion. The spontaneously emitted photon is reflected and focused along the direction of the exit tube, stimulating other excimers to emit photons in the same direction. These photons stimulate yet more excimers to release photons so that a high gain in photon intensity is achieved, resulting in an intense nanosecond pulse of monochromatic, coherent radiation

.

1.3.11. Quantum Yield

The electromagnetic radiation is used to effect a chemical transformation. The quantity of product produced by the absorption of a photon is described by the overall quantum yield, ϕ. The overall quantum yield is defined as the number of species (atoms, molecules, etc.) formed per photon absorbed, equation [1.4].

$$\phi = \frac{\text{No. of species formed}}{\text{No. of photons absorbed}} \qquad [1.4]$$

The $SO_4^{\cdot -}$ radical may be formed by 248 nm irradiation of $S_2O_8^{2-}$, reaction (1.39). The quantum yield may be estimated from the experimentally accessible parameters, $\varepsilon\phi = (2770 \pm 280)$ dm^3 mol^{-1} cm^{-1} and $\varepsilon = 1630$ dm^3 mol^{-1} cm^{-1}, to be $\phi = 1.7 \pm 0.2$.[52,69]

$$S_2O_8^{2-} + h\nu \rightarrow \phi\, SO_4^{\cdot -} \qquad (1.39)$$

1.4.1. References

1. R. A. Smith, in Air and Rain, Longman's Green, London 1845
2. M. Havas, T. C. Hutchinson and G. E. Likens, *Environ. Sci. Tech.*, 1984, **18**, 176A
3. C. L. Schofield, Acid/rain fisheries, in Proceedings of the International Symposium on Acidic Precipitation and Fishery Impacts in Northeast North America, Ed. R. E. Johnson, Ithaca, New York 1982
4. D. Camuffo, *Atmos. Environ.*, 1992, **26b**, 241
5. P. Brimblecombe, in The Big Smoke, Methuen, London 1987
6. W. M. Buchanan, in Smoke Nuisance Question, Griffin and Co., London 1857
7. S. Oden, *Water, Air, Soil Pollut.*, 1976, **6**, 137
8. A. S. Kallend, A. R. W. Marsh, J. H. Pickles and M. V. Proctor, *Atmos. Environ.*, 1983, **17**, 127
9. P. W. Atkins, in Physical Chemistry, 4th edition, Oxford University Press, Oxford 1990
10. P. Warneck, in Chemistry of the Natural Atmosphere, International Geophys. Series, Vol. 41, Academic Press 1988
11. R. P. Wayne, in Chemistry of Atmospheres, 2nd edition, Clarendon Press, Oxford 1991
12. P. Warneck, in Low Temperature Chemistry of the Atmosphere, Ed. G. K. Moortgat, NATO ASI Series, Vol. I 21, 1994
13. R. C. Easter and P. V. Hobbs, *J. Atmos. Sci.*, 1974, **31**, 1586
14. S. N. Pandis, A. S. Wexler and J. H. Seinfeld, *J. Phys. Chem.*, 1995, **99**, 9646
15. C. E. Junge, in The Modification of Aerosol Size Distribution in the Atmosphere, Final Tech. Report, Contract Da 91-591,EVC 2979, European Research Office, U. S. Army 1964
16. J. H. Topalian and D. C. Montague, *J. Atmos. Chem.*, 1989, **8**, 19
17. J. Lelieveld and P. J. Crutzen, *J. Atmos. Chem.*, 1991, **12**, 229

18. J. A. Gardner, L. R. Watson, Y. G. Adewuyi, P. Davidovits, M. S. Zahniser, D. R. Worsnop and C. E. Kolb, *J. Geophys. Res.*, 1987, **92**, 10887
19. I. N. Tang and J. H. Lee, in The Chemistry of Acid Rain, Ed. R. W. Johnson, G. E. Gordon, W. Calkins and A. Z. Elzerman, American Chemical Society, Washington D. C. 1987
20. L. R. Martin and D. E. Damschen, *Atmos. Environ.*, 1981, **15**, 1617
21. E. A. Betterton and M. R. Hoffmann, *Environ. Sci. Technol.*, 1988, **22**, 1415
22. M. R. Hoffmann, in Aerosol and Aqueous-Phase Chemistry, Oak Ridge, Tennessee 1986
23. W. L. Chameides, *J. Geophys. Res.*, 1984, **89**, 4739
24. E. Wilhelm, R. Battino and R. J. Wilcock, *Chem. Rev.*, 1977, **77**, 219
25. A. G. Clarke and M. Radojevic, *Atmos. Environ.*, 1987, **21**, 1115
26. M. Radojevic, B. J. Tyler, A. J. Wicks, M. J. Gray and T. W. Choularton, *Atmos. Environ.*, 1990, **24A**, 323
27. H. W. Georgii and D. Wotzel, *J. Geophys. Res.*, 1970, **75**, 1727
28. N. A. Esmen and R. B. Fergus, *Sci. Total Environ.*, 1976, **6**, 223
29. Committee on Aldehydes, in Formaldehyde and Other Aldehydes, Board on Toxicology and Environmental Health Hazards, Assembly of Life Sciences, National Research Council, National Academy Press, Washington D. C. 1981
30. U. Diester, R. Neeb, G. Helas and P. Warneck, *J. Phys. Chem.*, 1986, **90**, 3213
31. G. L. Kok, S. N. Gitlin and A. L. Lazrus, *J. Geophys. Res.*, 1986, **91**, 2801
32. J. Hoigne, H. Bader, W. R. Haag and J. Staehlin, *Water Res.*, 1985, **19**, 993
33. P. Warneck, *Fresenius J. Anal. Chem.*, 1991, **340**, 585
34. L. R. Martin, in Acid Precipitating Series, Ed. J. G. Calvert, Butterworth, Boston 1984
35. J. W. Munger, D. J. Jacob and M. R. Hoffmann, *J. Atmos. Chem.*, 1984, **1**, 335

36. C. C. Ang, F. Lipari and S. J. Swarin, *Environ. Sci. Technol.*, 1987, **21**, 102
37. R. J. Charleson, J. E. Lovelock, M. O. Andraea and S. G. Warren, *Nature*, 1987, **326**, 655
38. D. L. Baulch, R. A. Cox, R. F. Hampson, J. A. Kerr, J. Troe and R. T. Watson, *J. Phys. Chem. Ref. Data*, 1980, **9**, 295
39. R. A. Cox and D. Sheppard, *Nature*, 1980, **284**, 330
40. I. Barnes, V. Bastian, K. H. Becker and E. H. Fink, in Physico-chemical Behaviour of Atmospheric Pollutants, Ed. B. Versine and G. Angeletti, *Pro. Eur. Symp. 3rd*, Varese, Italy 1984
41. G. Black, *J. Chem. Phys.*, 1984, **80**, 1103
42. S. A. Penkett, *Natural Phys. Sci.*, 1972, **240**, 105
43. S. A. Penkett, B. M. R. Jones, K. A. Brice and A. E. J. Eggleton, *Atmos. Environ.*, 1979, **13**, 323
44. H. J. Maahs, *J. Geophys. Res.*, 1983, **88**, 10721
45. M. R. Hoffmann and J. O. Edwards, *J. Phys. Chem.*, 1975, **79**, 2096
46. S. M. Kunen, A. L. Lazrus, G. L. Kok and B. G. Heikes, *J. Geophys. Res.*, 1983, **88**, 3671
47. J. V. McArdle and M. R. Hoffmann, *J. Phys. Chem.*, 1983, **87**, 5627
48. L. R. Martin, in SO_2, NO and NO_2 Oxidation Mechanisms : Atmospheric Considerations, Acid Precipitation Series, Vol. 3, Butterworth, Boston 1984
49. R. E. Huie and N. C. Peterson, *Adv. Environ. Sci. Tech.*, 1983, **12**, 117
50. M. R. Hoffmann and S. D. Boyce, *Adv. Environ. Sci. Tech.*, 1983, **12**, 148
51. U. Diester and P. Warneck, *J. Phys. Chem.*, 1990, **94**, 2191
52. G. V. Buxton, S. McGowan, G. A. Salmon, J. E. Williams and N. D. Wood, *Atmos. Environ.*, 1995, **30**, 2483
53. P. Warneck and J. Ziajka, *Ber. Bunsenges. Phys. Chem.*, 1995, **99**, 59
54. M. Exner, H. Herrmann and R. Zellner, *Ber. Bunsenges. Phys. Chem.*, 1992, **96**, 470
55. G. A. Salmon, in Proceedings of the 6th European Symposium, Ed. G. Angeletti and G. Restelli, European Commission, Luxembourg 1993

56. S. E. Schwarz, *J. Geophys. Res.*, 1984, **89**, 11589
57. D. Behar, G. Czapski, J. Rabani, L. M. Dorfman and H. A. Schwarz, *J. Phys. Chem.*, 1970, **74**, 3209
58. C. J. Weschler, M. L. Mandich and T. E. Graedel, *J. Geophys. Res.*, 1986, **91**, 5189
59. T. E. Graedel, M. L. Mandich and C. J. Weschler, *J. Geophys. Res.*, 1986, **91**, 5205
60. J. W. T. Spinks and R. J. Woods, in An Introduction to Radiation Chemistry, John Wiley and Sons Inc., New York 1964
61. H. A. Bethe and J. Askin, in Experimental Nuclear Physics, ed. E. Segre, Wiley, New York 1953
62. G. V. Buxton, in Radiation Chemistry, in Principles and Applications, ed. Farhataziz and M. A. J. Rodgers, VCH Publishers, New York 1987
63. H. A. Schwarz, *J. Phys. Chem.*, 1969, **73**, 1928
64. H. A. Schwarz, *J. Chem. Edu.*, 1981, **58**, 101
65. A. K. Pikaev, in Pulse Radiolysis of Water and Aqueous Solutions, ed. E. Hart, Indiana University Press 1967
66. D. M. Stanbury, *Adv. Inorg. Chem.*, 1989, **3**, 69
67. A. B. Ross, W. G. Mallard, W. P. Helman, G. V. Buxton, R. E. Huie and P. Neta, NDRL - NIST Solution Kinetics Database ver. 3.0, NIST Standard Ref. Data, Gaithersburg, MD 1998
68. J. A. Barltrop and J. D. Coyle, in Principles of Photochemistry, John Wiley and Sons, New York 1975
69. Y. Tang, R. P. Thorn, R. L. Maudlin and P. H. Wine, *J. Photochem. Photobiol. A*, 1988, **44**, 243

Chapter 2

Experimental Techniques

2.1.1. Experimental

2.1.2. Pulse Radiolysis

This thesis contains a brief description of the pulse radiolysis facility. A more detailed description of the system and techniques used can be found elsewhere.[1,2,3] A diagram of the pulse radiolysis system used in this study is shown in Figure 2.1.

2.1.3. Van de Graaff Accelerator & Electron Beam Transport

A 3 MeV Van de Graaff accelerator (High Voltage Engineering Corporation, Model KS 3000) was used in all pulse radiolysis experiments and was operated at a terminal voltage of 2.5 MeV. This is the optimum voltage for the balance between performance and component lifetime. The accelerator was used in single pulse mode and each pulse could be varied in length over the range 5 ns to 2 μs.

The electron beam passed along an evacuated flight tube to the irradiation cell. It was directed and aligned by a series of electromagnets and was passed through a secondary emission chamber (S.E.C.), from which a measure of the pulse energy was obtained. The S.E.C. consists of three aluminium foils and was mounted just before the final exit window. When the electron beam passed through the chamber secondary electrons were ejected from the foils. By polarising the outer foils (+ve) with respect to the central one the emitted electrons from the latter were captured and the charge measured. The charge was then converted across a capacitor into a voltage reading.

Figure 2.1 *A schematic diagram of the pulse radiolysis set-up.*

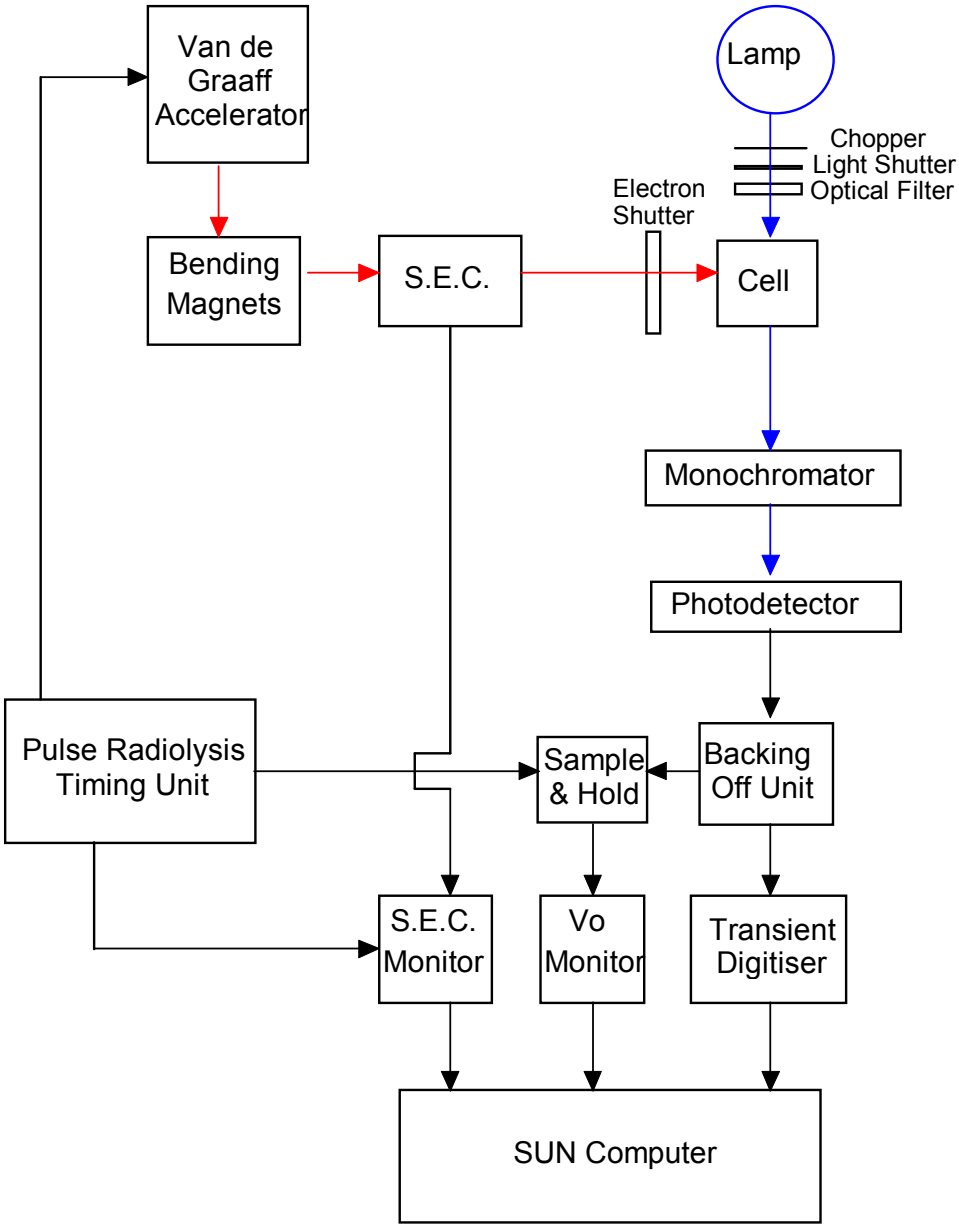

Figure 2.2 *Pulse radiolysis flow system.*

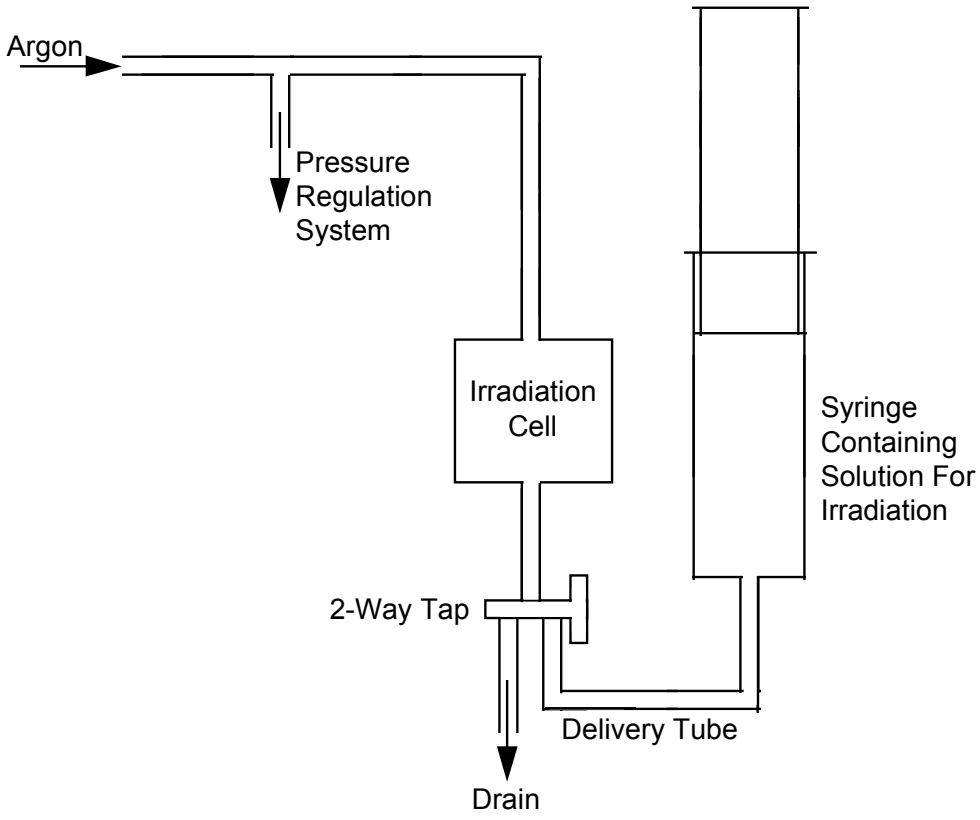

2.1.4. Flow System

The optical pulse radiolysis flow system used in this study centred around the cell, which had either a 2.5 cm or 1.0 cm path length. Also used was a 2 cm multipass cell with optical pathlength 7 cm. The cell was mounted at a distance of 40 mm for the 2.5 cm and multipass cells or 10 mm for the 1.0 cm cell. The gap between the cell and the end of the flight tube ensured uniform radiation of the cell. The cell was filled with solution from a reservoir glass syringe and kept under an inert atmosphere of argon. A diagram of the standard flow system is shown in Figure 2.2.

The temperature could be controlled using the variable temperature apparatus. Figure 2.3 shows a schematic diagram of the variable temperature cell.

Figure 2.3 *Variable temperature pulse radiolysis cell and cell holder.*

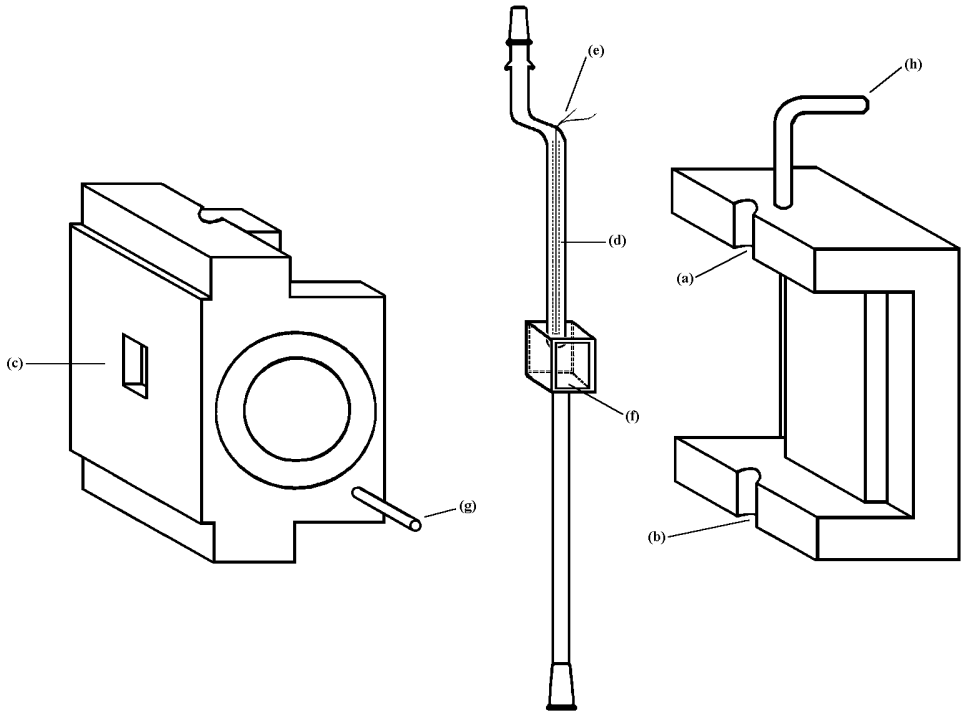

(a) and (b) Holes in which the cell is clamped

(c) Window of thin aluminium foil

(d) Pyrex glass envelope

(e) Thermocouple (g) Gas inlet

(f) Optical cell (h) Gas outlet

The enclosure is made from insulating plastic.

This apparatus was used with the 1.0 cm optical pathlength cell and was generally employed to determine the activation energy for a reaction. The temperature was varied by flowing nitrogen around the cell within the plastic enclosure. The nitrogen was passed through a heat exchange coil which was surrounded by dry ice (solid CO_2) in order to decrease the cell temperature. If an increase in temperature was required then the nitrogen was passed through

an in-line heating element which was adjusted by varying an applied voltage. A thermocouple enclosed within a glass capillary tube was used to measure the temperature within the cell.

2.1.5. Rapid Mix Apparatus

The rapid mix apparatus (R.M.A.), shown in Figure 2.4, allowed two solutions to be mixed together in the radiolysis cell seconds before the electron pulse was delivered.[4] This apparatus minimises any possible thermal reactions between species in the system being studied. The delay on the R.M.A. could be varied so that the time between mixing and irradiation was between 0 and 10 seconds. This delay followed the 1.5 s required for the mechanical action of mixing. Therefore a delay time of 0 s corresponds to firing a pulse 1.5 s after mixing is initiated. The cell in the R.M.A. was filled by the action of a compressed air driven piston on two injection syringes which forced the solutions together and ensured thorough mixing. The signal to inject was sent remotely from a computer which also allowed for the programmed delay before firing the electron pulse.

It was possible to heat one of the solutions within the R.M.A. by using a heating block surrounding one of the injection syringes. The solution with the highest thermal stability was heated in order to minimise thermal decomposition. A thermocouple was placed inside the heating block to measure the temperature of the solution prior to mixing, and another was placed inside the cell to measure the temperature after mixing and when the pulse was delivered.

Figure 2.4 *A schematic diagram of the rapid mix apparatus.*

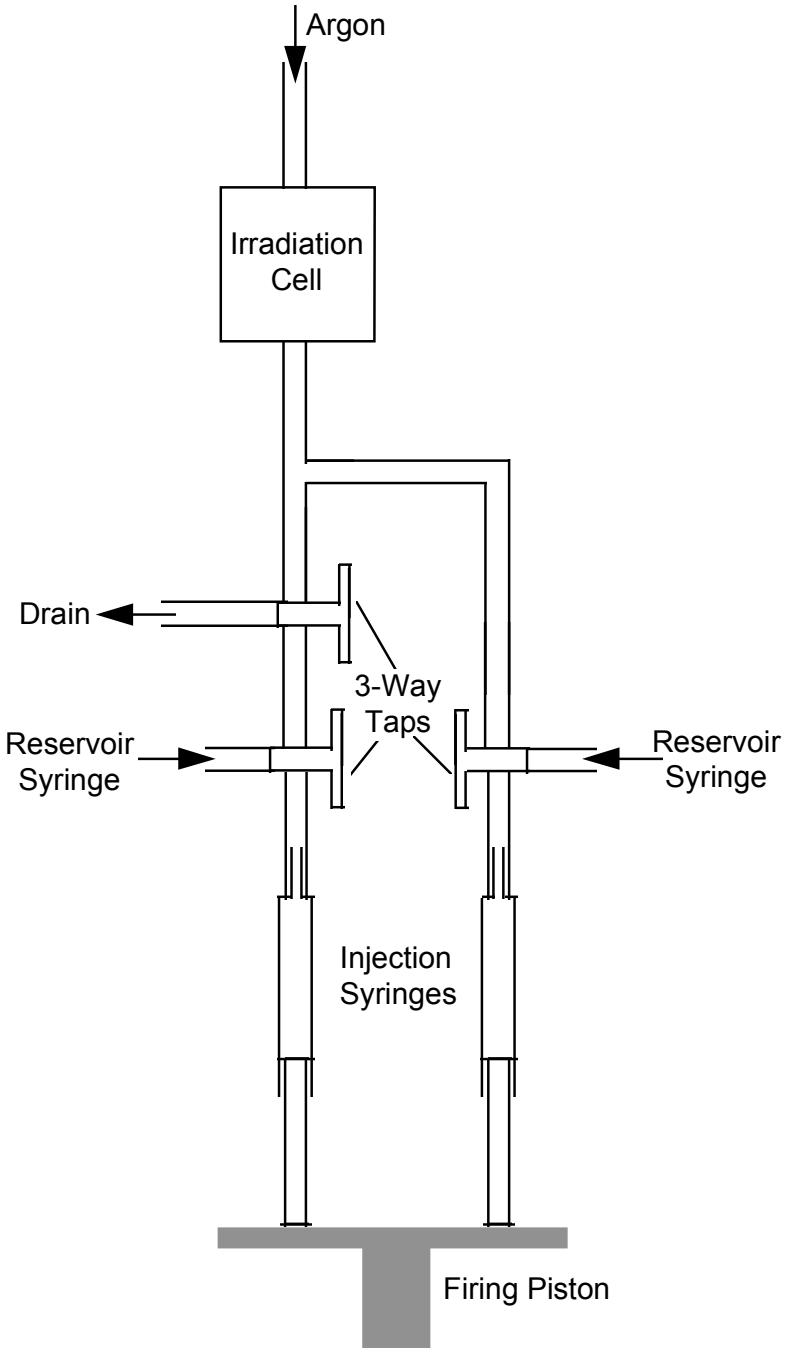

Figure 2.5 *A schematic diagram of the laser flash photolysis set-up.*

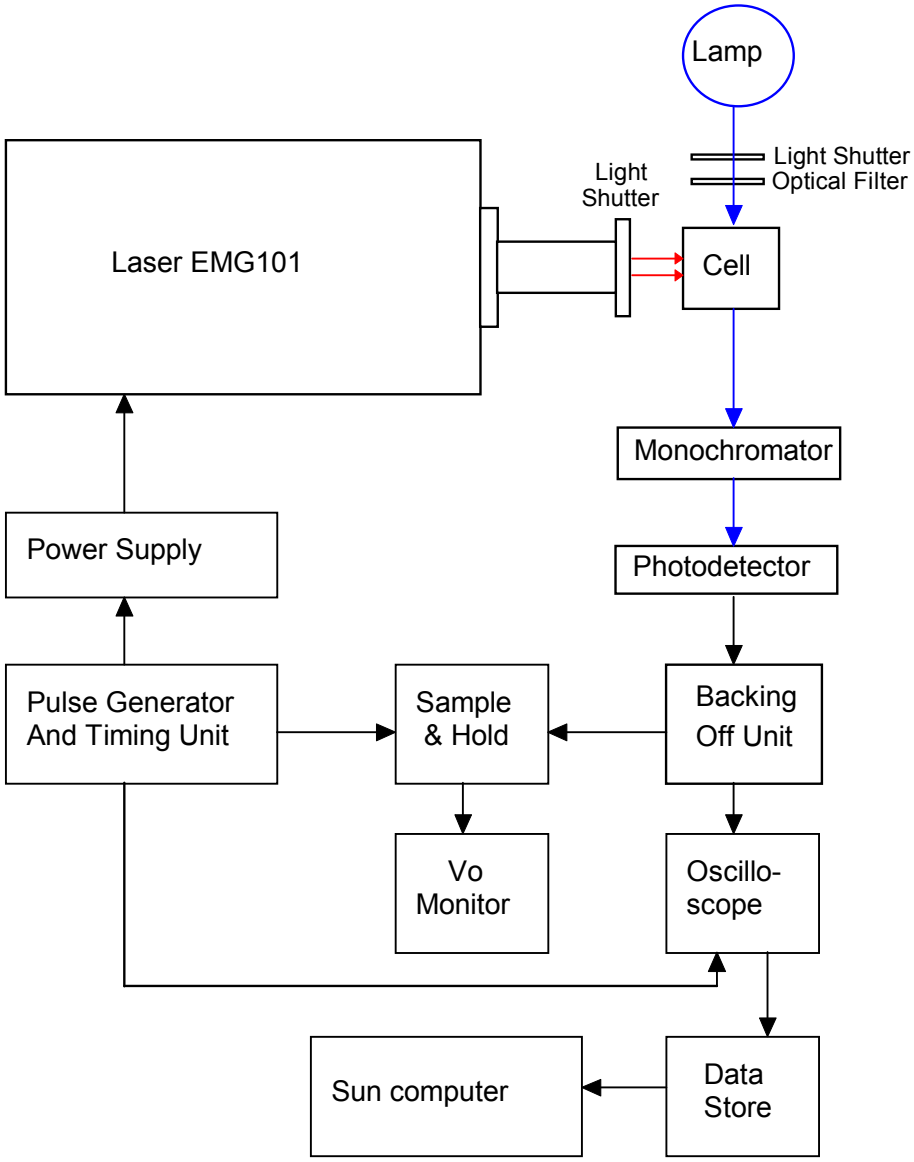

2.1.6. Laser Flash Photolysis

This thesis contains a brief description of the laser flash photolysis facility. A more detailed description of the system can be found elsewhere.[5,6,7] A schematic diagram of the laser flash photolysis system used in this study is shown in Figure 2.5.

Figure 2.6 *Laser flash photolysis flow system.*

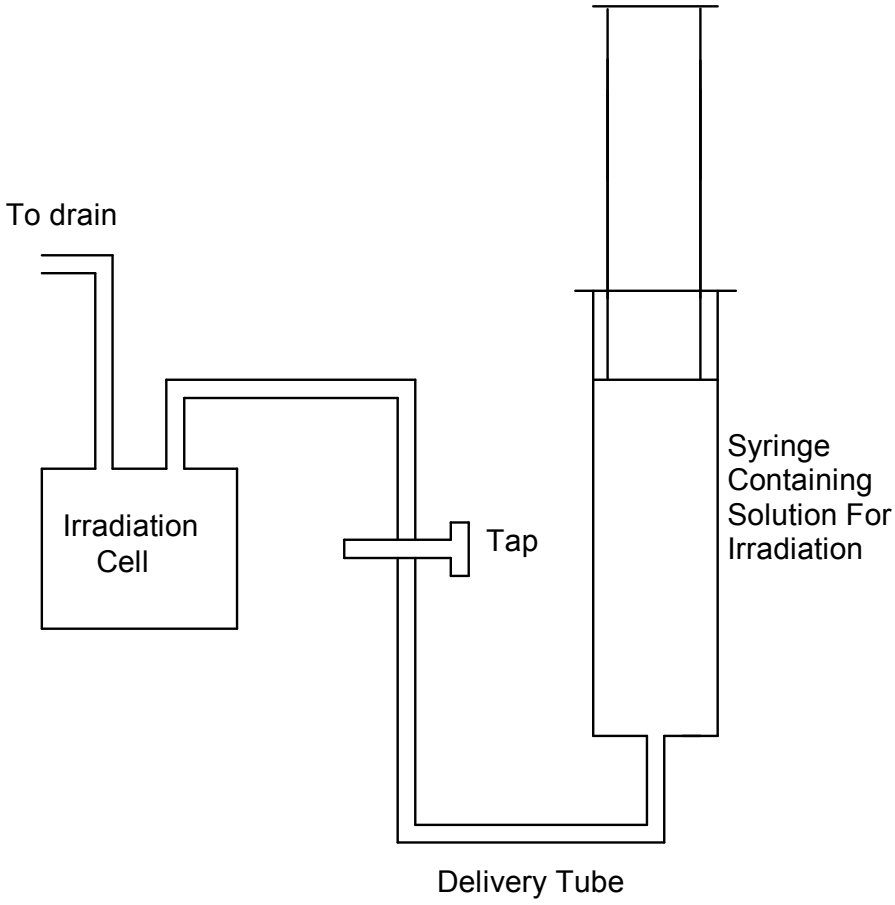

2.1.7. Laser System

The excimer laser (Physik Multigas laser EMG 101) was operated in single flash mode using irradiation wavelengths of 193 nm (ArF) and 248 nm (KrF). The optimum pulse energies at these wavelengths were 200 and 250 mJ, which were delivered in pulses of half-width 14 and 16 ns. Discharge voltages of between 25 and 32 kV were used. This allowed the pulse energy to be varied over a factor of *ca*. five and hence the radical yields could be reasonably well controlled.

2.1.8. Flow System

The laser flash photolysis flow system used in this study made use of a cell with optical path length of 1.0 cm and photolysis path length of 0.4 cm. The

cell was mounted at a distance of 30 cm from the exit window of the laser, which ensured uniform radiation. The cell was filled with solution from a reservoir glass syringe as shown in Figure 2.6. The temperature of the solution was controlled by immersing the syringe in a water bath and circulating water around the cell mountings. Allowing *ca*. 10 min. for thermal equilibration, this arrangement kept the temperature of solution in the cell within 2 ºC of that of the water bath. The temperature of the water bath was varied between 5 and 35 ºC using dry ice or a heater element as appropriate.

2.1.9. Analysing Light Sources

The choice of analysing light source was dependent on the chemical system being studied. The timescale of the reactions and the observation wavelength formed the basis for this choice. There are 3 lamps available and they complement each other to ensure full coverage for timescales from *ca*. 250 ns to 160 s over the spectral range 220 to 750 nm. For most experiments a xenon arc lamp (Wotan XB0 150/4, 150 or 250 W) was most suitable because of its wide spectral output range (230 to 750 nm). The lamp was operated in two modes, flashed- or normal-mode. In flashed-mode the lamp current was briefly (20 ms) increased from 14 A to 300 A for the 250 W lamp or from 7 A to 100 A for the 150 W lamp to produce an intense flash of light which was stable up to 200 μs.

In the pulse radiolysis system, the light beam was chopped by a rotating sector disc in order to prevent fatigue of the detectors and also to provide a trigger for the electron pulse. In normal-mode, without the flash circuit operating, the xenon lamp was restricted to time scales up to 500 μs due to arc instability. The tungsten lamp (Tungstram 150 W) also has a broad spectral range, 350 to 750 nm. It is a filament lamp and is therefore stable over longer periods of time than the xenon lamp. The deuterium lamp (Cathodean U.V. source R03) was used to observe long-lived intermediates which absorb in the U.V. region. It is also stable on long timescales but can only be used from 220 to 450 nm.

2.1.10. Optics

All of the lenses used in the optical system were made of quartz so that transmission was ensured in the U.V., visible and I.R. regions. The optical components were arranged so that a parallel sided beam passed through the radiolysis cell, and an image of the source was focused on the entrance slits of the monochromator. All optical components were adjusted daily to obtain the maximum possible light intensity and therefore the highest signal to noise ratio. A frequency-specific optical filter was placed across the light beam before the irradiation cell to reduce scattered light and minimise possible photolysis of the solution. These filters were chosen from a range of Chance Pilkington filters or a Ni/Co filter.

2.1.11. Monochromators and Detectors

The observation wavelength was selected by passing the light beam through one of two Bausch and Lomb high intensity grating monochromators. The U.V. (200 to 400 nm) and the visible (350 to 800 nm) monochromators covered all of the wavelengths used in this study. The monochromators were calibrated and checked regularly. The bandwidth used in all experiments was at or below a maximum of 10 nm. The light was converted to an electrical signal by a photodetector. In this study two detectors have been employed. An E.M.I. 9781B photomultiplier was used most frequently and was suitable for the wavelength range 200 to 600 nm. This photomultiplier was generally used in conjunction with a xenon lamp. If the xenon lamp was operated in flashed-mode then the photomultiplier used 2 dynodes and a fixed gain electronic amplifier. If the xenon lamp was operated in normal-mode then the photomultiplier used 4 or 5 dynodes and a variable gain amplifier. The latter set-up was also used when the deuterium or tungsten lamps were in operation.

2.2.1. Signal Processing

When the light had been converted to an electrical signal it was backed-off. Backing-off involves assigning to the V_o (light) level an absorbance of zero and inverting the trace so that log (V_S/V_o) becomes positive for an absorbance, where V_s is the signal voltage from the photomultiplier.[4] In this way, variations

in the light intensity are converted to absorbance readings. The electronic circuits used varied depending on the detector and light source in operation. The output following backing-off was in the form of an analogue signal and it was transferred to a transient digitiser (Gould 4072 oscilloscope), which converted it into a digital 1024 point data stream. The data stream was passed from the digitiser to a SUN Microsystems Sparcstation IPC where it was stored by CAPTURE as a 256 point data stream.[8] The data stream was reduced from 1024 to 256 points either by averaging four consecutive points or by recording only every fourth point. Stored along with the data stream were other parameters including the light level (V_o), pulse magnitude V(S.E.C.), wavelength and the absorbance at a selected time on the trace.

2.2.2. Data Analysis

In this study two software packages were used to analyse the kinetic absorbance-time traces, TREAT and FACSIMILE.

TREAT

TREAT[9] was used for traces which were to be analysed by simple first- or second-order kinetics. Rate constants and absorbances at specific times were obtained easily with this package. The mathematics which underlie this program are described in detail elsewhere.[10]

FACSIMILE

FACSIMILE[11] was used to analyse traces when the kinetics were more complex, and was also used to run simulations. FACSIMILE utilises a FORTRAN numerical integration program into which is placed the relevant and available kinetic data and a predicted mechanism. All of the unknown parameters, usually rate constants and absorption coefficients, were inserted as variables and varied until the most statistically significant set of values was obtained. The output was displayed graphically by FACSGRAF.[12]

2.2.3. Dosimetry

The S.E.C. meter was calibrated daily by a chemical dosimeter in terms of an absorbed dose per volt registered by the S.E.C. meter. Chemical dosimeters

have well defined Gε values when optical detection is employed, where Gε is the product of the G-value and the molar absorption coefficient, ε.[13]

2.2.4. Dosimetry by Optical Detection

When observing reactions using the flashed Xe lamp, an oxygen saturated solution containing 10^{-2} mol dm^{-3} potassium thiocyanate (KSCN) was used as the dosimeter, where $G\varepsilon[(SCN)_2\cdot^-]$ was taken to be 2.59×10^{-4} m^2 J^{-1} at 475 nm with a 10 nm bandwidth.[14] The formation of the $(SCN)_2\cdot^-$ radical occurs via the formation of (SCN)·, which rapidly combines with a thiocyanate ion, and is summarised in reaction (2.1).

$$\cdot OH + 2\ SCN^- \rightarrow (SCN)_2\cdot^- + OH^- \qquad (2.1)$$

The sensitivity of the S.E.C. meter was calculated from equation [2.1],

$$\text{Sensitivity / Gy V}^{-1} = \frac{(\text{OD / V})_{\text{dosimeter}}}{(G\varepsilon)_{\text{dosimeter}} \times l} \qquad [2.1]$$

where l is the optical path length of the cell in mm and $(\text{OD / V})_{\text{dosimeter}}$ is the optical density of the dosimeter per volt on the S.E.C. meter.

2.2.5. Calculation of Gε

Gε values of the transient species produced by irradiation may be calculated from equation [2.2], using the dosimeter value for the optical density per volt.

$$(G\varepsilon)_{\text{sample}} = \frac{(\text{OD / V})_{\text{sample}} \times (G\varepsilon)_{\text{dosimeter}}}{(\text{OD / V})_{\text{dosimeter}}} \qquad [2.2]$$

2.3.1. Materials and pH Measurements

Fluka supplied $Na_2S_2O_8$ (MicroSelect grade) and chloroacetone (further purified, see Section 2.3.3). All other chemicals used in this study were of AnalaR grade (BDH) or better and used as received. All solutions were prepared using distilled water which had been further purified and deionised by filtration (Millipore MilliQ organic free system, 18 MΩ cm resistivity or

higher). Gases (argon, nitrous oxide and oxygen) received from BOC were used to saturate the solutions. They were of the highest purity available and taken straight from the cylinder. The pH of the solutions was measured using a pH meter (Hanna HI 8314 membrane) which was calibrated daily using buffer solutions at pH 4.0, 7.0 and 9.2 (BDH reagent grade). The desired pH of the solution was obtained by the addition of $HClO_4$ or NaOH.

2.3.2. Preparation of Formaldehyde

Aqueous formaldehyde was prepared by the method outlined in Ref. 15. Briefly, argon was passed over heated paraformaldehye and bubbled through MilliQ water for *ca*. 1 hr. The concentration of formaldehyde was determined by its oxidation to formic acid using H_2O_2, followed by titration with NaOH.

2.3.3. Purification of Chloroacetone

Chloroacetone (Fluka) contains 5 % impurities, including *ca*. 1 % mesityl oxide,[16] $(CH_3)_2C{=}CHCOCH_3$, which has a maximum ε(245 nm) = 11 500 dm^3 mol^{-1} cm^{-1} in comparison to that of chloroacetone of ε(267 nm) = 18.2 dm^3 mol^{-1} cm^{-1}.[17,18] At this level of impurity, the majority of the 248 nm light was absorbed by mesityl oxide, forming a species with a large absorption centred at 270 nm. The chloroacetone was purified of mesityl oxide by oxidising the unsaturated carbon bond to a gem-diol using $KMnO_4$ and distillation.[19]

15 g $KMnO_4$ were dissolved in 150 ml water and cooled to < 4 ºC. 150 ml of chloroacetone at < 4 ºC were added and thoroughly mixed. When no further reaction was observed, 300 ml diethyl ether were added followed by further mixing. After leaving to settle for 30 min. the ether layer was extracted and transferred to 100 ml water in order to wash out any water soluble impurities, e.g. ions, organic acids. This was repeated twice. Upon separation the ether layer was warmed to boil off the ether, adding $CaCl_2$ to remove any residual water. The remaining liquid was filtered and distilled, discarding the first and last thirds of the distillate. The final product was a 50 ml yield of colourless liquid with the boiling point and spectrum of chloroacetone.

Figure 2.7 *Apparatus for degassing and saturation.*

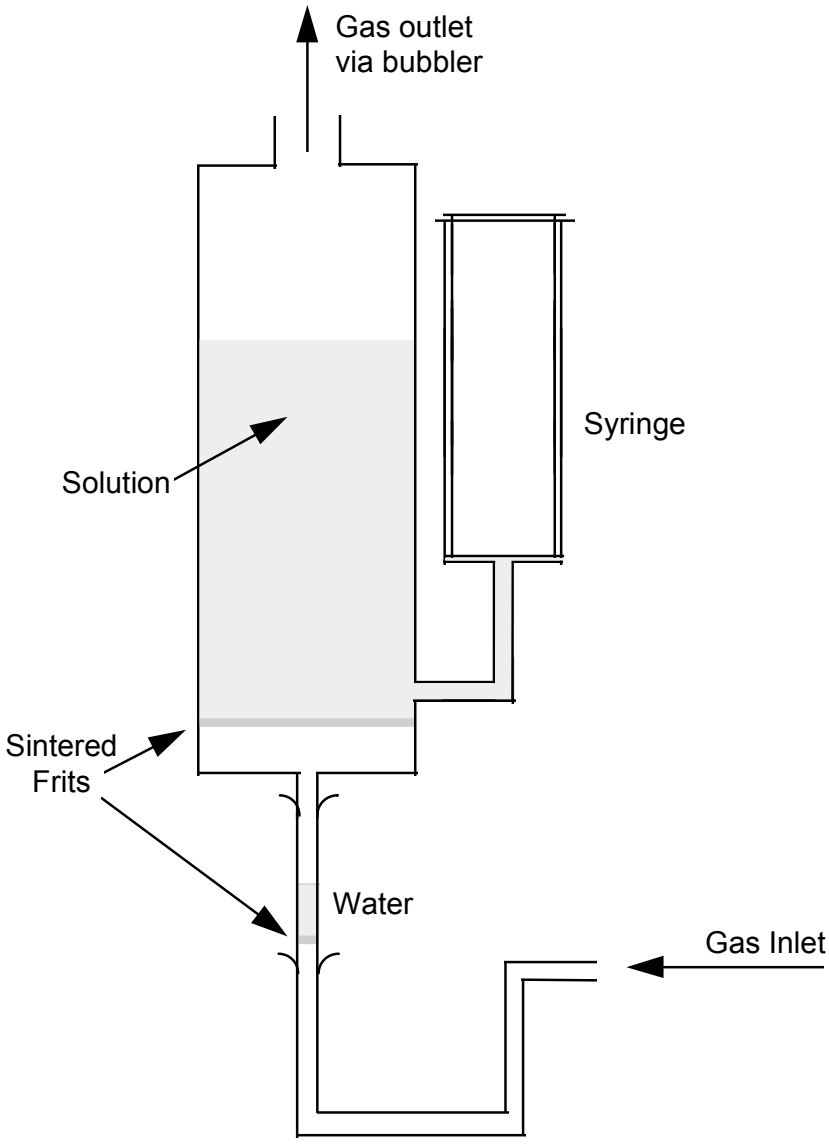

2.3.4. Deaeration and Saturation of Solutions

Solutions were deaerated by bubbling with argon or saturated with an appropriate gas prior to each irradiation session by using the syringe bubbler technique.[20] The apparatus for this technique is shown in Figure 2.7. The solution in the side arm of the bubbler was saturated by partially filling the

syringe with solution several times during the saturation period. After bubbling the solution for *ca*. 30 min. the syringe was filled and capped.

2.3.5. Cleaning of Glassware

In the majority of experiments the glassware was cleaned by the MICRO method. The glassware was soaked in a 2 % MICRO solution (International Products Corporation), and thoroughly rinsed with tap water before being rinsed with distilled water and then purified and deionised water. The permanganic acid cleaning method was used on new glassware and on glassware to be used with new chemicals. The permanganic acid method involved rinsing the glassware, as follows. Concentrated H_2SO_4 (containing a few grains of $KMnO_4$) was applied to the glassware for several minutes and rinsed off with distilled water. A mixture of 0.7 mol dm^{-3} HNO_3 and 3×10^{-3} mol dm^{-3} H_2O_2 was used to rinse away any residue. Finally the glassware was rinsed with distilled and then purified and deionised water.

2.4.1. References

1. J. W. T. Spinks and R. J. Woods, in An Introduction to Radiation Chemistry, 2nd Edition, John Wiley & Co. Ltd., New York 1976
2. G. A. Salmon and A. G. Sykes, in Methods in Enzymology, 227, Eds. J. F. Riordan and B. L. Vallee, 522, Academic Press 1992
3. T. J. Kemp, J. P. Roberts, G. A. Salmon and G. F. Thompson, *J. Phys. Chem.*, 1968, **72**, 1464
4. C. Kilner and S. R. Watkins, in Procedures for Operating the Van de Graaff Accelerator and Associated Equipment, C.R.R.C. 1988
5. Manual for the Lambda-Physik Excimer Laser EMG 101, Lambda Physik, Gottingen, Germany 1980
6. C. Kilner, in Procedures for Operating the Laser Flash Photolysis Facility and Associated Equipment, C.R.R.C. 1995
7. W. J. McElroy and S. J. Waygood, *J. Chem. Soc.*, *Faraday Trans.*, 1990, **86**, 2557
8. F. Wilkinson, CAPTURE Users' Manual, C.R.R.C. 1987
9. F. Wilkinson, TREAT Users' Manual, C.R.R.C. 1988
10. K. Laidler, in Chemical Kinetics, 3rd Edition, Pub. Harper Collins 1987
11. A. R. Curtis and W. P. Sweetenham, FACSIMILE/CHECKMAT Users' Manual, 1987, U.K.A.E.A., AERE R 12805
12. F. Wilkinson, FACSGRAF Ver. 6.0, C.R.R.C. 1996
13. E. M. Fielden, in The Dosimetry of Pulsed Radiation, International Commission on Radiation Units & Measurements, Report 34, Section 3, Washington, August 1982
14. G. V. Buxton and C. R. Stuart, *J. Chem. Soc., Faraday Trans*., 1995, **91**, 279
15. W. J. McElroy and S. J. Waygood, *J. Chem. Soc.*, *Faraday Trans.*, 1991, **87**, 1513
16. Fluka Technical Service, private communication
17. The Sadtler Handbook of Ultraviolet Spectra, Editor W. W. Simons, Heydon and Sons Ltd. Publishers, London 1979

18. P. Greenzaid, Z. Rappoport and D. Samual, *J. Chem. Soc.*, *Faraday Trans.*, 1967, **63**, 2131
19. J. McMurry, in Organic Chemistry, 3rd Ed., Brooks/Cole Publishing Co., California 1992
20. S. Gordon, E. J. Hart, M. S. Matheson, J. Rabani and J. K. Thomas, *Discuss. Faraday Soc.*, 1963, **36**, 193

Chapter 3

The Equilibrium $Cl^{\cdot} + Cl^{-} \leftrightarrow Cl_2^{\cdot -}$

3.1. Introduction

The equilibrium constant $K_{3.1}$ for reaction (3.1) is not well established. Literature values[1,2,3] are 17.7, 4700 and 1.9×10^5 dm^3 mol^{-1}. The rate constant of the forward reaction has been measured[4,5,6] to be 6.5×10^9, 8×10^9 and 1.9×10^{10} dm^3 mol^{-1} s^{-1}.

$$Cl\cdot + Cl^- \leftrightarrow Cl_2\cdot^- \quad (3.1)$$

In addition to the uncertainty regarding $K_{3.1}$, the kinetics of the reactions of $Cl\cdot$ and $Cl_2\cdot^-$ in aqueous solution have not been satisfactorily resolved. There have been reports of purely second-order,[1,7] largely first-order[2,8] and mixed first- and second-order[9] decays under similar experimental conditions. Rate constants for the second-order component range[1,10] from 7×10^7 to 2×10^{10} dm^3 mol^{-1} s^{-1} and are attributed to reactions (3.2a, b and c).

$$Cl\cdot + Cl\cdot \rightarrow Cl_2 \quad (3.2a)$$

$$Cl\cdot + Cl_2\cdot^- \rightarrow Cl_2 + Cl^- \quad (3.2b)$$

$$Cl_2\cdot^- + Cl_2\cdot^- \rightarrow Cl_2 + 2\,Cl^- \quad (3.2c)$$

From this evidence, it is apparent that the stability constant of $Cl_2\cdot^-$, equilibrium (3.1), and the fate of $Cl\cdot$ and $Cl_2\cdot^-$ in aqueous solution are in need of further investigation. This work aims to establish a reliable value for the stability constant of $Cl_2\cdot^-$ which is an essential prerequisite for detailed investigations into the reactivity of $Cl\cdot$ in aqueous solution, particularly in respect of the reactions likely to be important in cloud droplets and aerosols.

3.2. Experimental Approach

Experiments were performed using either laser flash photolysis or pulse radiolysis to produce $Cl\cdot$ atoms, which, in the presence of excess chloride, react to form $Cl_2\cdot^-$ by equilibrium (3.1). The former set of experiments were employed to obtain a value for the forward rate of equilibrium (3.1) by fitting

to a linear rate law the dependence of the rate of growth of $Cl_2\cdot^-$ on $[Cl^-]$. The latter were used to determine the reverse rate constant of equilibrium (3.1) by fitting to the appropriate rate law the non-linear rate of decay of $Cl_2\cdot^-$ with [t-BuOH]. The two rate laws, linear and non-linear, derived in Appendix 1 are extensions of widely-used expressions for the approach to equilibrium and the decay once equilibrium has been attained, respectively, to kinetic schemes in which significant reactions leading to a loss of yield occur.

3.3. Determination of k_1 by Laser Flash Photolysis

Laser flash photolysis (193 nm) of the chloride ion, reaction (3.3), was used to form chlorine atoms[11,12] in order to investigate the reaction of Cl· with chloride.

$$Cl^- + h\nu \rightarrow Cl\cdot + e^-_{aq} \qquad (3.3)$$

To confirm the high literature rate constants reported for this reaction, the growth of absorbance at 340 nm was observed following 193 nm laser photolysis of argon-saturated solutions containing chloride, with no added electron scavenger. A typical trace is shown in Figure 3.1. The first 50 ns of the traces from the onset of the flash were affected by the finite pulse length, the rise-time of the detection circuit and a short-lived interference, and were deleted before analysis. The growth of absorption obeyed first-order kinetics with k_{obs} proportional to $[Cl^-]$, see Figure 3.2, in accordance with the expected rate law for the approach to equilibrium, equation [A1.7], see Appendix 1.

$$k_{obs} \approx k_f + k_b + k_{loss} = k_{3.1}[Cl^-] + k_{-3.1} + k_{3.7} + k_{3.8} \qquad [A1.7]$$

The slope of the plot of k_{obs} *vs* $[Cl^-]$ yields $k_{3.1} = (8.5 \pm 0.7) \times 10^9$ dm^3 mol^{-1} s^{-1} in good agreement with the value obtained by Nagarajan and Fessenden,[5] who employed a different experimental method. The intercept of $(5 \pm 8) \times 10^5$ s^{-1} indicates that the rate of the back reaction and other reactions involving Cl· and $Cl_2\cdot^-$ are slow in comparison with the forward rate of equilibrium (3.1).

Figure 3.1 *The absorbance at 340 nm following 193 nm laser flash photolysis of an Ar-sat. solution containing [Cl⁻] = 10^{-3} mol dm^{-3} at pH ca. 6. The red line is a fitted first-order growth.*

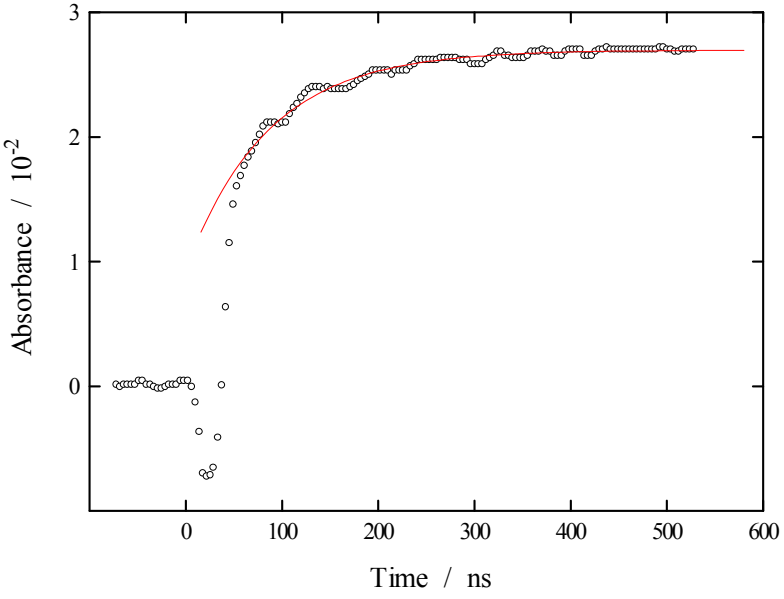

Figure 3.2 *Effect of [Cl⁻] on k_{obs} for the first-order formation of $Cl_2^{\cdot -}$. Error bars are ± 1 S.D.*

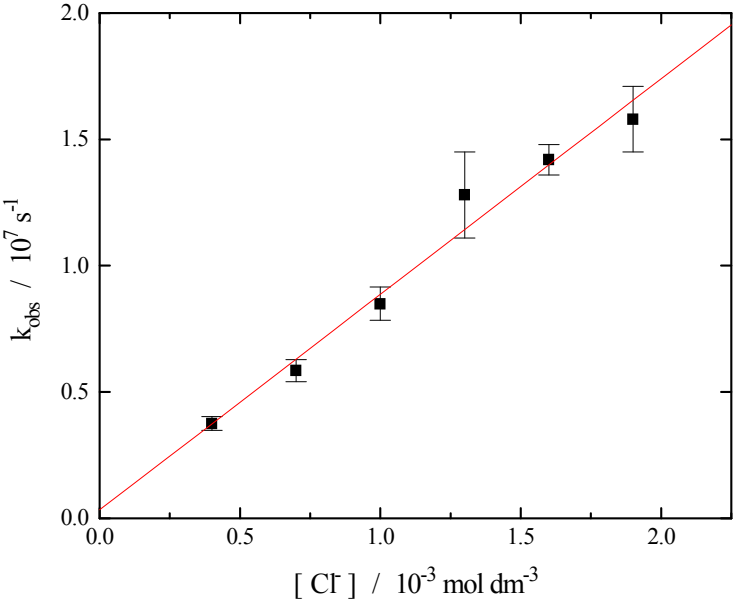

3.4. Absorption Coefficient of Cl·

An estimate of the molar absorption coefficient of Cl· at 340 nm was obtained by extrapolating the growth of absorption back to the mid-point of the photolysing flash and comparing this absorbance with that of the hydrated electron also formed in reaction (3.3), the decay of which was negligible over 500 ns. The absorption at 340 nm generated during the flash has contributions due to Cl· and e^-_{aq}. Taking $\varepsilon(e^-_{aq})$ at 720 and 340 nm as 1.9×10^4 and 1100 dm^3 mol^{-1} cm^{-1}, respectively,[13] $\varepsilon(Cl\cdot)$ was found to be (5000 ± 1000) dm^3 mol^{-1} cm^{-1}, in agreement with the values obtained by Treinin and Hayon,[14] Klaning and Wolff[4] and Nagarajan and Fessenden.[5] The absorbance at the end of the growth was consistent with that expected from e^-_{aq} and $Cl_2\cdot^-$, using an $\varepsilon(Cl_2\cdot^-)$ in the region of *ca*. 9600 dm^3 mol^{-1} cm^{-1}. Uncertainty in the values obtained was due largely to variability in the laser energy between successive pulses.

3.5. Formation and Decay of $Cl_2\cdot^-$

Chlorine atoms were formed by the reaction of chloride with $SO_4\cdot^-$, which was generated by pulse radiolysis of 10^{-3} mol dm^{-3} $Na_2S_2O_8$, reactions (1.28), (1.35) and (3.4), in near neutral argon saturated solution.

$$SO_4\cdot^- + Cl^- \rightarrow SO_4^{2-} + Cl\cdot \qquad (3.4)$$

$$k_{3.4} = 2.47 \times 10^8 \text{ dm}^3 \text{ mol}^{-1} \text{ s}^{-1} \text{ (Ref. 7)}$$

The growth and decay of the radicals were monitored by kinetic spectroscopy at 340 nm, where $\varepsilon(Cl_2\cdot^-)$ has a maximum value[2,15] of 9600 dm^3 mol^{-1} cm^{-1}. The ·OH radical generated by reaction (1.28) was converted to a relatively unreactive radical by the addition of t-BuOH, reaction (1.32). Solutions containing t-BuOH and $S_2O_8^{2-}$ are stable against daylight and thermal decomposition for several hours.[16]

The decay of $Cl_2\cdot^-$ was studied under conditions where reactions (1.28), (1.35) and (3.4) were very rapid, see Figure 3.3. Repeating the experiments of Adams *et al.,*[2] using a dose of 8 Gy, gave decays which obeyed mixed first- and

second-order kinetics. The second-order component was attributed to reactions (3.2a, b and c) and the first-order component to the reactions of Cl· and $Cl_2·^-$ with t-BuOH and water, reactions (3.5), (3.6), (3.7) and (3.8).

$$Cl· + \text{t-BuOH} \rightarrow \text{products} \qquad (3.5)$$

$$Cl_2·^- + \text{t-BuOH} \rightarrow \text{products} \qquad (3.6)$$

$$Cl· + H_2O \rightarrow \text{products} \quad [cf. \text{ reaction (3.9)}] \qquad (3.7)$$

$$Cl_2·^- + H_2O \rightarrow \text{products} \quad [cf. \text{ reaction (3.9)}] \qquad (3.8)$$

In order to investigate the contribution of reactions (3.2a, b and c) some experiments were performed at high dose (> 70 Gy per pulse). However the second-order rate of decay showed little variation with ionic strength, and increased with [t-BuOH] and decreasing $[Cl^-]$. This indicated the likely involvement of a reactive radical species derived from reaction (3.5), possibly $·CH_3$ as reported by Gilbert *et al*.[17] Strictly, the reactions of Cl· and $Cl_2·^-$ with $·CH_3$ would not be second-order, thus making analysis of the overall reaction scheme difficult. Therefore to avoid the complications of any radical-radical reactions, it was decided to conduct all experiments at very low dose. This ensured that the decays were first-order at all concentrations of chloride and t-BuOH.

No effect of $[S_2O_8^{2-}]$ on the rate of decay of $Cl_2·^-$ was expected, and this was found to be the case in a set of experiments with [t-BuOH] = 4×10^{-4}, $[Cl^-] = 10^{-3}$ and $[S_2O_8^{2-}]$ from 10^{-3} to 0.1 mol dm^{-3}. This result puts an upper limit of *ca*. 10^6 dm^3 mol^{-1} s^{-1} on the rate constant $k(Cl· + S_2O_8^{2-})$.

Figure 3.3 *The absorbance at 340 nm following pulse radiolysis of an Ar-saturated solution containing* $[Cl^-] = [S_2O_8^{2-}] = [t\text{-BuOH}] = 10^{-3}$ *mol dm*$^{-3}$ *at pH ca. 6 using a dose of ca. 1 Gy. The red line is a fitted first-order decay.*

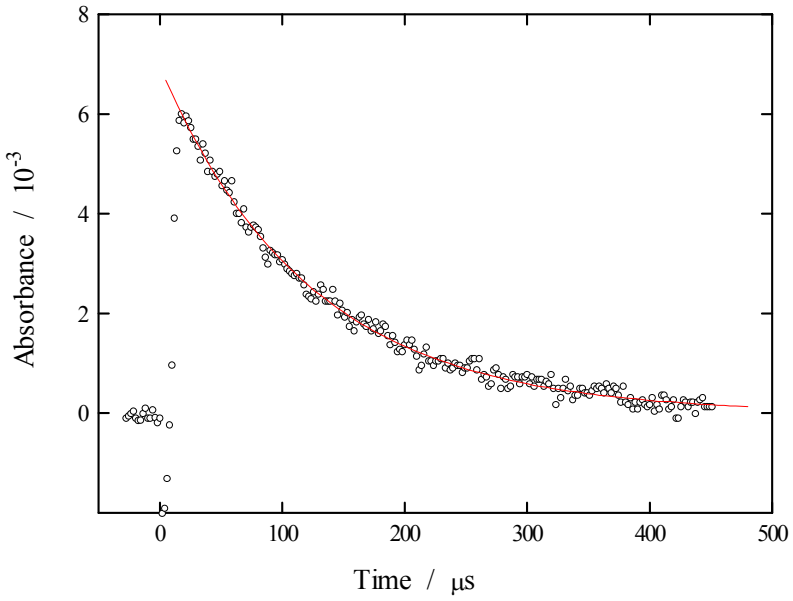

Figure 3.4 *Effect of [t-BuOH] on* k_{obs} *for the first-order decay of* $Cl_2^{\cdot-}$ *at* $[Cl^-] = 10^{-3}$ *mol dm*$^{-3}$*. The red line is a fit of the first four points using equation [3.1] and the blue line is a fit of all the points using equation [3.2]. Error bars are ± 1 S.D.*

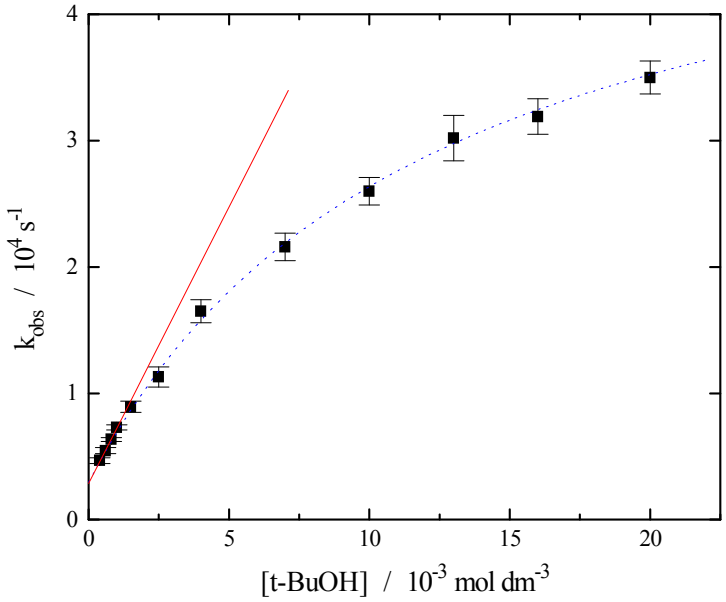

The reactions of Cl· and $Cl_2\cdot^-$ with water have been proposed[3,9,18] to involve a series of equilibria, reaction (3.9), which in neutral solution and $[Cl^-] < 0.1$ mol dm^{-3} lie far to the right. These equilibria are discussed in detail in reference 9.

$$Cl\cdot/Cl_2\cdot^- + H_2O \leftrightarrow HOClH\cdot \leftrightarrow H^+ + HOCl\cdot^- \leftrightarrow Cl^- + \cdot OH + H^+ \qquad (3.9)$$

The ·OH radical product of reaction (3.9) was removed by t-BuOH so that no equilibrium could be formed, and therefore reactions (3.7) and (3.8) behaved as simple first-order reactions.

3.6. Decay Kinetics of $Cl_2\cdot^-$

The effect of [t-BuOH] on k_{obs} for the first-order decay of $Cl_2\cdot^-$ is shown in Figure 3.4. On the assumption that equilibrium (3.1) is maintained then k_{obs} is given by equation [3.1], indicating a linear dependence on [t-BuOH].

$$k_{obs} = \frac{k_{3.7} + k_{3.8}K_{3.1}[Cl^-]}{1 + K_{3.1}[Cl^-]} + \left[\frac{k_{3.5} + k_{3.6}K_{3.1}[Cl^-]}{1 + K_{3.1}[Cl^-]}\right][t - BuOH] \qquad [3.1]$$

The marked deviation from linearity at higher [t-BuOH] suggests that there is significant departure from equilibrium. To better understand this behaviour, the exact rate law, equation [3.2], was derived by solving the rate equations pertaining to equilibrium (3.1) and reactions (3.5) to (3.8), see Appendix 1.

$$k_{obs} = \frac{k_{-3.1}(k_{3.5}[t - BuOH] + k_{3.7}) + (k_{3.1}[Cl^-] + k_{3.5}[t - BuOH] + k_{3.7})(k_{3.6}[t - BuOH] + k_{3.8})}{k_{3.1}[Cl^-] + k_{-3.1} + (k_{3.5} + k_{3.6})[t - BuOH] + k_{3.7} + k_{3.8}} \qquad .....[3.2]$$

Equation [3.2] simplifies to [3.1] when the inequality below is satisfied.

$$K_{3.1}[Cl^-] + 1 >> \frac{(k_{3.5} + k_{3.6})[t - BuOH] + k_{3.7} + k_{3.8}}{k_{-3.1}}.$$

Therefore the deviation from linearity can be seen to be a consequence of a small value for $k_{-3.1}$ and the associated high value for $K_{3.1}$.

The data of Figure 3.4 suggest that a limiting value of k_{obs} is reached with increasing [t-BuOH]. Accordingly, by taking the limit of equation [3.2] as [t-BuOH] tends to infinity it can be shown that the maximum rate of decay of $Cl_2\cdot^-$ in our experiments was dictated by the first-order dissociation of $Cl_2\cdot^-$ into Cl· and chloride, $k_{-3.1}$.

$$\lim_{[t\text{-}BuOH]\to\infty} k_{obs} \approx k_{-3.1}$$

3.7. Results

However, as indicated by the straight line in Figure 3.4, the dependence of k_{obs} on [t-BuOH] conforms to equation [3.1] over a limited range of [t-BuOH]. In Table 3.1 are listed values of the gradients and intercepts of such linear plots, obtained by a linear least squares treatment of k_{obs} *vs* [t-BuOH] for at least four concentrations. The range of [t-BuOH] was chosen so as to avoid departures from equilibrium (see equation [A1.12]), whilst maintaining efficient scavenging of ·OH by reaction (1.32).

Table 3.1 *Kinetic data for the decay of $Cl_2\cdot^-$ treated by equation [3.1].*

$[Cl^-]$ / 10^{-3} mol dm^{-3}	**[t-BuOH] range / 10^{-3} mol dm^{-3}**	**Intercept / s^{-1}**	**Gradient / dm^3 mol^{-1} s^{-1}**
1.0	0.4 to 1.0	3142 ± 78	(4.74 ± 0.11) × 10^6
1.25	0.4 to 1.3	2564 ± 236	(3.61 ± 0.26) × 10^6
1.5	0.6 to 1.5	2461 ± 34	(2.65 ± 0.04) × 10^6
2.0	0.8 to 2.0	2071 ± 211	(2.19 ± 0.28) × 10^6
3.0	1.0 to 2.2	2083 ± 70	(1.70 ± 0.04) × 10^6
5.0	1.0 to 5.0	1552 ± 142	(8.74 ± 0.04) × 10^5
10.0	3.0 to 12.0	1460 ± 164	(4.09 ± 0.20) × 10^5
20.0	6.0 to 18.0	1396 ± 138	(1.94 ± 0.11) × 10^5
50.0	15 to 45	1276 ± 162	(1.05 ± 0.05) × 10^5
70.0	25 to 70	1328 ± 114	(5.22 ± 0.23) × 10^4

The intercepts (I) and gradients (G) of these plots of k_{obs} *vs* [t-BuOH] are given by equations [3.3a] and [3.3b] (*cf*. equation [3.1]).

$$I = \frac{k_{3.7} + k_{3.8} K_{3.1}[Cl^-]}{1 + K_{3.1}[Cl^-]} \qquad [3.3a]$$

$$G = \frac{k_{3.5} + k_{3.6} K_{3.1}[Cl^-]}{1 + K_{3.1}[Cl^-]} \qquad [3.3b]$$

From the laser experiments outlined in Section 3.3., the rate constants $k_{3.1}$ and $k_{-3.1}$ were determined to be $(8.5 \pm 0.7) \times 10^9$ dm^3 mol^{-1} s^{-1} and $(5 \pm 8) \times 10^5$ s^{-1}, respectively, which together suggest a lower limit for the equilibrium constant of *ca*. 6×10^3 dm^3 mol^{-1}. Therefore the denominators of equations [3.3a] and [3.3b] are dominated by the $K_{3.1}[Cl^-]$ term at the chloride concentrations of Table 3.1.

Accordingly, equations [3.3a] and [3.3b] may be simplified to equations [3.4a] and [3.4b].

$$I = \frac{k_{3.7}}{K_{3.1}[Cl^-]} + k_{3.8} \qquad [3.4a]$$

$$G = \frac{k_{3.5}}{K_{3.1}[Cl^-]} + k_{3.6} \qquad [3.4b]$$

Equations [3.4a] and [3.4b] indicate a linear relationship between I and G and $1/[Cl^-]$. Therefore a plot of I and G versus $1/[Cl^-]$ from the data of Table 1 should give intercepts of $k_{3.6}$ and $k_{3.8}$ and gradients of $k_{3.5}/K_{3.1}$ and $k_{3.7}/K_{3.1}$, see Figure 3.5.

Figure 3.5 *Plots of the intercepts (I) and gradients (G) of equation [3.1] vs 1/[Cl⁻]. The data are listed in Table 3.1. °, I and ●, G.*

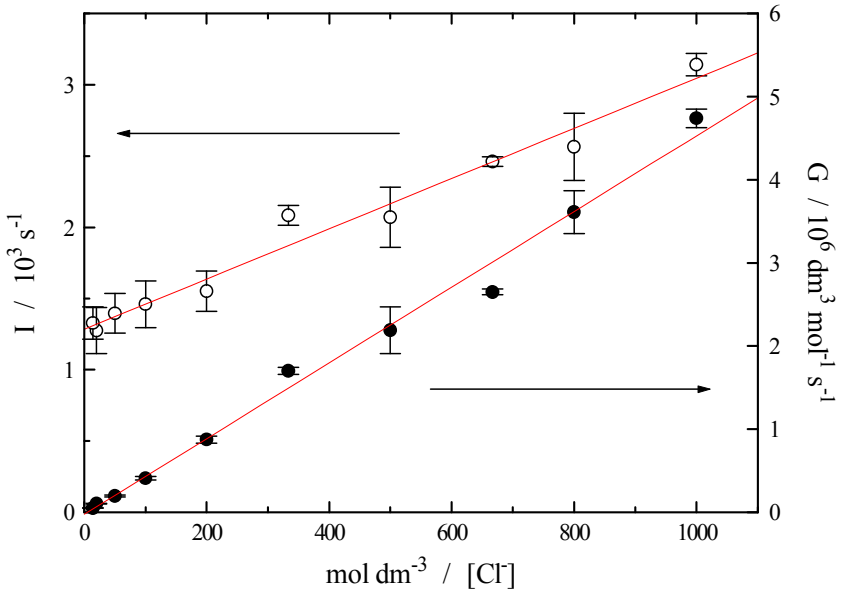

Plots of I and G *vs* 1/[Cl^-] gave straight lines, see Figure 3.5, from which the following were obtained : $k_{3.7}/K_{3.1}$ = (1.76 ± 0.10) mol dm^{-3} s^{-1}, $k_{3.5}/K_{3.1}$ = (4.55 ± 0.16) × 10^3 s^{-1}, $k_{3.8}$ = (1.28 ± 0.05) × 10^3 s^{-1} and $k_{3.6}$ = (–3 ± 8) × 10^4 dm^3 mol^{-1} s^{-1}. The last value is dictated by the scatter in the data and is not a true reflection of the magnitude of $k_{3.6}$, which we conclude is close to zero.

Replacing $K_{3.1}$ by $k_{3.1}/k_{-3.1}$ and substituting the value determined in this study of $k_{3.1}$ = (8.5 ± 0.7) × 10^9 dm^3 mol^{-1} s^{-1} gives equations [3.5] and [3.6].

$$k_{3.5} = (3.9 \pm 0.35) \times 10^{13} \;/\; k_{-3.1} \quad dm^3\ mol^{-1}\ s^{-1} \qquad [3.5]$$

$$k_{3.7} = (1.5 \pm 0.15) \times 10^{10} \;/\; k_{-3.1} \quad s^{-1} \qquad [3.6]$$

Inserting these relationships into equation [3.2] results in the equation being expressed in terms of $k_{-3.1}$ only. This value was, therefore, obtainable by fitting the experimentally determined dependences of k_{obs} on [t-BuOH] to equation [3.2] by the method of non-linear least squares, see Figure 3.4. This was done

using data for five concentrations of chloride, see Table 3.2. A weighted mean of the five values gives $k_{-3.1} = (6.0 \pm 0.2) \times 10^4$ s^{-1}, where the error represents the scatter only. Incorporating the error on $k_{3.1}$, upon which the value of $k_{-3.1}$ depends, gives $k_{-3.1} = (6.0 \pm 0.5) \times 10^4$ s^{-1}. Substituting $k_{-3.1}$ into [3.5] and [3.6] gives $k_{3.5} = (6.5 \pm 0.6) \times 10^8$ dm^3 mol^{-1} s^{-1} and $k_{3.7} = (2.5 \pm 0.3) \times 10^5$ s^{-1}.

Table 3.2 *Fitted values of $k_{-3.1}$ from equation [3.2]. Typical data are shown in Figure 3.4.*

$[Cl^-]$ / 10^{-3} mol dm^{-3}	**[t-BuOH] range / 10^{-3} mol dm^{-3}**	**$k_{-3.1}$ / 10^4 s^{-1}**
1.0	0.4 to 20.0	5.37 ± 0.20
1.5	0.6 to 30.0	5.98 ± 0.24
3.0	1.0 to 60.0	5.87 ± 0.19
5.0	1.0 to 100	5.90 ± 0.18
10.0	3.0 to 200	6.51 ± 0.15

3.8. Conclusions and Discussion

Rate constants determined at 25 °C in this study are listed in Table 3.3. The values of $k_{3.1}$ and $k_{-3.1}$ give an equilibrium constant $K_{3.1} = (1.4 \pm 0.1) \times 10^5$ dm^3 mol^{-1} in reasonable agreement with Jayson *et al.*[3] who obtained a value of 1.9×10^5 dm^3 mol^{-1} from studies at low pH. The discrepancy of *ca*. 30 % may be explained by these authors not taking into consideration the absorption due to Cl· which this study and earlier work[4,14] have shown to absorb at 340 nm with $\varepsilon \approx 5000$ dm^3 mol^{-1} cm^{-1}. At the lowest chloride concentration used (10^{-5} mol dm^{-3}) this may have contributed up to 30% of the absorbance.

Jayson *et al.* reported the rate constant of Cl· with water, $k_{3.7}$, to be 1.3×10^3 dm^3 mol^{-1} s^{-1}, which is 7.2×10^4 s^{-1} when multiplied by the molarity of water. However, this value was obtained from experiments with $[Cl^-]$ in the range 0.3

to 3 mol dm^{-3} where the results of the present study, and those of McElroy,[9] indicate that the predominant reaction is (3.8).

The value $K_{3.1}$ = 17.7 dm^3 mol^{-1}, reported by Wu *et al.*,[1] was obtained from an analysis of variations in the second-order rate of decay of $Cl_2\cdot^-$ with $[Cl^-]$. No first-order component to the decay was detected, even at the lowest $[Cl^-]$ of 5×10^{-4} mol dm^{-3}, contrary to many other studies. In addition, this very low $K_{3.1}$ would mean that $Cl_2\cdot^-$ is not observable at the $[Cl^-]$ used, as pointed out by Wagner *et al.*[19] For these reasons, the result of Wu *et al.* is considered to be erroneous.

Table 3.3 *Summary of the rate constants determined at 25 ºC in this study.*

Reaction	**Rate Constant / dm^3 mol^{-1} s^{-1}**	**Literature / dm^3 mol^{-1} s^{-1}**	**Ref.**
$Cl\cdot + Cl^-$	$(8.5 \pm 0.7) \times 10^9$	8×10^9	5
$Cl_2\cdot^- \rightarrow Cl\cdot + Cl^-$	$(6.0 \pm 0.5) \times 10^4$ [a]	N/A	N/A
$Cl\cdot$ + t-BuOH	$(6.5 \pm 0.6) \times 10^8$	*ca.* 10^9	19
$Cl_2\cdot^-$ + t-BuOH	*ca.* 0 [b]	*ca.* 700	8
$Cl\cdot$ + water	$(2.5 \pm 0.3) \times 10^5$ [a]	1.8×10^5 [a,c]	9
$Cl_2\cdot^-$ + water	$(1.3 \pm 0.1) \times 10^3$ [a]	1.3×10^3 [a]	9

[a] Units s^{-1} [b] See text [c] After adjusting for the revised $K_{3.1}$

Figure 3.6 *Simulation of $[Cl_2\cdot^-]$, $[Cl\cdot]$, $[SO_4\cdot^-]$, $Q_{3.1}(t)$ and k_{eff} vs time in a typical pulse radiolysis experiment. The $SO_4\cdot^-$ is formed at t = 0 and $[Cl^-]$ = [t-BuOH] = 10^{-3} mol dm^{-3}.*

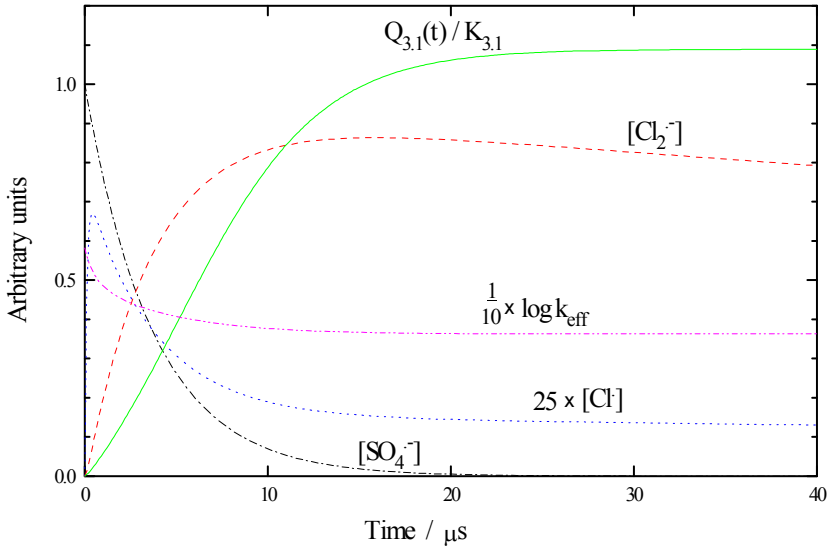

This study has found that the relationship $[Cl_2\cdot^-] = K_{3.1}[Cl^-][Cl\cdot]$ is valid only in the limit of low [t-BuOH]. When $[Cl^-] = 10^{-4}$ mol dm^{-3} even the reaction of Cl· with water, reaction (3.7), is sufficiently fast to cause a 30 % deviation from the equilibrium (3.1), *cf.* equation [A1.11]. This loss of equilibrium was observed by McElroy at very low $[Cl^-]$.

Conflict between the value $K_{3.1} = 1.4 \times 10^5$ dm^3 mol^{-1} and a recent determination by Adams *et al.*[2] of 4700 dm^3 mol^{-1} in neutral pH solution is resolved by considering the loss of equilibrium at low $[Cl^-]$. The rapid reactions leading to the formation and loss of Cl· create a situation in which $[Cl_2\cdot^-] \neq K_{3.1}[Cl^-][Cl\cdot]$, the correct relationship being $[Cl_2\cdot^-] = Q_{3.1}(t)[Cl^-][Cl\cdot]$, see equation [A1.16]. Figure 3.6 shows a FACSIMILE[20] simulation of $[Cl\cdot]$, $[Cl_2\cdot^-]$, $[SO_4\cdot^-]$ and $Q_{3.1}(t)$ as functions of time in a pulse radiolysis experiment.

The equilibrium quotient, $Q_{3.1}(t)$, is not constant during the growth of $Cl_2\cdot^-$ and this gives rise to a greater loss of $Cl_2\cdot^-$ than expected on the basis of equation

[3.2]. The first-order rate of loss of the total radical yield, $[R\cdot] = [Cl\cdot] + [Cl_2\cdot^-]$, is given by k_{eff} of equation [3.7], omitting for simplicity $k_{3.6}$, $k_{3.7}$ and $k_{3.8}$.

$$k_{eff} = -\frac{d\ln[R\cdot]}{dt} = \frac{k_{3.5}[t-BuOH]}{1 + Q_{3.1}(t)[Cl^-]} \qquad [3.7]$$

A simulation of k_{eff} in Figure 3.6 shows the time-dependence of the rate of loss of $Cl\cdot$ and $Cl_2\cdot^-$ during the approach to steady-state conditions. The difference between the values at $t = 0$ and at $t \rightarrow \infty$ is greater than two logarithmic units. In the work of Adams *et al.*,[2] a correction for the decay of $Cl_2\cdot^-$ during its growth assumed k_{eff} was constant at its long-time value, which resulted in too small a correction being applied to the yield of $Cl_2\cdot^-$. This, in turn, gave a smaller value of $K_{3.1}$. At low pH with no t-BuOH present, there are effectively no sinks for the $Cl\cdot$ atom except the $Cl_2\cdot^-$ self-reaction and so, under the conditions used by Jayson *et al.*,[3] equilibrium is maintained at all $[Cl^-]$.

An analogous situation to that encountered by Adams *et al.*[2] in their investigation of $K_{3.1}$ has been previously identified as a problem in the determination of rate constants by the competition method.[21,22,23,24] Frequently this technique relates the yield of $X_2\cdot^-$ (X = Br, I or SCN), after its formation from the $\cdot OH$ radical via the intermediate species $HOX\cdot^-$ and $X\cdot$, to the concentration of an added $\cdot OH$ scavenger, [S]. However the occurrence of fast reactions of the intermediate species, in particular $X\cdot$ + S, can decrease the yield of $X_2\cdot^-$ so that the expected relationship between $[X_2\cdot^-]$ and [S] is no longer obeyed.

In the present study one may associate X with Cl, $\cdot OH$ with $SO_4\cdot^-$ and S with t-BuOH. Then, although there is virtually no scavenging of $SO_4\cdot^-$ by t-BuOH ($k_{4.2} = 7.8 \times 10^5$ compared with $k_{3.4} = 2.47 \times 10^8$ dm^3 mol^{-1} s^{-1})[25] there is a significant decrease in the yield of $Cl_2\cdot^-$ with [t-BuOH], see Figure 3.7.

Figure 3.7 *Plot of $1/(G\varepsilon)_{corr}$ vs [t-BuOH], measured at 340 nm with $[Cl^-] = [S_2O_8^{2-}] = 10^{-3}$ mol dm^{-3} and at pH ca. 6.*

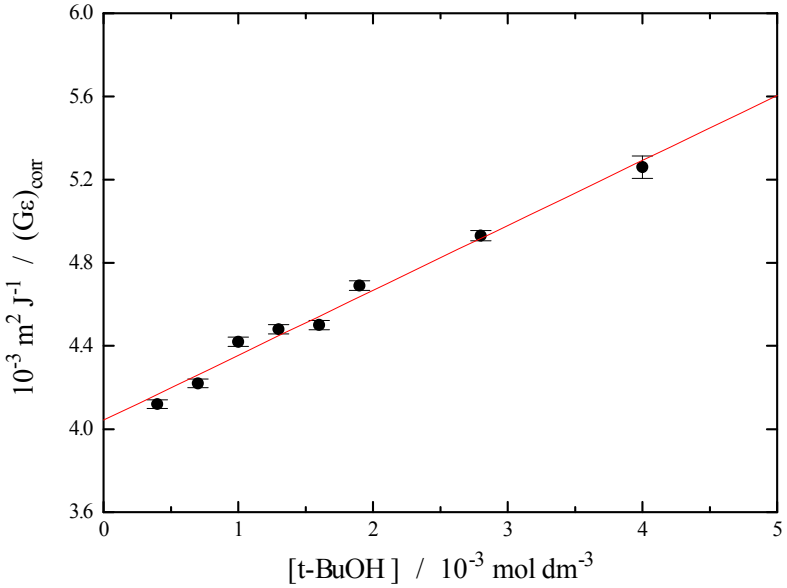

This is the result of a competition between t-BuOH and chloride for the intermediate Cl· atom, and therefore the relevant expression is equation [3.8].[26] $(G\varepsilon)_{corr}$ is the Gε of $Cl_2\cdot^-$ at the end of its growth after correction for the slight decay, as used by Adams *et al.*,[2] i.e. k_{eff} at $t \rightarrow \infty$, see equation [3.7].

$$\frac{1}{(G\varepsilon)_{corr}} = \frac{1}{(G\varepsilon)_o} + \frac{1}{(G\varepsilon)_o} \cdot \frac{k_{3.5}[t-BuOH]}{k_{3.1}[Cl^-]} \qquad [3.8]$$

The intercept of Figure 3.7 of $(4.04 \pm 0.04) \times 10^3$ J m^{-2} and gradient of $(3.12 \pm 0.16) \times 10$ J m^{-2} dm^3 mol^{-1} are given by equation [3.8], and therefore the values of $\varepsilon(Cl_2\cdot^-) = (9170 \pm 100)$ dm^3 mol^{-1} cm^{-1} and $k_{3.1} / k_{3.5} = (12.9 \pm 0.7)$ were obtained. These are close to the values determined in this investigation. The linear dependence of $1/(G\varepsilon)_{corr}$ on $1/[Cl^-]$ observed by Adams *et al.*,[2] which was attributed to the position of the equilibrium of reaction (3.1), was in fact governed by the competition described above. A minor difference was that the $[Cl^-]$ was varied at constant [t-BuOH] rather than the [t-BuOH] at constant $[Cl^-]$, although the same reactions were responsible for the variation.

3.10. References

1. D. Wu, D. Wong and B. Di Bartolo, *J. Photochem.*, 1980, **14**, 303
2. D. J. Adams, S. Barlow, G. V. Buxton, T. N. Malone and G. A. Salmon, *J. Chem. Soc., Faraday Trans.,* 1995, **91**, 3303
3. G. G. Jayson, B. J. Parsons and A. J. Swallow, *J. Chem. Soc., Faraday Trans. 1,* 1973, **69**, 1597
4. U. Klaning and T. Wolff, *Ber. Bunsenges. Phys. Chem.,* 1985, **89**, 243
5. V. Nagarajan and R. W. Fessenden, *J. Phys. Chem.,* 1985, **89**, 2330
6. A. Iwata, C. Yamanaka, N. Nakashima and Y. Izawa, *Anal. Chim. Acta,* 1993, **277**, 25
7. R. E. Huie and C. L. Clifton, *J. Phys. Chem.,* 1990, **94**, 8561
8. K. Hasegawa and P. Neta, *J. Phys. Chem.*, 1978, **82**, 854
9. W. J. McElroy, *J. Phys. Chem.*, 1990, 94, 2435
10. See reference 9 and references therein
11. L. I. Grossweiner and M. S. Matheson, *J. Phys. Chem.,* 1957, **61**, 1089
12. A. Iwata, N. Nakashima, M. Kusaba, Y. Izawa and C. Yamanaka, *Chem. Phys. Lett.,* 1993, **207**, 137
13. E. J. Hart and M. Anbar, in The Hydrated Electron, Wiley-Interscience, 1970
14. A. Treinin and E. Hayon, *J. Amer. Chem. Soc.,* 1975, **97**, 1716
15. B. H. Bielski, *Radiat. Phys. Chem.,* 1993, **41**, 527
16. G. Mark, M. N. Schuchmann, H-P. Schuchmann and C. von Sonntag, *J. Photochem. Photobiol. A-Chem.*, 1990, **55**, 157
17. B. C. Gilbert, J. K. Stell, W. J. Peet and K. J. Radford, *J. Chem. Soc., Faraday Trans. I*, 1988, **84**, 3319
18. M. Anbar and J. K. Thomas, *J. Phys. Chem.*, 1964, **68**, 3829
19. I. Wagner, J. Karthauser and H. Strehlow, *Ber. Bunsenges. Phys. Chem.*, **90**, 1986, 861
20. A. R. Curtis and W. P. Sweetham, FACSIMILE/CHECKMAT USER'S MANUAL, UKAEA, 1987, AERE R12805
21. S. R. Logan and G. A. Salmon, *Radiat. Phys. Chem.*, 1984, **24**, 593

22. G. E. Adams, J. W. Boag and B. D. Michael, *Trans. Faraday Soc.*, 1965, **61**, 1417
23. S. P. Mezyk, *Can. J. Chem.*, 1994, **72**, 1116
24. A. J. Elliot and A. S. Simsons, *Radiat. Phys. Chem.*, 1984, **24**, 229
25. A. B. Ross, W. G. Mallard, W. P. Helman, G. V. Buxton, R. E. Huie and P. Neta, NDRL-NIST Solution Kinetics Database, Ver. 3.0, NIST Standard Ref. Data, Gaithersburg, MD 1998
26. M. Ebert, J. P. Keene, A. J. Swallow and J. H. Baxendale, in Pulse Radiolysis, Academic Press, London 1965

Chapter 4

The Equilibrium $SO_4^{\cdot -} + Cl^- \leftrightarrow SO_4^{2-} + Cl^{\cdot}$

4.1. Introduction

The forward reaction of equilibrium (4.1), *cf.* reaction (3.4), has been thought to be a major sink for $SO_4^{\cdot -}$ in the atmospheric aqueous phase due to its high rate constant and the relatively high chloride concentration.[1,2]

$$SO_4^{\cdot -} + Cl^- \leftrightarrow Cl^{\cdot} + SO_4^{2-} \quad (4.1)$$

However, this work and other studies[3,4] have shown there to be a similarly high rate constant for the reverse reaction. Considering that the condensation nuclei for cloud droplets consist predominantly of sulfate salts,[2] it may be expected that the sulfate concentration would result in equilibrium (4.1) being pushed to the left. Hence there may be little or no loss of $SO_4^{\cdot -}$ by this route. In the only previous determination of equilibrium constant $K_{4.1}$, the decay of $SO_4^{\cdot -}$ was modelled numerically to find a value for $k_{-4.1}$ from a reaction scheme involving equilibria (3.1) and (4.1) and the self-reactions of $SO_4^{\cdot -}$ and $Cl_2^{\cdot -}$.[3] No reactions with water were included in the model, perhaps accounting for the poor fits reported at lower $[Cl^-]$, and a negative intercept was obtained in the plot of k_{obs} *vs* $[Cl^-]$ that could not be explained.

$$Cl^{\cdot} + Cl^- \leftrightarrow Cl_2^{\cdot -} \quad (3.1)$$

4.2. Experimental Approach

The kinetics of the double equilibrium, reactions (3.1) and (4.1), have been studied by pulse radiolysis, reactions (1.28) and (1.35). Expressions describing the effect of $[Cl^-]$ and $[SO_4^{2-}]$ on the rate of growth and decay of $Cl_2^{\cdot -}$ and $SO_4^{\cdot -}$ were derived, which explain the negative intercept found in previous work. The rate constants of $SO_4^{\cdot -}$ with t-BuOH, $S_2O_8^{2-}$ and water were redetermined.

4.3. Reactions of $SO_4^{\cdot -}$ with t-BuOH and Water

The decay of $SO_4^{\cdot -}$ was monitored in solutions containing 10^{-3} mol dm^{-3} persulfate and [t-BuOH] in the range (0.1 to 30) $\times 10^{-3}$ mol dm^{-3}, with 0.1 mol dm^{-3} sulfate used to adjust the ionic strength to 0.3 mol dm^{-3}, see Figure 4.1.

Figure 4.1 *The absorbance at 450 nm following pulse radiolysis of an argon-saturated solution containing [t-BuOH] = 10^{-4} and [$S_2O_8^{2-}$] = 10^{-3} mol dm^{-3} at natural I and pH ca. 6 using a dose of ca. 0.3 Gy. The red line is a fitted first-order decay.*

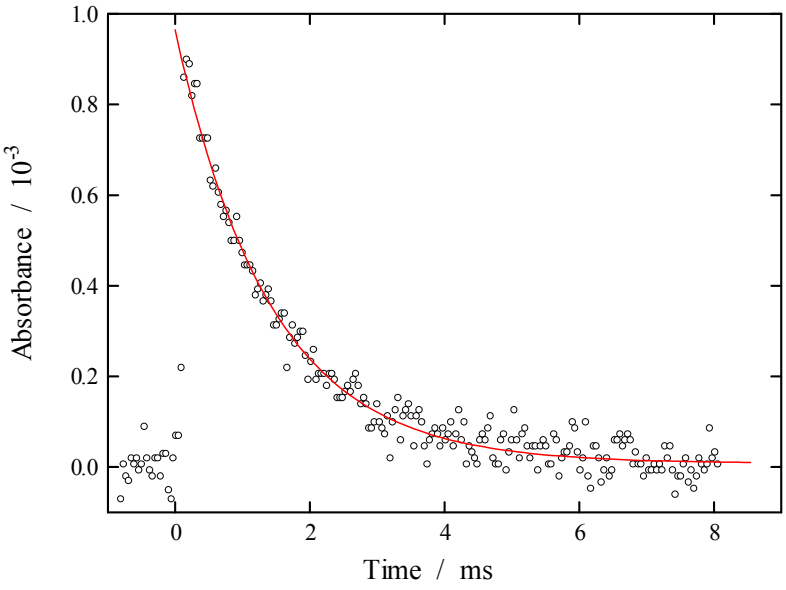

Figure 4.2 *Effect of [t-BuOH] on k_{obs} for the first-order decay of $SO_4^{\cdot-}$. °, natural I and ●, I = 0.3 mol dm^{-3}. Error bars are ± 1 S.D.*

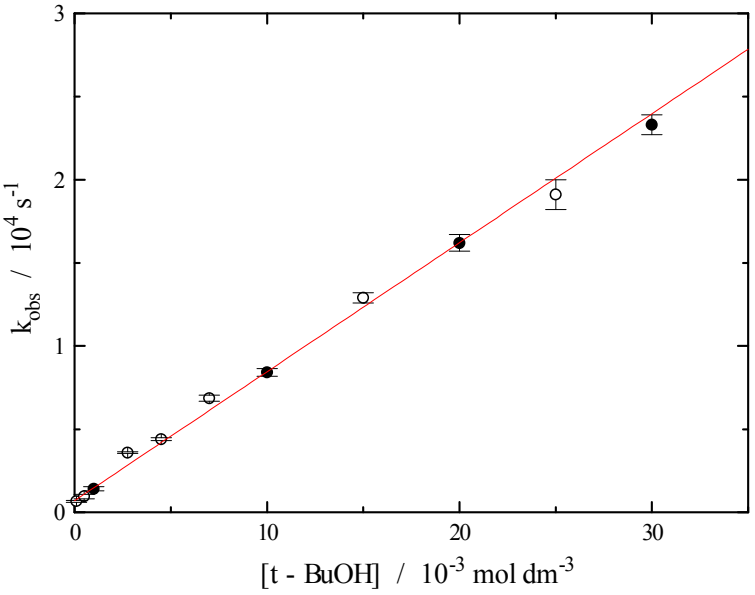

In some experiments, no sulfate was added and MilliQ water which had been further purified by distillation from alkaline $KMnO_4$ was used in order to check whether impurities or the presence of sulfate were affecting the rate of decay. No difference was observed, see Figure 4.2, and therefore the first-order decay of $SO_4{\cdot}^-$ was attributed solely to reactions (4.2), (4.3) and (4.4). Using a dose of 1 Gy, a significant contribution from the self-reaction of $SO_4{\cdot}^-$ was expected at the lowest [t-BuOH], therefore when [t-BuOH] $\leq 10^{-3}$ mol dm^{-3} the dose was reduced to *ca*. 0.3 Gy.

$$SO_4{\cdot}^- + \text{t-BuOH} \rightarrow \text{products} \qquad (4.2)$$

$$SO_4{\cdot}^- + H_2O \rightarrow SO_4^{2-} + H^+ + {\cdot}OH \qquad (4.3)$$

The gradient and intercept of the plot of k_{obs} *vs* [t-BuOH] indicate that $k_{4.2} = (7.8 \pm 0.2) \times 10^5$ dm^3 mol^{-1} s^{-1} and $(k_{4.3} + k_{4.4} \times 10^{-3}) = (690 \pm 120)$ s^{-1}. This value of $k_{4.2}$ is in agreement with previous determinations.[5]

4.4. Reaction of $SO_4{\cdot}^-$ with $S_2O_8^{2-}$

The rate constant for reaction (4.4) is not well established.

$$SO_4{\cdot}^- + S_2O_8^{2-} \rightarrow SO_4^{2-} + S_2O_8{\cdot}^- \qquad (4.4)$$

Literature values range from $< 10^4$ to 6.1×10^5 dm^3 mol^{-1} s^{-1},[6,7,8] and have been obtained from experiments in which the first-order decay is a minor sink for the radical compared with its self-reaction. In this study, the rate of decay of $SO_4{\cdot}^-$ was measured in solutions containing 10^{-3} mol dm^{-3} t-BuOH and persulfate in the range 10^{-3} to 0.1 mol dm^{-3}, using sulfate to maintain the ionic strength at 0.3 mol dm^{-3}. As above, the dose was limited to *ca*. 0.3 Gy. Some experiments were performed with no sulfate in order to check whether the possible reverse reaction of (4.4) was affecting the decays. No significant effect was observed. The ionic strength was determined solely by $S_2O_8^{2-}$ in these experiments.

Figure 4.3 *Effect of $[S_2O_8^{2-}]$ on k_{obs} for the first-order decay of $SO_4^{\cdot-}$. °, natural I and ●, I = 0.3 mol dm^{-3}. Error bars are ± 1 S.D.*

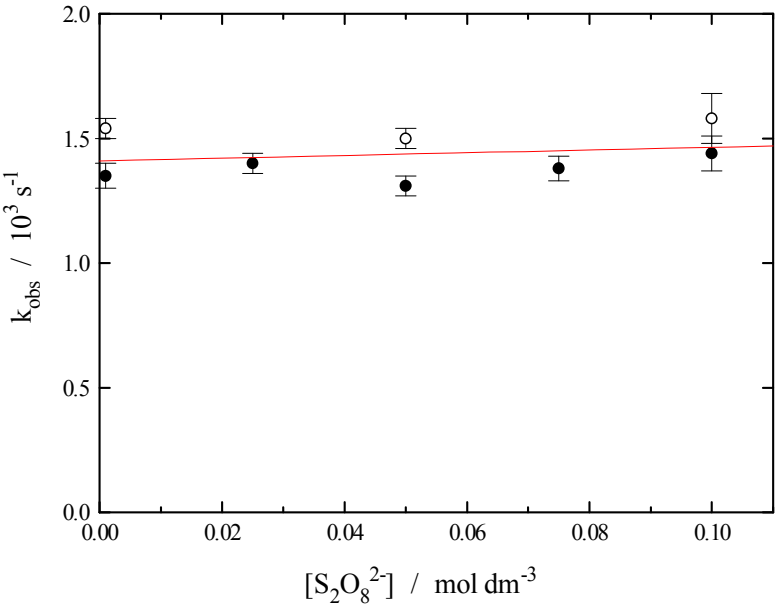

Little variation in the rate of decay occurred over the range of persulfate concentration, see Figure 4.3. The average value of $k_{obs} = (1.45 \pm 0.22) \times 10^3$ s^{-1} (error is 2σ from 32 experiments) corresponds with the rate expected from reactions (4.2) and (4.3) only, and whilst the error limit permits a value of up to 4.4×10^3 dm^3 mol^{-1} s^{-1} for $k_{4.4}$ this seems unlikely in the absence of a clear trend in the data. Linear regression gives the value (540 ± 1000) dm^3 mol^{-1} s^{-1}, and therefore we suggest that the rate constant for reaction (4.4) is $< 1.5 \times 10^3$ dm^3 mol^{-1} s^{-1}. This means that the intercept of Figure 4.2 is predominantly due to reaction (4.3), and hence $k_{4.3} = (690 \pm 120)$ s^{-1}.

This is a little higher than other reported values for $k_{4.3}$ which are typically 360 to 660 s^{-1},[7] and it may be that the self-reaction of $SO_4^{\cdot-}$ was affecting the slowest decays even at 0.3 Gy. Taking[8] $2k(SO_4^{\cdot-} + SO_4^{\cdot-}) = 8.9 \times 10^8$ dm^3 mol^{-1} s^{-1} it was estimated that this reaction could contribute between 100 to

200 s^{-1} to the rate of decay, which would mean our value of $k_{4.3}$ is more in line with the literature values.

The rate constant for reaction (4.4) determined in this study is somewhat lower than previous reports. The reason for the discrepancy is not clear, however it is believed that the results of Figure 4.2 provide stronger evidence for a low value than do the mixed-order analyses of previous determinations for a high value. Indeed, if $k_{4.4}$ were 6.1×10^5 dm^3 mol^{-1} s^{-1} then the rate of decay at 0.1 mol dm^{-3} persulfate would be *ca*. 40 times faster than observed in our experiments.

4.5. Effect of $S_2O_8^{2-}$ on the Reactions of Cl· and $Cl_2\cdot^-$

No influence of ionic strength up to 0.3 mol dm^{-3} was expected for the reactions of Cl· and $Cl_2\cdot^-$ in our experiments, nor any discernible reaction with persulfate. Our previous study[9] reported no significant variation in the rate of decay of $Cl_2\cdot^-$ over the range $[S_2O_8^{2-}] = 10^{-3}$ to 0.1 mol dm^{-3} confirming that ionic strength and persulfate have little effect on the reactions. For the reason that persulfate appears to be unreactive towards $SO_4\cdot^-$ and $Cl\cdot/Cl_2\cdot^-$ it was considered to be a suitable neutral salt in our experiments.

4.6. Kinetics of the Simultaneous Equilibria (3.1) and (4.1)

In studying the kinetics of these, and any, equilibria, one must consider firstly the growth or decay of the radicals corresponding to the approach to equilibrium, and secondly the decay of the radicals once equilibrium has been established.

In the present study, $SO_4\cdot^-$ was produced during the pulse and decayed by reaction with chloride until an equilibrium with Cl· had been reached. Simultaneously, Cl· reacted with chloride until the equilibrium with $Cl_2\cdot^-$ was reached. The solutions to the differential equations for this kinetic scheme indicate that the rates of these processes are described by $\lambda(1)$ and $\lambda(2)$, see Appendix 2. The rate of decay of the radicals at equilibrium is described by $\lambda(3)$, comprising the reactions of Cl·, $Cl_2\cdot^-$ and $SO_4\cdot^-$ with water and t-BuOH.

Thus, the concentration / time profile for $Cl_2\cdot^-$ is given by equation [4.1].

$$[Cl_2\cdot^-] = C_1 e^{\lambda(1)t} + C_2 e^{\lambda(2)t} + C_3 e^{\lambda(3)t} \quad [4.1]$$

Using existing literature values for the rate constants,[3,9] it can be calculated that $|\lambda(1)| >> |\lambda(2)| >> |\lambda(3)|$, with half-lives, i.e. ln 2 / λ(i), of the order 50 ns, 1 μs and 100 μs for i = 1, 2 and 3, respectively. Therefore the first term in equation [4.1] is so fast that it shrinks to zero on the time-scale of the electron pulse, and can be neglected. Physically, this means the overall rate of approach to equilibrium, comprising the growth of $Cl_2\cdot^-$ and fast decay of $SO_4\cdot^-$, is determined by $\lambda(2)$. Hence equation [4.1] reduces to an expression involving only two terms, representing the first-order growth and decay of $Cl_2\cdot^-$, equation [4.2]. Similarly, the biexponential decay of $SO_4\cdot^-$ is given by equation [4.3].

$$[Cl_2\cdot^-] = C_2 e^{\lambda(2)t} + C_3 e^{\lambda(3)t} \quad [4.2]$$

$$[SO_4\cdot^-] = C_4 e^{\lambda(2)t} + C_5 e^{\lambda(3)t} \quad [4.3]$$

In order to test the double equilibrium mechanism, experiments were performed over a range of sulfate and chloride concentrations with [t-BuOH] = 10^{-3} mol dm^{-3} and ionic strength 0.3 mol dm^{-3}, using $Na_2S_2O_8$ as a neutral salt. The rate of growth and decay of $Cl_2\cdot^-$ and the fast decay of $SO_4\cdot^-$ were measured. Efforts to observe the slow decay of $SO_4\cdot^-$ were frustrated by its low concentration and the interfering absorption of $Cl_2\cdot^-$. Typical traces obtained in these experiments are shown in Figures 4.4, 4.6 and 4.8, and the kinetic data in Figures 4.5, 4.7 and 4.9. Fitting the data in Figures 4.5 and 4.7 to equation [A2.13] by the method of non-linear least squares analysis, while fixing the other rate constants at the values of Ref. 9 and the present study, gave estimates for $k_{4.1}$ and $k_{-4.1}$. Equation [A2.13] indicates that $\lambda(2)$ has the limits $k_{4.1}[Cl^-]$ and $k_{-3.1}$ as $[SO_4^{2-}]$ and $[Cl^-]$ tend to zero, respectively, with which literature values[9,10] of 6.18×10^8 $[Cl^-]$ s^{-1} and 6×10^4 s^{-1} and the results of this study, are consistent.

Figure 4.4 *The absorbance at 340 nm following pulse radiolysis of an argon-saturated solution containing* $[SO_4^{2-}] = 0.1$ *and* $[Cl^-] = [t\text{-BuOH}] = [S_2O_8^{2-}] = 10^{-3}$ *mol dm*$^{-3}$ *at pH ca. 6 using a dose of ca. 1 Gy. The red line is a fitted first-order growth.*

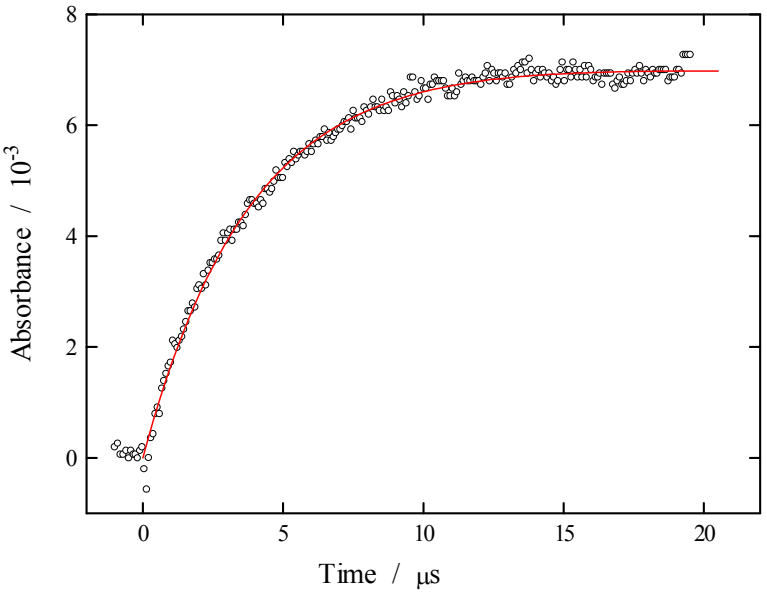

Figure 4.5 *Effect of* $[Cl^-]$ *on* k_{obs} *for the first-order growth of* $Cl_2^{\cdot-}$, °, *and fast decay of* $SO_4^{\cdot-}$, ●, *in 0.1 mol dm*$^{-3}$ SO_4^{2-}. *Error bars are ± 1 S.D.*

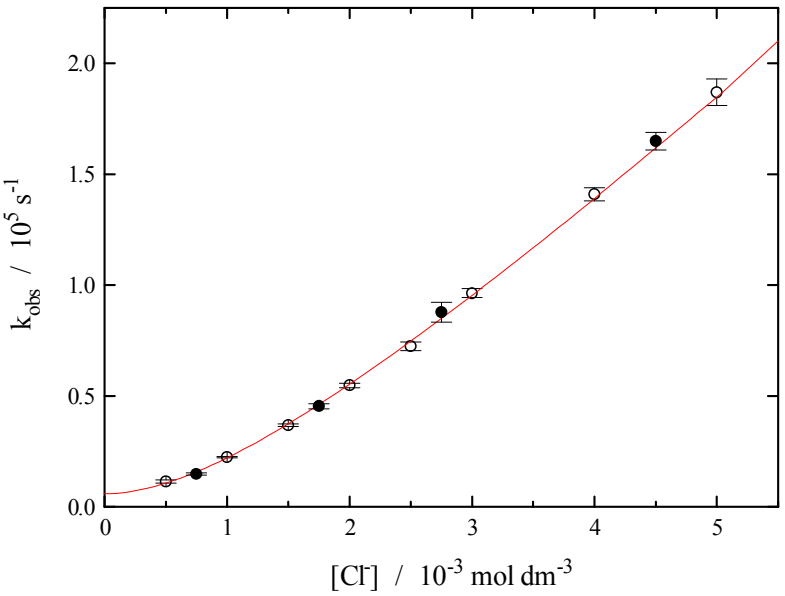

Figure 4.6 *The absorbance at 450 nm following pulse radiolysis of an argon-saturated solution containing* $[SO_4^{2-}] = 0.092$, $[S_2O_8^{2-}] = 8 \times 10^{-3}$ *and* $[Cl^-] = [t\text{-BuOH}] = 10^{-3}$ *mol dm*$^{-3}$ *at pH ca. 6 using a dose of ca. 1 Gy. The red line is a fitted first-order decay to a plateau.*

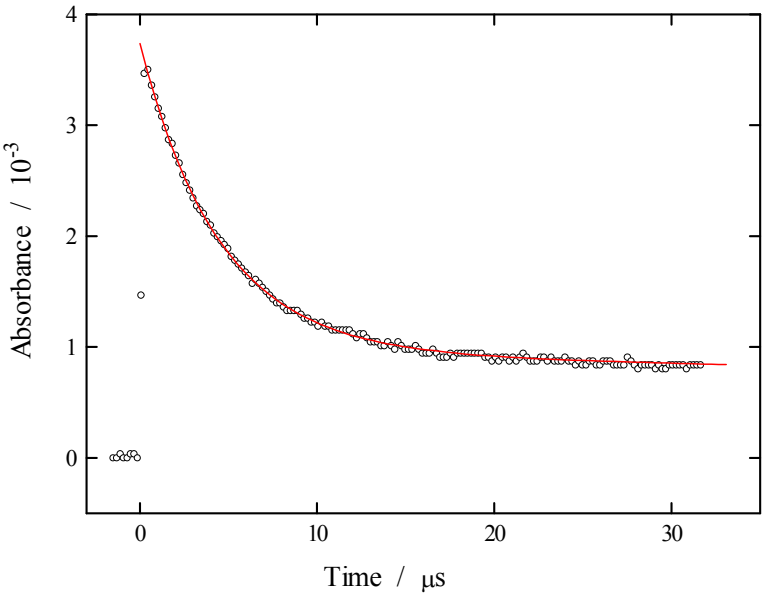

Figure 4.7 *Effect of* $[SO_4^{2-}]$ *on* k_{obs} *for the first-order growth of* $Cl_2^{\cdot-}$, °, *and fast decay of* $SO_4^{\cdot-}$, ●, *in* 10^{-3} *mol dm*$^{-3}$ Cl^-. *Error bars are ± 1 S.D.*

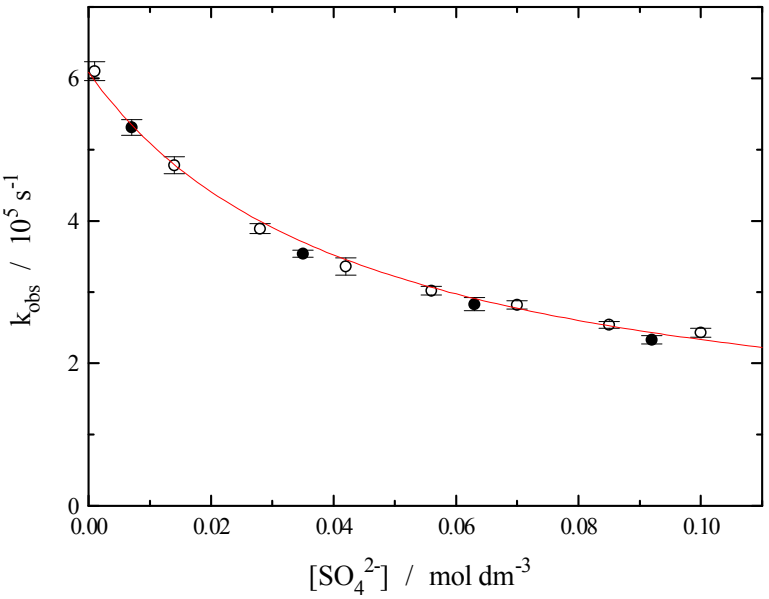

Figure 4.8 *The absorbance at 340 nm following pulse radiolysis of an argon-saturated solution containing* $[SO_4^{2-}] = 0.1$ *and* $[Cl^-] = [t\text{-BuOH}] = [S_2O_8^{2-}] = 10^{-3}$ *mol dm*$^{-3}$ *at pH ca. 6 using a dose of ca. 1 Gy. The red line is a fitted first-order decay.*

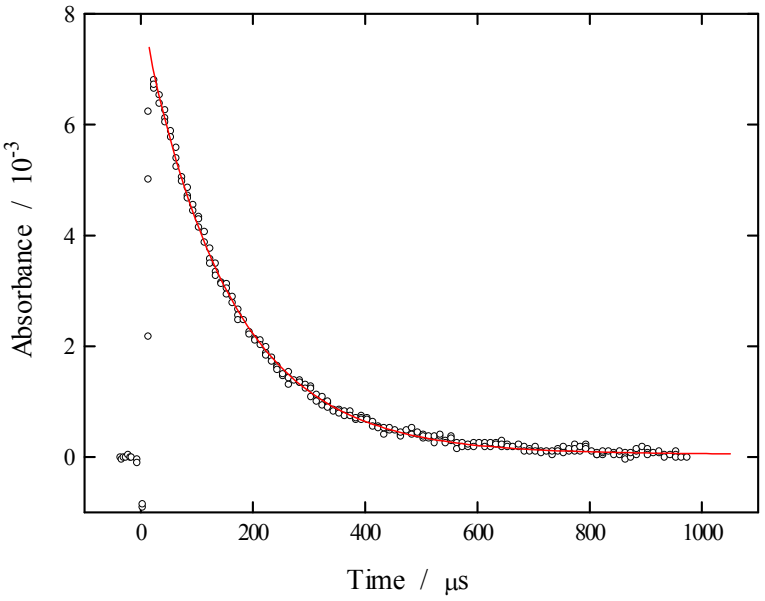

Figure 4.9 *Effect of* $[SO_4^{2-}]$ *on* k_{obs} *for the first-order decay of* $Cl_2^{\cdot-}$ *at* $[Cl^-] = [t\text{-BuOH}] = 10^{-3}$ *mol dm*$^{-3}$*. Error bars are ± 1 S.D.*

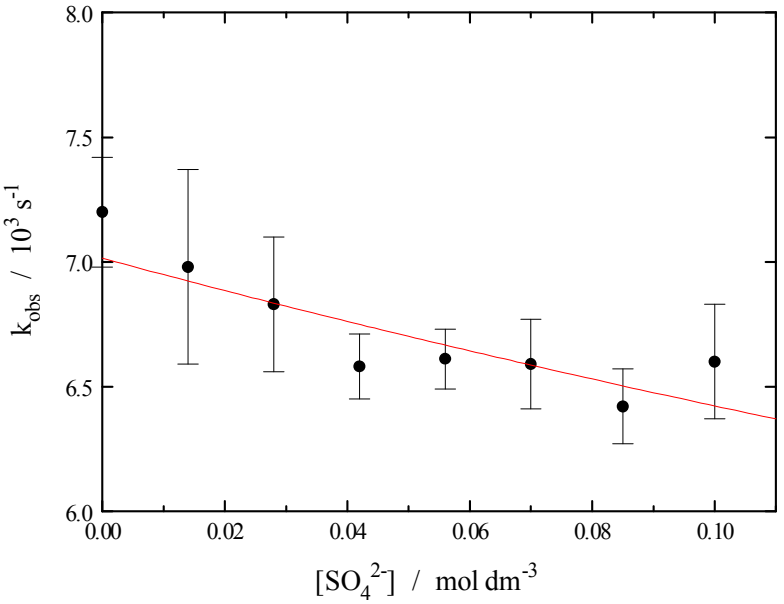

Table 4.1 *Fitted values of $k_{4.1}$ and $k_{-4.1}$ from equation [A2.13] using the data shown in Figures 4.5 and 4.7.*

Rate constant	Fitted from Fig. 4.5 / dm^3 mol^{-1} s^{-1}	Fitted from Fig. 4.7 / dm^3 mol^{-1} s^{-1}	Average value / dm^3 mol^{-1} s^{-1}
$k_{4.1}$	$(5.7 \pm 0.1) \times 10^8$	$(6.4 \pm 0.1) \times 10^8$	$(6.1 \pm 0.2) \times 10^8$
$k_{-4.1}$	$(2.0 \pm 0.1) \times 10^8$	$(2.2 \pm 0.1) \times 10^8$	$(2.1 \pm 0.1) \times 10^8$

4.7. Results and Discussion

The best-fit values of the data in Figures 4.5 and 4.7 to equation [A2.13] were $k_{4.1} = (6.1 \pm 0.2) \times 10^8$ and $k_{-4.1} = (2.1 \pm 0.1) \times 10^8$ dm^3 mol^{-1} s^{-1}, see Table 4.1, in agreement with other determinations of these rate constants.[1,4,10] The data for the decay of $Cl_2\cdot^-$, once equilibrium had been attained, were not fitted to equation [A2.18] due to their lack of precision, see Figure 4.9. However the solid line, which is the expected rate of decay using rate constants from Ref. 9 and the present study, indicates that the correct trend is followed with $[SO_4^{2-}]$.

Obviously, the fitted values of $k_{4.1}$ and $k_{-4.1}$ depend on those chosen for the fixed rate constants in equations [A2.13] and [A2.18] and so it is appropriate to consider the reliability of these data. There is no serious disagreement in the literature on the magnitude of $k_{3.1}$ for which measured values lie in the range $(6.5 \text{ to } 8.5) \times 10^9$ dm^3 mol^{-1} s^{-1}.[9,11,12] It is believed that the higher value, reported by our laboratory, is the more reliable as it was obtained from relatively simple first-order growth kinetics in contrast to the results of Klaning and Wolff[11] and Nagarajan and Fessenden,[12] which were obtained, respectively, by competition kinetics in alkaline solutions containing ClO^- and by monitoring the return to equilibrium following laser photolysis of $Cl_2\cdot^-$.

The value of $k_{-3.1}$ is more uncertain as it has been calculated from $k_{3.1}$ and the equilibrium constant $K_{3.1}$, which has been the subject of disagreement in the literature.[9] Our recent determination of $K_{3.1} = 1.4 \times 10^5$ dm^3 mol^{-1} is in agreement with the long-standing literature value of 1.9×10^5 dm^3 mol^{-1},[13]

suggesting that $k_{-3.1}$ is in the range (4 to 6) × 10^4 s^{-1}. Strong evidence for the higher of these values comes from plots of k_{obs} *vs* [t-BuOH] for the rate of decay of $Cl_2\cdot^-$, which have the limiting value $k_{-3.1}$ as [t-BuOH] is increased (see Section 3.6). The highest k_{obs} measured in our laboratory have been in the range (6 to 7) × 10^4 s^{-1} at 0.1 mol dm^{-3} t-BuOH and 10^{-3} mol dm^{-3} chloride.

Rate constants for the reactions leading to loss of Cl·, i.e. those with t-BuOH ($k_{3.5}$), water ($k_{3.7}$), and persulfate, show agreement in the literature. Values for t-BuOH of (6.2 and 6.5) × 10^8 dm^3 mol^{-1} s^{-1} have been obtained in our laboratory using two different experimental methods.[4,9] The rate constant of the water reaction has been found generally to be in the range (1.6 to 2.5) × 10^5 s^{-1} by a number of laboratories using different experimental methods.[1,9,11,14]

The $Cl_2\cdot^-$ and $SO_4\cdot^-$ loss reactions were not considered in the fitting of λ(2) due to their low rate constants (see Appendix 2), and therefore have no effect on the fitted values in Table 4.1. Disagreement exists over the rate constant for the reaction of $Cl_2\cdot^-$ with water, $k_{3.8}$. The reason for the difference between our value of 1.3 × 10^3 s^{-1} and that of Jacobi *et al.*,[14] who reported < 610 s^{-1} from experiments in acidic solution, is unclear. However it is curious that experiments performed in alkaline solution, also by Jacobi *et al.*,[14] to determine $k(Cl_2\cdot^- + OH^-)$, have an intercept on the plot of k_{obs} *vs* $[OH^-]$ more consistent with our value than the upper limit of 610 s^{-1}.

$$Cl\cdot/Cl_2\cdot^- + H_2O \leftrightarrow HOClH\cdot \leftrightarrow H^+ + HOCl\cdot^- \leftrightarrow Cl^- + \cdot OH + H^+ \qquad (3.9)$$

A resolution of the discrepancy between these observations is achieved by considering the reverse reactions of equilibrium (3.9), which are significant at high $[Cl^-]$ and low pH.[13,15] Under the acidic conditions used by Jacobi *et al.*, i.e. pH 4 and $[Cl^-]$ up to 0.1 mol dm^{-3} with no ·OH scavenger, the $Cl_2\cdot^-$ decays only to its equilibrium concentration. The subsequent decay proceeds by radical-radical reactions, which occur slowly at low radical concentrations, and

therefore very little loss of $Cl_2\cdot^-$ takes place. In our previous work and in the alkaline experiments of Jacobi *et al.*, the removal of ·OH by t-BuOH and the effect of high pH, respectively, ensure that equilibrium (3.9) lies far to the right and therefore the first-order decay by reactions (3.7) and (3.8) occurs to completion. This reaction scheme is discussed further in Section 5.7.8.

Investigations by DeFelippis *et al.*[16] of a double equilibrium mechanism involving $Br_2\cdot^-$, Br· and $N_3\cdot$, similar to that of $Cl_2\cdot^-$, Cl· and $SO_4\cdot^-$ studied in this work, revealed a non-linear dependence of the rate of formation of $N_3\cdot$ on $[Br^-]$. A rate law comparable to equation [A2.8] was derived from two differential equations (*cf.* equations [A2.1] and [A2.3]) and the mass-balance relation, $[Br_2\cdot^-] + [Br\cdot] + [N_3\cdot] = [Br_2\cdot^-]_o$, which relies upon the condition that no loss reactions occur, i.e. that f = 0 in equation [A2.2]. In the present study, the use of a mass-balance relation, $[Cl_2\cdot^-] + [Cl\cdot] + [SO_4\cdot^-] = [SO_4\cdot^-]_o$, would not be valid due to the high reactivity of Cl· towards water and t-BuOH. These reactions cause a significant loss of the radical yield during the approach to equilibrium, and necessitate additional terms in the rate law. Hence equation [A2.8] (and therefore [A2.13]) is an extension of the expression derived in Ref. 16 to kinetic schemes involving fast loss reactions.

DeFelippis *et al.*[16] expressed concern that an equilibrium reported by Alfassi *et al.*[17] between the dibromide anion and azide radicals, $Br_2\cdot^- + N_3^- \leftrightarrow 2Br^- + N_3\cdot$, actually involved the bromine atom equilibrium $Br\cdot + N_3^- \leftrightarrow Br^- + N_3\cdot$. In combination with $Br\cdot + Br^- \leftrightarrow Br_2\cdot^-$, this resulted in a double equilibrium mechanism rather than the single equilibrium proposed by Alfassi *et al.* Subsequent argument by Huie *et al.*,[3] presumably in support of Alfassi *et al.*, that the mechanism whereby equilibrium is attained is not relevant to the determination of the equilibrium constant, is incorrect. This is verified by the present study, in which the determination of the equilibrium constant, $K_{4.1}$, depends on knowledge of the relevant kinetic equations for the mechanism by which equilibrium is attained.

4.8. Conclusions

The rate constants obtained at 25 ºC and 0.3 mol dm^{-3} ionic strength in this study are listed in Table 4.2. Only the forward reaction of equilibrium $K_{4.1}$ was influenced by ionic strength, and so it was possible to obtain a value for $K_{4.1}$ at infinite dilution by substituting $k_{4.1}$ ($I \rightarrow 0$) = 2.47×10^8 dm^3 mol^{-1} s^{-1} in place of the high ionic strength value.[10] This gives $K_{4.1}$ ($I \rightarrow 0$) = 1.2. The thermodynamic equilibrium constant, $K_{4.1}$ ($I \rightarrow 0$), allows a calculation of the reduction potential of Cl· to be made in relation to that of $SO_4{\cdot}^-$, which shows $SO_4{\cdot}^-$ to be the stronger oxidant by 5 mV, see equation [4.4].[18]

$$\Delta E^\circ = \frac{RT \ln K_{4.1}}{F} \approx 5 \times 10^{-3} \text{ V} \qquad [4.4]$$

Based on $E^o(SO_4{\cdot}^-/SO_4^{2-})$ = 2.43 V, $E^o(Cl{\cdot}/Cl^-)$ is calculated to be *ca*. 2.42 V, in agreement with estimates of between 2.2 and 2.6 V.[19] The reduction potential of $Cl_2{\cdot}^-$ may also be calculated from $K_{3.1} = 1.4 \times 10^5$ dm^3 mol^{-1} to be 2.12 V,[9] also in agreement with previous reports of between 2.09 and 2.30 V.[19]

Table 4.2 *Rate constants determined in this study at 25 ºC and I = 0.3 mol* dm^{-3}.

Reaction	Rate constant / dm^3 mol^{-1} s^{-1}	Literature / dm^3 mol^{-1} s^{-1}	Reference
$SO_4{\cdot}^-$ + water	690 ± 120 [a]	360 to 660 [a]	(see text)
$SO_4{\cdot}^-$ + t-BuOH	$(7.8 \pm 0.2) \times 10^5$	*ca*. 8×10^5	5
$SO_4{\cdot}^-$ + $S_2O_8^{2-}$	$< 1.5 \times 10^3$	$< 10^4$	(see text)
$SO_4{\cdot}^-$ + Cl^-	$(6.1 \pm 0.2) \times 10^8$	6.18×10^8 [b]	10
Cl· + SO_4^{2-}	$(2.1 \pm 0.1) \times 10^8$	1.7×10^8	4
Equilibrium 4.1	$K_{4.1} = (2.9 \pm 0.2)$ [c]	$K_{4.1} = 1.9$ [c,d]	3

[a] Units s^{-1} [b] At I = 0.4 mol dm^{-3} [c] No units [d] At I = 0.1 mol dm^{-3}

Despite differences in the experimental method and analysis, our value for $K_{4.1}$ is in agreement with that of Huie *et al.*,[3] who reported 1.9 at 0.1 mol dm^{-3} ionic strength. The present study has been performed over a wider concentration range than that of Huie *et al.*, and elucidated characteristic features of the double equilibrium mechanism that are often obscured by numerical modelling. Our analysis has shown that the negative intercept obtained by Huie *et al.* arises from the erroneous assumption of a linear dependence on the rate of decay of $SO_4{\cdot}^-$ with $[Cl^-]$, whereas the correct dependence is given by equation [A2.13], see Figure 4.5. The decrease in the rate of growth with $[SO_4^{2-}]$ is another aspect of the double equilibrium mechanism observed in this study and by Huie *et al*. These trends have also been exhibited in experiments using NO_3^- in place of SO_4^{2-}, suggesting that there is an equilibrium between $NO_3{\cdot}$ and $Cl{\cdot}$, reaction (4.5).[20] Although this is at variance with a number of studies which have assumed irreversibility, further experiments have provided strong evidence for an equilibrium reaction, and much of the disagreement between previous authors has been resolved.[21]

$$NO_3{\cdot} + Cl^- \leftrightarrow Cl{\cdot} + NO_3^- \qquad (4.5)$$

In relation to the chemistry of cloud water, it is an interesting observation that there is such interplay amongst the strongly oxidising radicals, i.e. $\cdot OH$, $SO_4{\cdot}^-$, $NO_3{\cdot}$, $Cl{\cdot}$. It is apparent that any of these radicals may undergo conversion to another by a direct reaction and therefore that no one radical acts as a sink. Instead, the radicals will be equilibrated according to the chloride, sulfate, nitrate and H^+ concentrations so that each contributes to the chemistry within the cloud droplet. For example, at high $[Cl^-]$ the balance of the equilibria is such that the radical chemistry of $Cl{\cdot}$ and $Cl_2{\cdot}^-$ will be important, whilst at high $[SO_4^{2-}]$ that of $SO_4{\cdot}^-$ will predominate. Given that these radicals react with organic species to form a differing range of products,[22] some variation in the organic composition of the cloud droplet may be expected as a result of the inorganic ion concentrations.

Figure 4.10 *Simulation of $[Cl_2^{\cdot -}]$, $[Cl^{\cdot}]$, $[SO_4^{\cdot -}]$, $Q_{3.1}(t)$, $Q_{4.1}(t)$ and k_{eff} vs time in a typical experiment. The $SO_4^{\cdot -}$ is formed at t = 0, [t-BuOH] = $[Cl^-] = 10^{-3}$ and $[SO_4^{2-}] = 0.1$ mol dm^{-3}.*

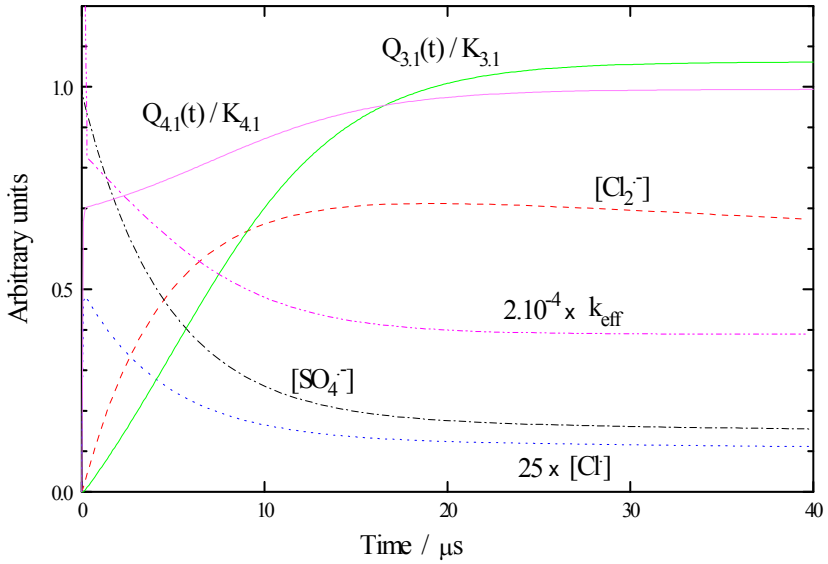

For comparison with the single equilibrium of Chapter 3, see Figure 3.6, in Figure 4.10 is shown a FACSIMILE[23] simulation of the approach to equilibrium for the double equilibrium mechanism. As discussed in Section 4.7, the rate of loss of the radical yield $[R^{\cdot}] = [Cl_2^{\cdot -}] + [Cl^{\cdot}] + [SO_4^{\cdot -}]$, given by k_{eff} of equation [4.5], is significant during the approach to equilibrium and therefore the mass-balance relationship $[Cl_2^{\cdot -}] + [Cl^{\cdot}] + [SO_4^{\cdot -}] = [SO_4^{\cdot -}]_o$ cannot be used.

$$k_{eff} = -\frac{d\ln[R^{\cdot}]}{dt} = \frac{k_{3.5}[t-BuOH]}{Q_{3.1}(t)[Cl^-] + 1 + ([SO_4^{2-}]/Q_{4.1}(t)[Cl^-])} \qquad [4.5]$$

$Q_{3.1}(t)$ and $Q_{4.1}(t)$ are the equilibrium quotients for $K_{3.1}$ and $K_{4.1}$, respectively. At $t \rightarrow \infty$, equation [4.5] takes the form of equation [A2.17].

4.9. References

1. W. J. McElroy, *J. Phys. Chem.*, 1990, **94**, 2435
2. P. Warneck, in Chemistry of the Natural Atmosphere, Academic Press Inc., London, 1988
3. R. E. Huie, C. L. Clifton and P. Neta, *Radiat. Phys. Chem.*, 1991, **38**, 477
4. G. V. Buxton, M. Bydder, G. A. Salmon and J. E. Williams, to be published
5. P. Neta, R. E. Huie and A. B. Ross, *J. Phys. Chem. Ref. Data*, 1988, **17**, 1027
6. Z.-C. Bao and J. R. Barker, *J. Phys. Chem.*, 1996, **100**, 9780
7. See reference 6 and references therein
8. W. J. McElroy and S. J. Waygood, *J. Phys. Chem.*, 1990, **86**, 2557
9. G. V. Buxton, M. Bydder, G. A. Salmon, *J. Chem. Soc.*, *Faraday Trans.*, 1998, **94**, 653
10. R. E. Huie and C. L. Clifton, *J. Phys. Chem.*, 1990, **94**, 8561
11. U. Klaning and T. Wolff, *Ber. Bunsenges. Phys. Chem.*, 1985, **89**, 243
12. V. Nagarajan and R. W. Fessenden, *J. Phys. Chem.*, 1985, **89**, 2330.
13. G. G. Jayson, B. J. Parsons and A. J. Swallow, *J. Chem. Soc., Faraday Trans. 1*, 1973, **69**, 1597
14. H.-W. Jacobi, H. Herrmann and R. Zellner, *Ber. Bunsenges. Phys. Chem.*, 1997, **101**, 1909
15. M. Anbar and J. K. Thomas, *J. Phys. Chem.*, 1964, **68**, 3829
16. M. R. DeFelippis, M. Faraggi and M. H. Klapper, *J. Phys. Chem.*, 1990, **94**, 2420
17. Z. B. Alfassi, A. Harriman, R. E. Huie, S. Mosseri and P. Neta, *J. Phys. Chem.*, 1987, **91**, 2120
18. P. W. Atkins, in Physical Chemistry 4th ed., Oxford University Press Publishers, Oxford 1990
19. D. M. Stanbury, in Advances in Inorganic Chemistry Vol. 33, Academic Press Publishers 1989
20. G. V. Buxton, J. L. Eccles, G. A. Salmon, Proceedings of EUROTRAC Symposium '92, SPB Academic Publishing, The Netherlands 1993

21. G. V. Buxton, G. A. Salmon, J. Wang, *Phys. Chem. Chem. Phys.*, 1999, **1**, 3589

22. B. C. Gilbert, J. K. Stell, W. J. Peet and K. J. Radford, *J. Chem. Soc.*, *Faraday Trans. 1*, 1988, **84**, 3319

23. A. R. Curtis and W. P. Sweetham, FACSIMILE/CHECKMAT USER'S MANUAL, UKAEA, 1987, AERE R12805

Chapter 5

The Reactions of Cl· with Solutes

5.1. Introduction

The Cl· atom may be formed in cloud droplets by the reaction of chloride with strongly oxidising radicals such as NO_3·, SO_4·$^-$ and ·OH,[1,2,3,4] which are well known atmospheric species. In the presence of chloride equilibrium (3.1) is established, for which $K_{3.1} = 1.4 \times 10^5$ dm^3 mol^{-1}.[5]

$$Cl\cdot + Cl^- \leftrightarrow Cl_2\cdot^- \qquad (3.1)$$

The chloride concentrations typically found in cloud water of 10^{-4} mol dm^{-3} mean that Cl_2·$^-$ is likely to be the predominant form of radical chlorine in the atmospheric aqueous phase.[6] Perhaps for this reason, and because of the scarcity of available data, most atmospheric chemistry models have included the reactions of Cl_2·$^-$ whilst neglecting those of the Cl· atom.[7] However, this study and previous work[5,8,9] show that Cl· reacts rapidly with many species and can therefore contribute to the loss of Cl_2·$^-$ through equilibrium (3.1) even at high chloride concentrations. For example, in the presence of 1 mol dm^{-3} chloride the diffusion controlled rate constant for a Cl· reaction would give rise to an apparent rate constant for Cl_2·$^-$ of *ca*. 6×10^4 dm^3 mol^{-1} s^{-1}, see equation [5.1] (*cf*. equation [3.1] with $k_{3.6} = k_{3.7} = k_{3.8} = 0$).

$$k_{obs} = \frac{k[S]}{1 + K_{3.1}[Cl^-]} = \frac{8 \cdot 5 \times 10^9 [S]}{1 \cdot 4 \times 10^5} \approx 6 \times 10^4 [S]\ s^{-1} \qquad [5.1]$$

Many Cl_2·$^-$ rate constants have been reported to be of this magnitude,[10,11,12] some having been determined at [Cl$^-$] < 1 mol dm^{-3}, without due consideration of the accompanying Cl· reactions. Since many reactions of the Cl· atom occur at close to the diffusion controlled limit, their effect on the Cl_2·$^-$ decay can be substantial. Additionally, a loss of equilibrium at relatively low solute concentrations means that kinetic data do not, in general, conform to equation [5.1]. In the above example, non-equilibrium conditions apply when [S] > 0.1 mol dm^{-3}, insofar as the ratio [Cl_2·$^-$]/[Cl$^-$][Cl·] deviates from $K_{3.1}$ by more than 10 % (*cf*. equation [A1.11]). Prior to Ref. 5, studies of the reactions of Cl· and

$Cl_2\cdot^-$ did not take this non-equilibrium behaviour into account, and so rate constants derived using equilibrium (3.1) and equation [5.1] must be regarded with some caution.

The current work aims to study the reactions of Cl· independently of equilibrium (3.1), using the photolysis of chloroacetone as a source of Cl· atoms. In this way complications such as loss of equilibrium, first- and second-order reactions of $Cl_2\cdot^-$ and ionic strength effects on $Cl_2\cdot^-$ reactions are avoided. A similar approach has been used to study the reactions of the Br· atom independently of the $Br\cdot + Br^- \leftrightarrow Br_2\cdot^-$ equilibrium.[13] Whilst the present accumulation of rate data is intended primarily to be of use in the modelling of aqueous phase cloud chemistry, it is hoped that future studies involving $Cl_2\cdot^-$ will benefit from an increased knowledge of the Cl· side of equilibrium (3.1).

5.2. Experimental Approach

Chloroacetone was purified by the method described in Section 2.3.3. In aqueous solution the hydrolysis of chloroacetone has been suggested,[16] reaction (5.1), resulting in chloride contamination which is undesirable due to the formation of $Cl_2\cdot^-$ by reaction (3.1).

$$CH_3COCH_2Cl + H_2O \rightarrow CH_3COCH_2OH + Cl^- + H^+ \qquad (5.1)$$

To test whether reaction (5.1) had a significant effect in our experiments, a stock solution of 0.2 mol dm^{-3} chloroacetone was prepared and stored at room temperature for several hours. The pH was monitored over this period and found to remain constant at pH *ca*. 5. Aliquots of the stock solution were periodically removed and diluted to 2×10^{-2} mol dm^{-3}, before saturating with argon and subjected to LFP. Any build-up of chloride from reaction (5.1) would have resulted in variation in the traces over the course of the experiment, similar to the effect of multiple pulsing (see below), however no such variation was observed. These results indicate that chloroacetone does not hydrolyse on the time-scale of an experimental session. The slight acid pH of the stock

solution was therefore due to reactions that occurred during storage, perhaps a carbonyl condensation, reaction (5.2),[14] followed by hydrolysis, reaction (5.1).

$$2\ CH_3COCH_2Cl \rightarrow \text{aldol} \rightarrow H_2O + \text{product} \qquad (5.2)$$

The discoloration of purified chloroacetone over a period of months was attributed to a build-up of the product of reaction (5.2), which is presumably chlorinated mesityl oxide, and for this reason fresh batches were prepared regularly. Since a stoichiometric amount of H^+ is produced, the pH of the stock solution gives an indication of the purity and hence it was estimated that the impurity concentration (comprising of chloride and the product of reaction (5.2)) was < 0.01 %.

5.3. Laser Flash Photolysis

The photolysis of chloroacetone has been demonstrated to produce chlorine atoms.[15,16] In this study, chlorine atoms were generated by the 248 nm laser photolysis of Ar-saturated solutions containing chloroacetone, reactions (5.3) and (5.4).

$$CH_3COCH_2Cl + h\nu \rightarrow {}^1[CH_3COCH_2Cl]^* \qquad (5.3)$$

$${}^1[CH_3COCH_2Cl]^* \rightarrow \cdot CH_2COCH_3 + Cl\cdot \qquad (5.4)$$

The photolysis of 2×10^{-2} mol dm^{-3} chloroacetone produced an immediate absorbance at 320 nm followed by a first-order decay to a plateau, the rate of which was increased by the addition of t-BuOH, see Figure 5.3.

Variation was observed with increasing number of pulses to the same solution, and for this reason each recorded trace was the result of a single pulse only. Simulations using FACSIMILE[17] confirmed that this variation could be explained by a build-up of chloride produced from the Cl· decay, and hence the formation of strongly absorbing $Cl_2\cdot^-$ in subsequent pulses.

Figure 5.1 *Spectra at 100 ns (open data points) and 5 μs (closed data points) following LFP of an Ar-saturated solution containing 2 × 10^{-2} mol dm^{-3} chloroacetone and 10^{-2} mol dm^{-3} t-BuOH at pH ca .6.*

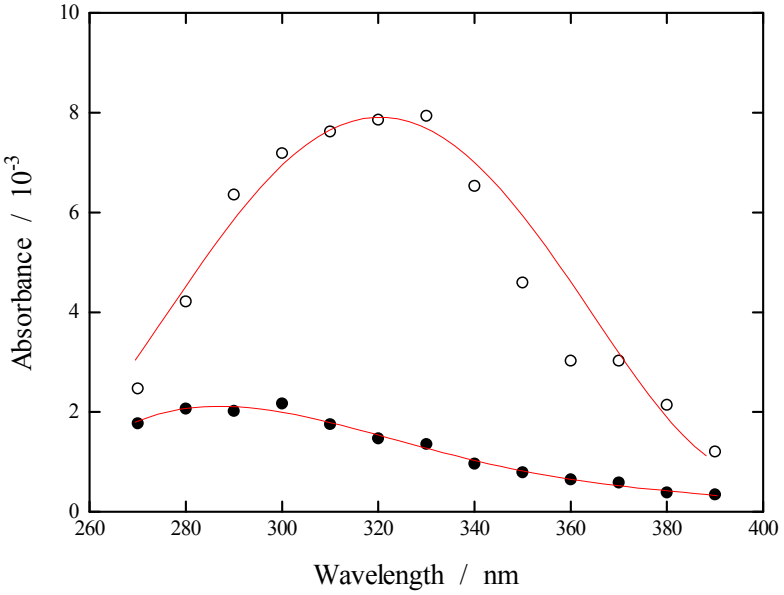

In the presence of 10^{-2} mol dm^{-3} t-BuOH, > 95 % of the Cl· was converted to t-BuOH radicals, none of which absorbs in the range 260 to 400 nm. Figure 5.1 shows the spectra at 100 ns and at the plateau, in agreement with spectra reported in the literature for the Cl· atom[9,16] and the $\cdot CH_2COCH_3$ radical,[18] which has a molar absorption coefficient of 800 dm^3 mol^{-1} cm^{-1} at 295 nm. From this, the yield of $\cdot CH_2COCH_3$ was calculated to be (2.5 ± 0.5) × 10^{-6} mol dm^{-3} and, because [Cl·] = [$\cdot CH_2COCH_3$], it was possible to make an estimate of ε(Cl·). Correcting for *ca*. 0.8 half-lives of the Cl· decay during the first 100 ns, gave a value of ε(Cl·) ≈ 4500 dm^3 mol^{-1} cm^{-1} at 320 nm which, although approximate because of the large correction, is in agreement with literature values (see Chapter 3).

In the absence of t-BuOH, the decay was slower and was attributed to reactions of the Cl· atom with chloroacetone and water, reactions (5.5) and (3.7).

$$Cl\cdot + CH_3COCH_2Cl \rightarrow Cl^- + \text{products} \qquad (5.5)$$

$$Cl\cdot + H_2O \rightarrow Cl^- + \text{products} \qquad (3.7)$$

Figure 5.2 *Spectra at 100 ns (open data points) and 10 μs (closed data points) following LFP of Ar- (□) and O_2- (Δ) saturated solutions containing 5×10^{-3} mol dm^{-3} chloroacetone at pH ca .6. Also shown are data from Figure 5.1 (°) multiplied by 0.5.*

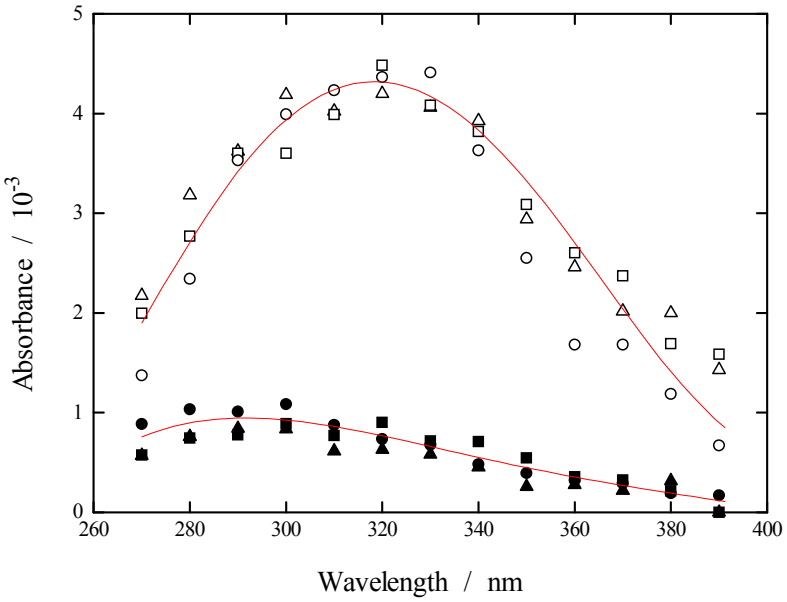

There was a slight decay of the plateau compared with the previous system, which could not be explained by the self-reaction of the organic radicals on the time-scales used. Therefore it was thought that the chloride concentration, from impurity in the chloroacetone and as the product of reactions (5.5) and (3.7), may have been sufficient to form the $Cl_2\cdot^-$ radical via equilibrium (3.1), for which $k_{3.1} = 8.5 \times 10^9$ dm^3 mol^{-1} s^{-1} and $\varepsilon(Cl_2\cdot^-) = 9600$ dm^3 mol^{-1} cm^{-1}.[5] The $Cl_2\cdot^-$ would then decay, giving rise to a decaying plateau. This was confirmed by simulations using FACSIMILE and the observation that, upon reducing the chloroacetone concentration from 2×10^{-2} to 5×10^{-3} mol dm^{-3} (and hence $[Cl\cdot]_o$ from 2.5×10^{-6} to $< 10^{-6}$ mol dm^{-3}), little decay of the plateau occurred. Spectra taken under these conditions are shown in Figure 5.2, with the data from Figure 5.1 included for comparison (scaled by a factor 0.5).

These spectra may be explained in terms of Cl· and $\cdot CH_2COCH_3$ absorptions only, and give no indication of an absorption due to triplet chloroacetone, as

suggested by Treinin and Hayon.[16] Saturating the solutions with O_2, which is known to quench triplets at the diffusion controlled rate, made no difference to the spectra and rate of decay, suggesting that reaction (5.6) is an insignificant decay route for singlet chloroacetone in comparison to reaction (5.4), or that the triplet absorption is small in the region 260 to 400 nm.

$$^1[CH_3COCH_2Cl]^* \rightarrow {}^3[CH_3COCH_2Cl]^* \qquad (5.6)$$

To obtain an estimate of the rate constant for the reaction of Cl· with chloroacetone, $k_{5.5}$, the decay at 320 nm was monitored over the range $[CH_3COCH_2Cl] = (5 \text{ to } 20) \times 10^{-3}$ mol dm^{-3}. The effect of the slight decaying plateau with these slower reactions meant that the first-order fits were less good than those obtained when reactive solutes were present, however the rate was found to increase linearly with gradient, $k_{5.5} = (1.3 \pm 0.2) \times 10^7$ dm^3 mol^{-1} s^{-1}, and intercept, $k_{3.7} = (2.5 \pm 0.5) \times 10^5$ s^{-1}. Some contribution to the rate of decay was expected from the impurities, but using an impurity concentration of < 0.01 % and rate constant of up to 10^{10} dm^3 mol^{-1} s^{-1}, this was estimated to be < 10 % of the observed rate. Rate constant $k_{5.5}$ was also measured by pulse radiolysis using an experimental method less sensitive to chloride impurity (see Section 5.6).

5.4. Reactions of Cl· with Organic Solutes

The decays at 320 nm following laser flash photolysis were analysed for the reactions of Cl· with a number of organic species, see Table 5.1. Under all conditions the absorption-time profile fitted a first-order decay to a plateau, which was due to $\cdot CH_2COCH_3$ and products from reactions of the Cl· atom, see Figure 5.3. The gradients from the plots of k_{obs} *vs* [S] were used to determine the rate constants at 10 ºC intervals from 5 to 35 ºC, see Figure 5.4.

The rate constants for reaction with HCO_2H and CH_3CO_2H were determined at pH 1. The rate constant for reaction with acetone was determined in O_2-saturated solution in order to quench the absorbing acetone triplet. The life-

time of the triplet was measured to be < 1 μs under these conditions, and therefore the first 1 μs of the traces was deleted before analysis. No variation in the rate of decay of Cl· was observed over the range of concentration used, suggesting an upper limit for the rate constant of 5×10^6 dm^3 mol^{-1} s^{-1}. The rate constant for reaction with formaldehyde was determined by pulse radiolysis only, since the laser photolysis experiments showed no variation of k_{obs} with [HCHO]. This is attributed to a carbonyl condensation reaction between HCHO and chloroacetone, effectively removing HCHO from the solution.[14]

Table 5.1 *Rate constants and activation energies for the reactions with organic species measured in this study.*

Species, S	**[S] range / 10^{-3} mol dm^{-3}**	**k at 25 °C / dm^3 mol^{-1} s^{-1}**	**E_a / kJ mol^{-1}**
CH_3COCH_2Cl [a]	0 to 30	$(1.1 \pm 0.1) \times 10^7$	-[b]
" "	5 to 20	$(1.3 \pm 0.2) \times 10^7$	-
CH_3COCH_3	2.5 to 10	$< 5 \times 10^6$	-
CH_3OH	0.1 to 1.0	$(1.0 \pm 0.2) \times 10^9$	12 ± 2
CH_3CH_2OH	0.1 to 0.7	$(1.7 \pm 0.3) \times 10^9$	15 ± 2
$CH_3CH(OH)CH_3$	0.25 to 1.0	$(1.5 \pm 0.1) \times 10^9$	17 ± 1
$(CH_3)_3COH$	0.2 to 1.4	$(6.2 \pm 0.3) \times 10^8$	21 ± 2
HCHO [a]	0.2 to 0.8	$(1.4 \pm 0.1) \times 10^9$	-
CH_3CHO	0.5 to 2.0	$(6.3 \pm 0.4) \times 10^8$	15 ± 2
$HCOO^-$ (pH 6)	0.1 to 0.4	$(4.2 \pm 0.5) \times 10^9$	16 ± 2
HCOOH (pH 1)	2.5 to 10.0	$(1.3 \pm 0.1) \times 10^8$	9 ± 1
CH_3COO^- (pH 6)	0.1 to 0.4	$(3.7 \pm 0.4) \times 10^9$	14 ± 2
CH_3COOH (pH 1)	10 to 40	$(3.2 \pm 0.2) \times 10^7$	8 ± 1

[a] Result from pulse radiolysis [b] Not measured

Figure 5.3 *The absorbance at 320 nm following photolysis of 2 × 10^{-2} mol dm^{-3} chloroacetone and (0.4 to 1.6) × 10^{-3} mol dm^{-3} t-BuOH in argon-saturated solution at pH ca. 6 and 5 ºC. The black lines are fitted first-order decays to a plateau.*

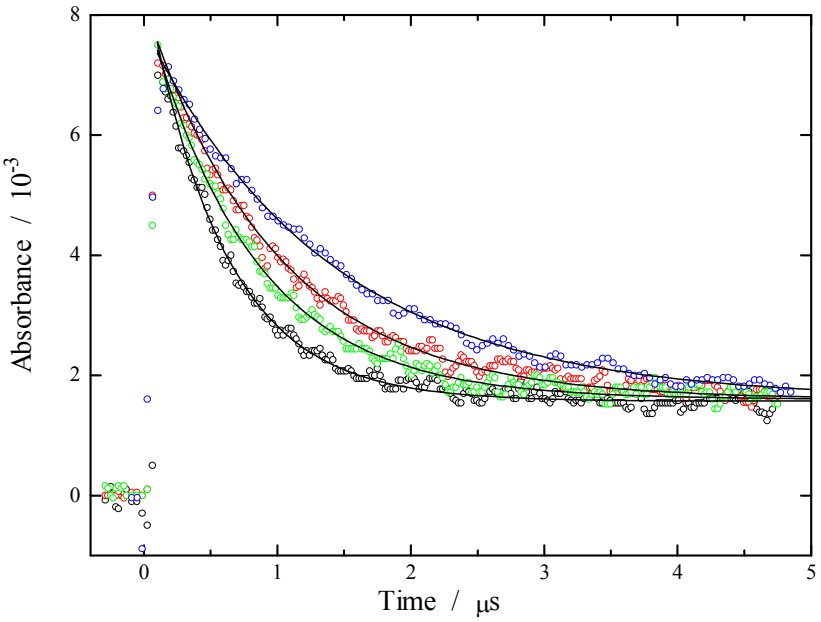

Figure 5.4 *The dependence of k_{obs} on [t-BuOH] for the first-order decay of Cl· at temperatures of 5, 15, 25 and 35 ºC.*

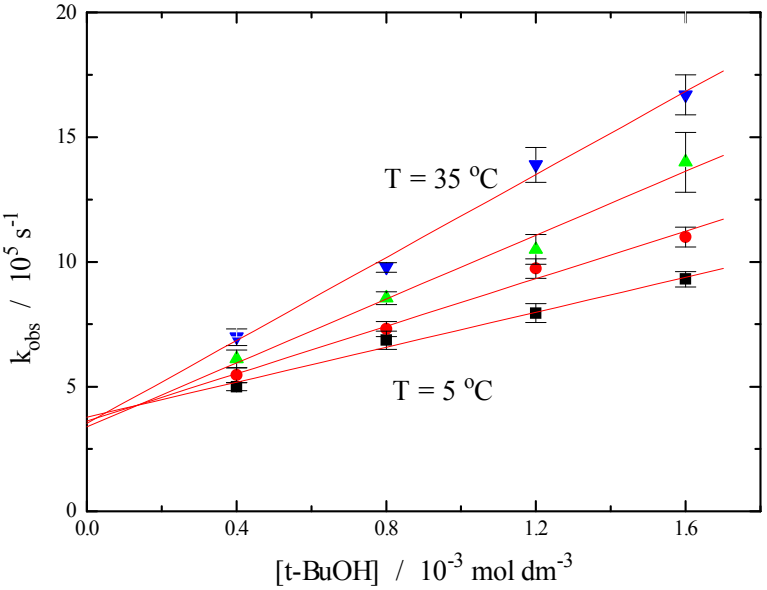

5.5. Reactions of Cl· with Inorganic Solutes

The rate constants for the reactions of Cl· with a number of inorganic species were measured at 25 ºC, see Table 5.2. The pH was adjusted to ensure that the ions were present almost entirely in their basic form, using pK_a values from Ref. 19, whilst avoiding making the solutions alkaline. Although some of these species absorb at 248 nm, yields of the photolysis products were small at the concentrations used and did not contribute significantly to the absorption at 320 nm. Experiments to investigate the reaction of Cl· with the hydroxide ion, studied by Klaning and Wolff,[9] gave traces with large, slowly decaying absorptions upon LFP. This was attributed to OH^- catalysis of reaction (5.2),[14] the product of which presumably photolyses like the mesityl oxide impurity. Therefore all experiments were performed at pH ≤ 7. The reaction of Cl· with ClO_4^- was investigated but no variation was observed in the rate of decay, suggesting an upper limit for the rate constant of 5×10^5 dm^3 mol^{-1} s^{-1}.

Table 5.2 *Rate constants for inorganic species determined in this study.*

Species, S	**[S] range / 10^{-3} mol dm^{-3}**	**E° / V**	**k at 25 °C / dm^3 mol^{-1} s^{-1}**
OCN^- [a]	0.1 to 0.7	2.66	$(2.2 \pm 0.4) \times 10^9$
NO_3^-	2.5 to 10.0	2.5	$(7.6 \pm 0.8) \times 10^7$
SO_4^{2-}	2.5 to 10.0	2.43	$(1.7 \pm 0.2) \times 10^8$
ClO_3^- [a]	0.1 to 2.5	2.1	$(5.0 \pm 0.1) \times 10^8$
OH^- [b]	Not known	1.9	1.8×10^{10}
SCN^- [a]	0.05 to 0.25	1.63	$(5.3 \pm 0.3) \times 10^9$
HCO_3^-	0.1 to 0.7	1.5	$(2.4 \pm 0.5) \times 10^9$
N_3^- [a]	0.05 to 0.25	1.33	$(5.2 \pm 0.4) \times 10^9$
NO_2^- [a]	0.05 to 0.30	1.04	$(5.0 \pm 0.2) \times 10^9$
HSO_3^- [a,c]	0.25 to 4.0	0.63	$(2.8 \pm 0.3) \times 10^8$

[a] Measured by J. E. Williams [b] From Ref. 9 [c] Probably HSO_3^--chloroac. adduct

Figure 5.5 *Spectrum following the reaction of ·OH with chloroacetone from pulse radiolysis of N_2O-saturated solutions containing 5×10^{-4} mol dm^{-3} chloroacetone at pH ca. 6.*

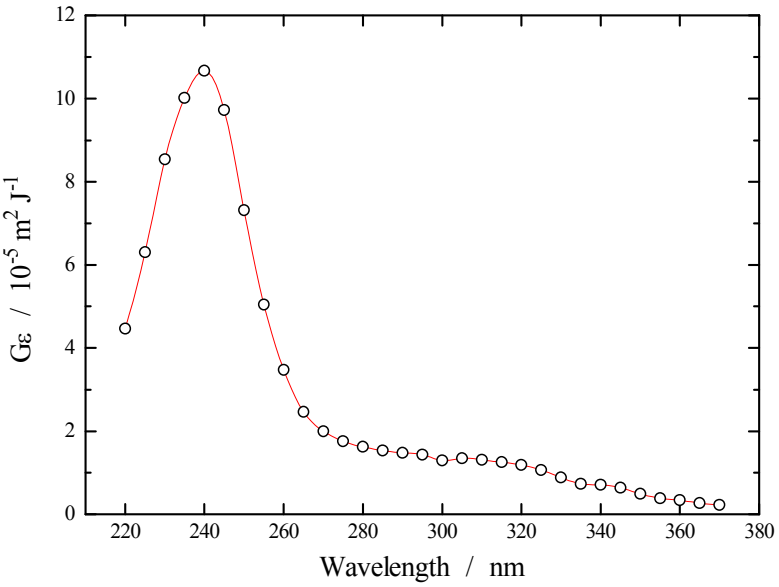

5.6. Pulse Radiolysis

The rate constant of reaction (5.5) was determined by measuring the rate of decay of $Cl_2\cdot^-$ in solutions containing $[S_2O_8^{2-}] = 0.1$, [t-BuOH] = 5×10^{-4}, $[Cl^-]$ = (1 to 5) $\times 10^{-3}$ and [chloroacetone] = (0 to 3) $\times 10^{-2}$ mol dm^{-3}. The chloride impurity in the chloroacetone was negligible in comparison to these chloride concentrations. Gradients of k_{obs} *vs* [chloroacetone] were plotted *vs* 1/$[Cl^-]$ (*cf.* Figure 3.5) from which were obtained $k_{5.5}/K_{3.1}$ = (81 ± 6) s^{-1} and k($Cl_2\cdot^-$ + chloroacetone) = (2.5 ± 1.0) $\times 10^4$ dm^3 mol^{-1} s^{-1}. Hence $k_{5.5}$ = (1.1 ± 0.1) $\times 10^7$ dm^3 mol^{-1} s^{-1}. In a similar way, k(Cl· + HCHO) and k($Cl_2\cdot^-$ + HCHO) were found to be (1.4 ± 0.1) $\times 10^9$ and (1.8 ± 0.5) $\times 10^5$ dm^3 mol^{-1} s^{-1}.

The spectrum of the products of ·OH + chloroacetone was measured in N_2O-saturated solution containing 5×10^{-4} mol dm^{-3} chloroacetone, see Figure 5.5. Two maxima were observed at 240 nm, with Gε = 1.1×10^{-4} m^2 J^{-1}, and *ca.* 300 nm, with Gε = 1.5×10^{-5} m^2 J^{-1}. These perhaps arise from the two different

radicals that can be formed by H-abstraction from either the $-CH_3$ or $-CH_2Cl$ groups of chloroacetone. The overall rate constant, measured by observing the growth of product at 240 nm, was found to be $(1.4 \pm 0.1) \times 10^8$ dm^3 mol^{-1} s^{-1}, in line with the value of $k(\cdot OH + CH_3COCH_3)$ of 1.1×10^8 dm^3 mol^{-1} s^{-1}.[20]

5.7.1. Discussion

The values determined for the reactions of Cl· with t-BuOH and water are in agreement with our previous work performed in chloride solution,[5] the accord between which serves to confirm the value of the equilibrium constant, $K_{3.1}$, which was in some dispute. A number of rate constants have been cited recently, different to those of the present study, e.g. $k(Cl\cdot + \text{t-BuOH}) = 3 \times 10^8$ and $k(Cl\cdot + CH_3CH(OH)CH_3) = 6 \times 10^9$ dm^3 mol^{-1} s^{-1}.[21] The reason for discrepancy is not known due to the unavailability of experimental details, and it is understood that there are no plans to publish this information.[22]

In relation to the determination of rate constants using equilibrium (3.1) and equation [5.1] (see Section 5.1), a recent paper by Jacobi *et al.* has presented a number of rate constants of the $Cl_2\cdot^-$ radical,[12] ranging from 1.4×10^3 (acetone) to 4.8×10^5 dm^3 mol^{-1} s^{-1} (tetrahydrofuran). However two assumptions made in that study, namely that a $[Cl^-]$ of 0.1 mol dm^{-3} was sufficient to suppress any influence of the Cl· atom reactions and that equilibrium (3.1) was always maintained, are incorrect. This is verified in the case of t-BuOH. Firstly, with $k(Cl\cdot + \text{t-BuOH}) = 6.2 \times 10^8$ dm^3 mol^{-1} s^{-1}, it can be calculated from equation [5.1] that an effective $Cl_2\cdot^-$ rate constant of 4.4×10^4 dm^3 mol^{-1} s^{-1} would be observed at 0.1 mol dm^{-3} chloride. This compares with the value obtained by Jacobi *et al.* of 2.6×10^4 dm^3 mol^{-1} s^{-1}, which is undoubtedly lowered by the non-linearity of k_{obs} *vs* [t-BuOH] (see Figure 3.4). Secondly, at the highest [t-BuOH] of 0.5 mol $dm^{-3,}$ the condition under which equilibrium (3.1) is maintained, i.e. equation [A1.12], is not met.

Although with some species there is clearly a significant reaction of the $Cl_2\cdot^-$ radical, e.g. CH_3COCH_3 and HCO_2H, it would seem that most of the rate

constants are dominated by the Cl· atom contribution, see Table 5.3. In view of this, the disagreement between Jacobi *et al.*[12] and Hasegawa and Neta[10] regarding the magnitude of the $Cl_2^{\cdot -}$ rate constants, which was attributed to the formation of a less reactive $NaCl_2^{\cdot}$ complex at high ionic strength, may be seen to be a consequence of the different chloride and solute concentrations used. Following from this, it is evident that the reported activation energies and ionic strength effects reported by Jacobi *et al.* cannot be simply attributed to the $Cl_2^{\cdot -}$ reactions.

It is disappointing that these points were not addressed, despite reports in the literature and presentations at a number of conferences.[5,23,24,25] One further presumption of Jacobi *et al.* was that the $Cl_2^{\cdot -}$ radical reacts by an H-abstraction mechanism. Whilst this is certainly plausible, it remains to be proven by product studies and should not be assumed.

Table 5.3 *A comparison of the effect of Cl· atom reactions on the rate of decay of* $Cl_2^{\cdot -}$.

Species	**Cl· rate constant[a] / dm^3 mol^{-1} s^{-1}**	**From eq. [5.1][b] / dm^3 mol^{-1} s^{-1}**	**$Cl_2^{\cdot -}$ rate constant[c] / dm^3 mol^{-1} s^{-1}**
CH_3OH	1.0×10^9	7.1×10^4	5.1×10^4
CH_3CH_2OH	1.7×10^9	1.2×10^5	1.2×10^5
$CH_3CHOHCH_3$	1.5×10^9	1.1×10^5	1.9×10^5
$(CH_3)_3COH$	6.2×10^8	4.4×10^4	2.6×10^4
HCHO	1.4×10^9	1.0×10^5	3.6×10^4
CH_3COCH_3	$< 5 \times 10^6$	< 360	1.4×10^3
HCO_2H	1.3×10^8	9.3×10^3	8.0×10^4
CH_3CO_2H	3.2×10^7	2.3×10^3	1.5×10^3

[a] This work [b] Taking $[Cl^-] = 0.1$ mol dm^{-3} [c] From Ref. 12, $[Cl^-] = 0.1$ mol dm^{-3}

Figure 5.6 *Plot of log $k_{Cl\cdot}$ vs log $k_{\cdot OH}$ showing the similarity of the rate constants at 25 °C. The line represents $k_{Cl\cdot} = k_{\cdot OH}$.*

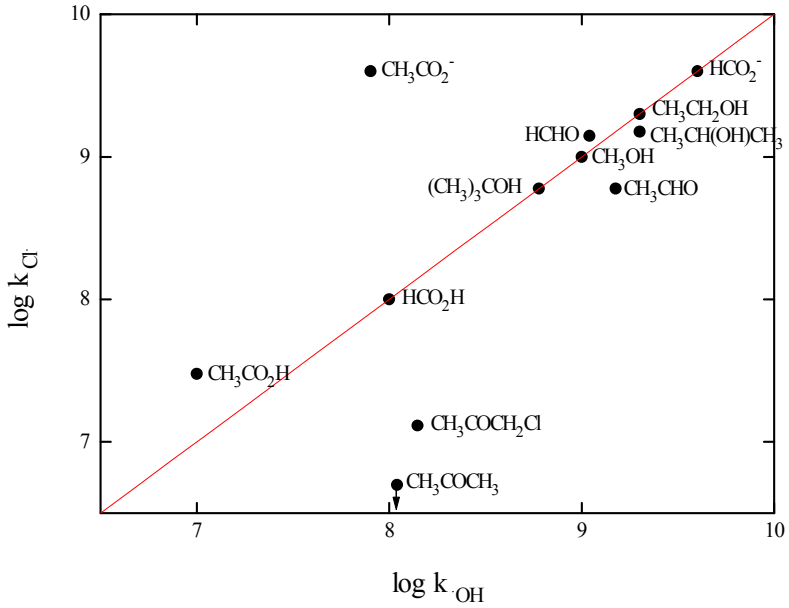

5.7.2. Organic Species

It may be seen from Figure 5.6 and Table 5.4 that the rate constants of the Cl· reactions with organic species correlate with those of the ·OH radical and are generally orders of magnitude greater than those of NO_3· and SO_4·$^-$, which are also somewhat correlated. The similarity between the ·OH and Cl· rate constants at 25 °C is fortuitous, since the activation energies are different and hence the values will not agree as well at different temperatures.

5.7.3. Ketones and Aldehydes

The ·OH radical reacts with ketones and aldehydes by H-abstraction from C-H groups.[26,27,28] The mechanism for the Cl· reactions is not known. In contrast to ·OH there is a significant difference between the Cl· atom rate constants for chloroacetone and acetone. Both are more than 10 times smaller than the ·OH equivalents, see Table 5.4. In trying to understand these results it is noted that a significant difference between chloroacetone and acetone in aqueous solution is the extent to which they undergo hydration; 7 % and 0.1 % at 25 °C, respectively.[29,14]

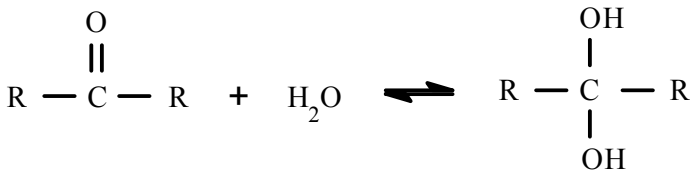

The hydration does not affect the number of available C-H bonds, however it does introduce O-H groups to the molecule with which the Cl· atom is known to react.[8] If the absence of an O-H group in acetone is the reason for its apparent non-reactivity with the Cl· atom, then an H-abstraction from C-H is ruled out as the dominant reaction mechanism. This could also account for the small rate constant of Cl· with chloroacetone, because of the small fraction of hydrated molecules present.

Table 5.4 *Comparison of Cl·, ·OH, $SO_4^{\cdot-}$ and NO_3· radical rate constants and activation energies (in parentheses), using data from Ref. 7 and 11.*

Species, S	**10^{-8} k $_{Cl\cdot}$ /dm^3 mol^{-1} s^{-1}**	**10^{-8} k $_{\cdot OH}$ /dm^3 mol^{-1} s^{-1}**	**10^{-6} k $_{SO4\cdot-}$ /dm^3 mol^{-1} s^{-1}**	**10^{-6} k $_{NO3\cdot}$ /dm^3 mol^{-1} s^{-1}**
CH_3COCH_2Cl	0.12	1.4	-[a]	-
CH_3COCH_3	<0.05	1.1	-	0.0044
CH_3OH	10 (12)[b]	9.7 (5)	8.8 (18)	0.51 (19)
CH_3CH_2OH	17 (15)	19	42 (15)	2.4 (15)
$(CH_3)_3COH$	6.2 (21)	6.0 (10)	0.84	0.066
$CH_3CHOHCH_3$	15 (17)	19 (5)	81 (7)	3.2 (11)
HCHO	14	7.7 (8.5)	14 (11)	0.78 (37)
CH_3CHO	6.3 (15)	24	20	0.49
HCO_2^-	42 (16)	32 (4)	110	57 (18)
HCO_2H	1.3 (9)	1.3 (8)	0.46	0.42 (28)
$CH_3CO_2^-$	37 (13)	0.75 (15)	4.3 (10)	2.5 (32)
CH_3CO_2H	0.32 (8)	0.18 (11)	0.014	0.018 (31)

[a] No literature value available [b] Numbers in parentheses are E_a in kJ mol^{-1}

Hence, in general, there may be a relationship between the Cl· atom rate constant and the extent of hydration of the carbonyl species. With this in mind it is of interest to consider the reactions with the aldehydes HCHO and CH_3CHO, which are 99.9 % and 55 % hydrated, respectively.[14,30] The Cl· atom rate constants show a significant decrease between HCHO and CH_3CHO, again following the extent of hydration, which is opposite to the trend observed with the ·OH radical rate constants. Therefore, whilst ·OH reacts faster with the unhydrated forms of the molecule,[27] it seems that Cl· reacts faster with the hydrated forms. A preference for the Cl· atom to react with hydrated carbonyl compounds implicates the O-H group as the site of reaction, in line with similar findings by Gilbert *et al*.[8]

The reason why an H-abstraction mechanism may be less favourable than electron-transfer is because it would involve considerable charge separation in the transition state, as suggested by Gilbert *et al*. This would increase the energy requirement of the reaction.

$$Cl\cdot + H{-}R \longrightarrow [\, Cl^{\delta-} \cdots H^{\delta+} \cdots R \,] \longrightarrow Cl^- + H^+ + R\cdot$$

5.7.4. Acids

To compare the ·OH and Cl· reactions with RCO_2^- and RCOOH it is necessary to consider firstly the mechanism by which ·OH reacts with these species. The 40-fold difference between k(·OH + HCO_2^-) and k(·OH + HCO_2H) cannot be rationalised in terms of a lower C-H bond strength and it is thought that, whilst ·OH can abstract an H from C-H in both HCO_2^- and HCO_2H, it may also add to HCO_2^- followed by the elimination of water.

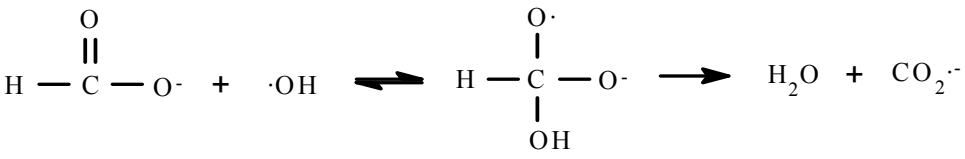

The addition-elimination mechanism is not as favourable with the neutral species because of its lower resonance, which makes the C=O group less available. This explanation for the lower rate constant of HCO_2H in

comparison to HCO_2^- follows that of the similar situation observed with HCO_3^- and CO_3^{2-}, where the greater negative charge of CO_3^{2-} facilitates ·OH addition.[31,32] The more similar rate constants of $CH_3CO_2^-$ and CH_3CO_2H indicate that addition followed by the elimination of methanol is not favourable, and therefore H-abstraction from C-H is the predominant mechanism in both cases. In contrast to ·OH, the magnitude of the Cl· rate constants depends only on the presence or absence of a negative charge. Presumably an electron-transfer is the mechanism for the ions, and with the neutral molecules Gilbert *et al.* have reported electron-transfer from the O-H group as the only mechanism.[8]

5.7.5. Alcohols

There is a remarkable similarity between the rate constants of Cl· measured in this study and those of the ·OH radical. Gilbert *et al.*[8] reported that the reaction of Cl· with t-BuOH is 67 % H-abstraction from C-H and 33 % electron transfer from O-H and that, in general, Cl· atoms react by a combination of electron-transfer and H-abstraction, using ESR identification of the products to obtain branching ratios. However an important reaction not considered was that of Cl· with water, reaction (3.7), which produces ·OH radicals. This would have led to the formation of H-abstraction products from the subsequent ·OH reactions, which would have been attributed to the Cl· reactions. Also, as discussed in the case of t-BuOH, there was a tendency for electron-transfer products to react with the solutes used, e.g. $(CH_3)_3CO\cdot$ + Ti(III), leading to an enhancement of the ratio of H-abstraction to electron-transfer products. For these reasons, the results of Gilbert *et al.* may have shown H-abstraction to be more significant than is the case.

In summary, the results of this study and Gilbert *et al.*[8] are consistent with a mechanism for reaction with oxygen containing organic species by which Cl· attacks at the O-H group, presumably by electron-transfer. The possibility of an H-abstraction reaction from C-H has not been discounted although it is likely to be a less favoured pathway. We observe therefore that, despite broad similarity in the pattern of reactivity of Cl· and ·OH, their reaction mechanisms are

essentially different. This undermines the arguments of Hasegawa and Neta[10] and Jacobi *et al.*[12] in the case of $Cl_2\cdot^-$ and H·, that a similar pattern of reactivity indicates a similar reaction mechanism.

5.7.6. Activation Energies

Activation energies for the Cl· reactions have been found to lie in the range (8 to 21) kJ mol^{-1} for all the organic molecules studied, and are often about 10 kJ mol^{-1} higher than the equivalent ·OH reactions. The activation energies of the fast Cl· atom reactions ($k > 10^9$ dm^3 mol^{-1} s^{-1}) are close to that of the diffusion process of *ca*. 17 kJ mol^{-1},[33a,b] suggesting that the rate of diffusion is the limiting step in these reactions. The activation energies of the fast ·OH radical reactions are rather less, e.g. 4 kJ mol^{-1} for HCO_2^-.[34] This may be understood using an equation for the observed rate constant, k_{obs}, expressed in terms of its component steps of diffusion and reaction, equation [5.2], see Appendix 3.

$$\frac{1}{k_{obs}} = \frac{1}{k_{diff}} + \frac{1}{k_{react}} \qquad [5.2]$$

For a reaction limited by diffusion, $k_{react} >> k_{diff}$ so that k_{obs} is largely determined by k_{diff}, and hence the measured activation energy is that of the diffusion process. This seems to be the case with many Cl· reactions. In situations other than this limiting case, the observed rate constant is a more complicated function of the intermediate rate constants and consequently the activation energy has contributions from several processes. The activation energies of the ·OH reactions conform to this analysis. For example, Elliot *et al.*[34] have found that the activation energy of the fast reaction of ·OH with HCO_2^- is almost independent of the diffusion term except at low temperatures.

The fact that many of the reactions of the Cl· atom are limited by diffusion makes it difficult to assess its true reactivity, i.e. the properties of k_{react}, since the observed rate constants of *ca*. 5×10^9 dm^3 mol^{-1} s^{-1} with activation energies of *ca*. 17 kJ mol^{-1} are seemingly describing little more than the diffusion of the

reactive species towards each other, k_{diff}. Since diffusion is not a limiting process in the gas-phase, the gas-phase rate constants are more directly a measure of k_{react}, and hence the Cl· and ·OH gas-phase data better reflect the relative reactivity of these species. A marked difference between aqueous- and gas-phase data is the much faster rate constants of Cl· over ·OH in the gas-phase.[35,36] This demonstrates that the Cl· atom is a more reactive species than the ·OH radical. Hence in the aqueous phase it is reasonable that the rate constants should more often be controlled by diffusion rather than by the reaction step.

5.7.7. Inorganic Species

Figure 5.7 shows a plot of the rate constants of the Cl· atom reactions with ions as a function of the Gibbs free energies of reaction. The Gibbs free energy changes were calculated from $\Delta G^o = FE^o$, taking $E^o(Cl\cdot/Cl^-) = 2.41$ V and the reduction potentials of the other ions from Stanbury.[37] According to the Marcus theory of outer-sphere electron transfer for a reaction affected by diffusion,[38,39] a relationship between the rate constant, k_{obs}, and the driving force, ΔG^o, is expected according to equations [5.3] to [5.5].

$$\log k_{obs} = \log k_{diff} + \log\left(\frac{1}{1 + e^x}\right) \qquad [5.3]$$

$$x = \frac{\Delta G^{\neq}}{RT} \qquad [5.4]$$

$$\Delta G^{\neq} = \frac{\lambda}{4}\left(1 + \frac{\Delta G^o}{\lambda}\right)^2 \qquad [5.5]$$

Figure 5.7 *Plot of log k_{obs} vs ΔG^o for the reactions of Cl· atoms. The red line is the curve expected from equation [5.3].*

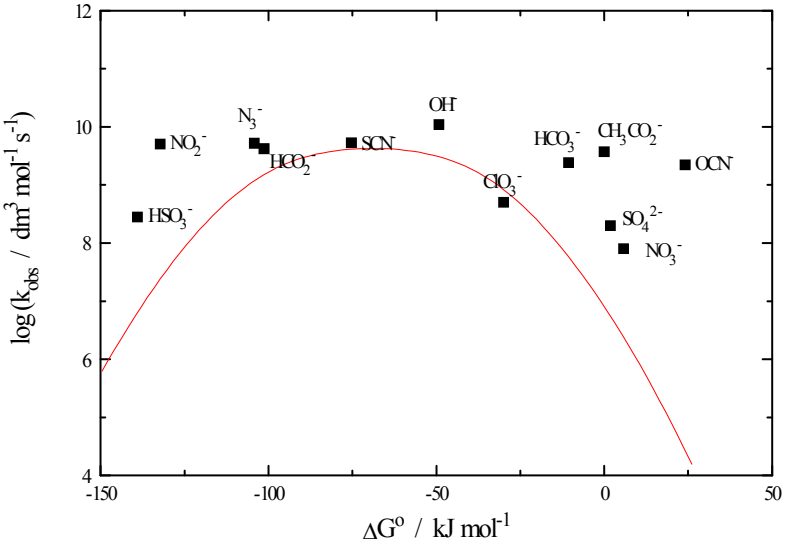

This behaviour is not obviously exhibited in Figure 5.7, using a diffusion controlled rate constant of $k_{diff} = 8.5 \times 10^9$ dm^3 mol^{-1} s^{-1} and a reorganisational energy of $\lambda = 70$ kJ mol^{-1}, and there are many points greater than one order of magnitude from the line. This perhaps suggests that a common reorganisational energy does not exist across the diverse range of anions studied. Also, different reaction pathways may occur, e.g. the formation of an adduct with OCN^- seems likely as this has been observed with $SO_4\cdot^-$ and ·OH,[40,41] in which case equation [5.3] is not applicable. The rate constants shown in Figure 5.7 are generally at, or near to, the diffusion controlled limit. As may be seen from equation [5.2], this means that the component of relevance to the Marcus theory, k_{react}, is of minor importance in the expression for k_{obs} in comparison to k_{diff}.

It is notable that the data point for HSO_3^- at greatest ΔG^o is considerably lower than the diffusion controlled limit, unlike the other species with low reduction potentials. This may have been due to the formation of a less reactive S(IV)-chloroacetone adduct which, using the correlation by Olson and Hoffmann[42] and hydration constant of chloroacetone,[29] would have an equilibrium constant of greater than 10^4 dm^3 mol^{-1}. This high value means that free HSO_3^- would not exist in an appreciable quantity in solutions containing the chloroacetone

concentrations required for our experiments. Therefore the rate constant obtained in this study is almost certainly that of Cl· with the HSO_3^--chloroacetone adduct. A further observation is the low reactivity of Cl· towards $S_2O_8^{2-}$ and ClO_4^- (rate constants are 1.8×10^6 and $< 5 \times 10^5$ dm^3 mol^{-1} s^{-1}, respectively),[43] which suggests that the reduction potentials of these ions are rather higher than that of chloride.

5.7.8. Reaction with Water

The intercepts on the plots of k_{obs} *vs* [S], corresponding to the reactions of Cl· with water and chloroacetone, were in the range (3 to 5) $\times 10^5$ s^{-1} over all temperatures. No significant trend with temperature was observed. The effect of acidity on the rate of decay was investigated in Ar-saturated solutions containing 5×10^{-3} mol dm^{-3} chloroacetone, revealing little variation across the pH range 1 to 6. As is presently understood, the reaction of Cl· with water proceeds by reaction (3.9).[5,46]

$$Cl\cdot + H_2O \leftrightarrow H_2OCl\cdot \leftrightarrow H^+ + HOCl\cdot^- \leftrightarrow \cdot OH + Cl^- + H^+ \qquad (3.9)$$

However, there is some uncertainty regarding the species involved in this reaction. Treinin and Hayon[16] found evidence for a weakly bound complex, H_2O-Cl·, and Klaning and Wolff[9] concluded that Cl· exists in aqueous solution as an oxygen acid. Furthermore, recent studies have derived potential energy surfaces of the H_2O-Cl· complex[44] and presented evidence that it is a three-electron bonded species.[45] From these reports it is reasonable to suppose that the Cl· atom exists in aqueous solution in a complex with a water molecule, thus rendering superfluous the first equilibrium of reaction (3.9).

The equilibrium $Cl\cdot + H_2O \leftrightarrow H_2OCl\cdot$ was introduced by McElroy[46] to explain the lack of an $[H^+]$ dependence on the rate of decay of $Cl\cdot/Cl_2\cdot^-$ by reaction with water over the pH range 2.2 to 4.8, and from the results of conductivity experiments by Wagner *et al*.[47] Whilst the results of the present study confirm the lack of an $[H^+]$ dependence, it is uncertain whether it is necessary to

introduce an equilibrium between Cl· and H_2OCl· as an explanation, especially in light of work suggesting that they are not different species. Removing it from reaction (3.9) results in reaction (5.7), where Cl· (aq) is used to denote the complexed water-Cl· species.

$$\text{Cl·(aq)} \overset{K_A}{\leftrightarrow} \text{H}^+ + \text{HOCl·}^- \overset{K_B}{\leftrightarrow} \text{·OH} + \text{Cl}^- + \text{H}^+ \qquad (5.7)$$

This is essentially the scheme proposed by Jayson *et al.*,[4] by whom the values of $K_A = (7.2 \times 10^4 / 2.1 \times 10^{10}) = 3.4 \times 10^{-6}$ mol dm^{-3} and $K_B = (6.1 \times 10^9 / 4.3 \times 10^9) = 1.4$ mol dm^{-3} were obtained. Using more recent determinations of the rate of dissociation of Cl· (aq), a new value of $K_A = 5 \times 10^{-6}$ mol dm^{-3} has been estimated. This comes from the first-order rate of decay of Cl· (aq) in the absence of solutes, *ca*. 2.5×10^5 s^{-1}, and the reported rate constant for proton transfer to a negatively charged base of 5×10^{10} dm^3 mol^{-1} s^{-1}.[48] FACSIMILE simulations of reaction (5.7) using these values show little effect of [H^+] on the rate of decay of Cl· (aq), indicating that an equilibrium Cl· + $H_2O \leftrightarrow H_2OCl$· is not required to explain the results of this study.

More detailed simulations in the presence of chloride, taking rate constants from Buxton *et al.*[5] for equilibrium (3.1) and inserting a reaction between ·OH and Cl_2·$^-$,[47] qualitatively agree with the observations of both McElroy[46] and Jacobi *et al.*[49] (see Tables 5.5 and 5.6 and Section 4.7). The expected [H^+] dependence for the formation of Cl_2·$^-$ from ·OH radicals is also displayed.[4,50] Therefore it is unclear why McElroy, who used an almost identical reaction scheme to Table 5.5, proposed Cl· + $H_2O \leftrightarrow H_2OCl$· to explain his results. Under the conditions used by McElroy, second-order reactions dominated the decay of the radicals so that the reaction of interest, reaction (5.7), may have been obscured.

The reduction potentials $E°(Cl·/Cl^-) = 2.41$ V and $E°(·OH, H^+/H_2O) = 2.72$ V taken from Stanbury[37] suggest a free energy of reaction (5.7) of $\Delta G° = +30$ kJ

mol^{-1}, which agrees with that calculated from the equilibrium constants of +29 kJ mol^{-1}. This consistency substantiates the values used for K_A and K_B.

Table 5.5 *Reactions used in the FACSIMILE simulations.*

Reaction	Rate constant / $dm^3\ mol^{-1}\ s^{-1}$	Reference
$Cl\cdot\ (aq) \leftrightarrow HOCl\cdot^- + H^+$	$k_{forward} = 2.5 \times 10^5\ s^{-1}$	This work
	$k_{reverse} = 5 \times 10^{10}$	48
$HOCl\cdot^- \leftrightarrow \cdot OH + Cl^-$	$k_{forward} = 6.1 \times 10^9\ s^{-1}$	4
	$k_{reverse} = 4.3 \times 10^9$	4
$Cl\cdot + Cl^- \leftrightarrow Cl_2\cdot^-$	$k_{forward} = 8.5 \times 10^9$	5
	$k_{reverse} = 6 \times 10^4\ s^{-1}$	5
$Cl_2\cdot^- + H_2O \rightarrow Cl^- + HOCl\cdot^- + H^+$	$1.3 \times 10^3\ s^{-1}$	5, 46
$Cl_2\cdot^- + Cl_2\cdot^- \rightarrow$ products	*ca.* 1×10^9	45
$Cl_2\cdot^- + \cdot OH \rightarrow$ products	1×10^9	46
$\cdot OH + \cdot OH \rightarrow$ products	5.5×10^9	19

T*able 5.6* *Results of simulations of the rate of decay of $Cl_2\cdot^-$ under the conditions used by different authors.*

Author	$[H^+]$ / mol dm^{-3}	$[Cl^-]$ / mol dm^{-3}	Radical Yield / mol dm^{-3}	Effect on rate of decay
Buxton *et al.* [a]	10^{-6} to 0.1	$< 10^{-6}$	10^{-6}	Slight decrease at the highest $[H^+]$.
McElroy [b]	(0.16 to 63) $\times 10^{-4}$	10^{-2}	5×10^{-6}	Little change. Decay is mainly $Cl_2\cdot^- + Cl_2\cdot^-$.
Jacobi *et al.* [c]	10^{-10} to 10^{-4}	0.1	2×10^{-7}	Fast at pH > 7 and slow at pH 4.

[a] This study [b] Ref. 46 [c] Ref. 49

5.8. Conclusions

In this study a large number of previously unmeasured rate constants have been determined, see Tables 5.1 and 5.2. These data show the Cl· atom to be one of the most reactive one-electron oxidants known in aqueous solution, in many instances more reactive than the ·OH radical. The present study and that of Gilbert *et al.*[8] have found strong evidence that electron-transfer is a dominant pathway for the Cl· atom reactions with organic and inorganic solutes. There is a need for product studies in order to further verify this result.

Owing to the high reactivity of the Cl· atom, its reactions contribute significantly to the decay of $Cl_2^{\cdot -}$ through equilibrium (3.1) even at a $[Cl^-]$ of 0.1 mol dm^{-3}, see Table 5.3. In cloud droplets, where the $[Cl^-]$ is typically of the order 10^{-4} mol dm^{-3}, it is evident that the Cl· chemistry will predominate over that of $Cl_2^{\cdot -}$. Therefore in modelling studies of atmospheric chemistry, it is necessary to consider the reactions of Cl· as well as the reactions of $Cl_2^{\cdot -}$. In addition, evidence from the literature has been collected which suggests that Cl· is bonded to a water molecule in aqueous solution, forming H_2OCl·. This will have consequences for the uptake of gas-phase Cl· by cloud droplets and, coupled with the rapid dissociation of the aquated species by reaction (5.7), may result in a significant enhancement of this sink for gas-phase Cl· atoms.

5.9. References

1. H. Herrmann, M. Exner and R. Zellner, *Ber. Bunsenges. Phys. Chem.*, 1991, **95**, 598
2. G. V. Buxton, G. A. Salmon, J. Wang, *Phys. Chem. Chem. Phys.*, 1999, **1**, 3589
3. R. E. Huie and C. L. Clifton, *J. Phys. Chem.*, 1990, **94**, 8561
4. G. G. Jayson, B. J. Parsons and A. J. Swallow, *J. Chem. Soc., Faraday Trans. 1*, 1973, **69**, 1597
5. G. V. Buxton, M. Bydder, G. A. Salmon, *J. Chem. Soc., Faraday Trans.*, 1998, **94**, 653
6. P. Warneck, in Chemistry of the Natural Atmosphere, International Geophys. Series, Vol. 41, Academic Press 1988
7. H. Herrmann, B. Ervens, P. Nowacki, R. Wolke and R. Zellner, *Chemosphere*, 1999, **38**, 1223
8. B. C. Gilbert, J. K. Stell, W. J. Peet and K. J. Radford, *J. Chem. Soc., Faraday Trans. 1*, 1988, **84**, 3319
9. U. Klaning and T. Wolff, *Ber. Bunsenges. Phys. Chem.*, 1985, **89**, 243
10. K. Hasegawa and P. Neta, *J. Phys. Chem.*, 1978, **82**, 854
11. A. B. Ross, W. G. Mallard, W. P. Helman, G. V. Buxton, R. E. Huie and P. Neta, NDRL-NIST Solution Kinetics Database, Ver. 3.0, NIST Standard Ref. Data, Gaithersburg, MD 1998
12. H.-W. Jacobi, F. Wicktor, H. Herrmann and R. Zellner, *Int. J. Chem. Kinet.*, 1999, **31**, 169
13. G. Merenyi and J. Lind, *J. Am. Chem. Soc.*, 1994, **116**, 7872
14. J. McMurray, in Organic Chemistry, Brooks/Cole Publishing Company, California 1992
15. A. N. Strachan and F. E. Blacet, *J. Am. Chem. Soc.*, 1955, **77**, 5254
16. A. Treinin and E. Hayon, *J. Amer. Chem. Soc.,* 1975, **97**, 1716
17. A. R. Curtis and W. P. Sweetham, FACSIMILE/CHECKMAT USER'S MANUAL, UKAEA, 1987, AERE R12805
18. M. Nakashima and E. Hayon, *J. Phys. Chem.*, 1971, **75**, 1910

19. D. F. Shriver, P. W. Atkins and C. H. Langford, in Inorganic Chemistry, Oxford University Press, Oxford 1990

20. G. V. Buxton, C. L. Greenstock, W. P. Helman and A. B. Ross, *J. Phys. Chem. Ref. Data*, 1988, **17**

21. R. Mertens and C. von Sonntag, *J. Photochem. Photobiol. A:Chem.*, 1995, **85**, 1

22. C. von Sonntag, private communication

23. G. V. Buxton, M. Bydder, G. A. Salmon and J. Wang, Proceedings of the 1st Workshop of the EUROTRAC-2 Sub-project CMD, Ed. M. Ammann and R. Lorenzen, ETH-Zurich 1997

24. G. V. Buxton, M. Bydder and G. A. Salmon, Proceedings of the EUROTRAC-2 Symposium 98, Ed. P. M. Borrell and P. Borrell, Garmisch, WIT Press, Southampton 1999

25. H. Herrmann, private communication

26. W. J. McElroy and S. J. Waygood, *J. Chem. Soc.*, *Faraday Trans.*, 1991, **87**, 1513

27. M. N. Schuchmann and C. von Sonntag, *J. Am. Chem. Soc.*, 1988, **110**, 5698

28. G. V. Buxton, T. N. Malone and G. A. Salmon, *J. Chem. Soc.*, *Faraday Trans.*, 1997, **93**, 2889

29. P. Greenzaid, Z. Rappoport and D. Samual, *J. Chem. Soc.*, *Faraday Trans.*, 1967, **63**, 2131

30. J. L. Kurz, *J. Am. Chem. Soc.*, 1967, **89**, 3524

31. G. V. Buxton, N. D. Wood and S. Dyster, *J. Chem. Soc.*, *Faraday Trans.*, 1988, **84**, 1113

32. D. R. McCracken and G. V. Buxton, *Nature*, 1981, **292**, 439

33a. E. F. Caldin, in Fast Reactions in Solution, Blackwell Scientific Publications, Oxford 1964

33b. E_a of the viscosity of water is *ca*. 17 kJ mol^{-1} over the range 5 to 35 °C, Handbook of Chemistry and Physics, 55th ed., Ed. R. C. Weast, CRC Press, Ohio 1974

34. A. J. Elliot, D. R. McCracken, G. V. Buxton and N. D. Wood, *J. Chem. Soc., Faraday Trans.*, 1990, **86**, 1539
35. J. V. Michael, D. F. Nava, W. A. Payne and L. J. Stief, *J. Chem. Phys.*, 1979, **70**, 3652
36. L. Nelson, O. Rattigan, R. Neavyn, H. Sidebottom, J. Treacy and O. J. Nielsen, *Int. J. Chem. Kinet.*, 1990, **22**, 1111
37. D. M. Stanbury, *Advances in Inorganic Chemistry*, 1989, **33**, 69
38. R. A. Marcus and N. Sutin, *Biochimica et Biophysica Acta.*, 1985, **881**, 265
39. R. D. Cannon, in Electron Transfer Reactions, Butterworths Publishers, UK 1980
40. R. E. Huie and C. L. Clifton, *J. Phys. Chem.*, 1990, **94**, 8561
41. J. G. Leopold and M. Faraggi, *J. Phys. Chem.*, 1977, **81**, 803
42. T. M. Olson and M. R. Hoffmann, *J. Phys. Chem.*, 1988, **92**, 4246
43. J. Wang, PhD Thesis, University of Leeds, Leeds 1999
44. M. Roeslova, G. Jacoby, U. Kaldor and P. Jungwirth, *Chem. Phys. Lett.*, 1998, **293**, 309
45. M. D. Sevilla, S. Summerfield, I. Eliezer, J. Rak and M. C. R. Symons, *J. Phys. Chem. A*, 1997, **101**, 2910
46. W. J. McElroy, *J. Phys. Chem.*, 1990, **94**, 2435
47. I. Wagner, J. Karthauser and H. Strehlow, *Ber. Bunsenges. Phys. Chem.*, 1986, **90**, 861
48. F. A. Cotton and G. Wilkinson, in Advanced Inorganic Chemistry, 4th Ed., John Wiley, New York 1980
49. H.-W. Jacobi, H. Herrmann and R. Zellner, *Ber. Bunsenges. Phys. Chem.*, 1997, **101**, 1909
50. M. Anbar and J. K. Thomas, *J. Phys. Chem.*, 1964, **68**, 3829

Chapter 6

The Equilibrium $SO_4^{\cdot -} + NO_3^- \leftrightarrow SO_4^{2-} + NO_3^{\cdot}$

6.1. Introduction

The nitrate radical has been much studied in aqueous solution as a consequence of its relevance to the chemistry within atmospheric cloud droplets.[1,2] Despite this attention, certain important characteristics of the $NO_3\cdot$ radical are not well established e.g. the maximum of $\varepsilon(NO_3\cdot)$ has literature values from 250 to 1300 $dm^3\ mol^{-1}\ cm^{-1}$, and $E^o(NO_3\cdot/NO_3^-)$ is estimated to lie within the range 2.3 and 2.6 V.[1,3] By studying equilibrium (6.1) it is possible to establish $\varepsilon(NO_3\cdot)$ and $E^o(NO_3\cdot/NO_3^-)$ in relation to the well known values for the $SO_4\cdot^-$ radical.

$$SO_4\cdot^- + NO_3^- \leftrightarrow SO_4^{2-} + NO_3\cdot \qquad (6.1)$$

In light of recent work in our laboratory regarding the equilibria between $Cl\cdot$, $NO_3\cdot$ and $SO_4\cdot^-$,[2,4] it is of considerable interest to examine equilibrium (6.1), for which the value of $K_{6.1}$ should act as a test of consistency of the previous results, see equations [6.1] and [6.2].

$$\left(\frac{[Cl\cdot][SO_4^{2-}]}{[Cl^-][SO_4^{-}]}\right)_{eq} \cdot \left(\frac{[Cl^-][NO_3]}{[Cl\cdot][NO_3^-]}\right)_{eq} = \left(\frac{[SO_4^{2-}][NO_3]}{[SO_4^-][NO_3^-]}\right)_{eq} \qquad [6.1]$$

$$K_{4.1} \cdot 1 / K_{4.5} = K_{6.1} \qquad [6.2]$$

The equilibrium constants $K_{4.1}$ ($I\rightarrow0$) = 1.2 and $K_{4.5}$ ($I\rightarrow0$) = 3.3 are those of the $Cl\cdot$ atom with $SO_4\cdot^-$ and $NO_3\cdot$, respectively,[4,2] as is clear from equation [6.1]. They combine according to equation [6.2] to predict $K_{6.1}$ ($I\rightarrow0$) = 0.36 at infinite dilution, which is close to the value 0.28 reported by Logager *et al.*[5]

In the study of Logager *et al.*, the absorbance due to the $SO_4\cdot^-$ and $NO_3\cdot$ radicals was measured at fixed $[NO_3^-]$ over a range of $[SO_4^{2-}]$ to determine the equilibrium constant. This method relies upon accurate values for $\varepsilon(SO_4\cdot^-)$ and $\varepsilon(NO_3\cdot)$, the latter of which is the subject of large variation in the literature. Therefore agreement between the value of Logager *et al.* and the estimate from equation [6.2] is perhaps fortuitous and in need of verification. To this end an

investigation of equilibrium (6.1) has been undertaken, adopting a kinetic approach whereby kinetic rather than absorbance data are used to determine the equilibrium constant. This method has the advantage that the absorption coefficients of the radicals are not required to a high degree of accuracy.

6.2. Experimental Approach

Experiments were performed using pulse radiolysis to produce e_{aq}^- which reacts with $S_2O_8^{2-}$ to produce the $SO_4^{\cdot -}$ radical, reactions (1.28) and (1.35).[6] The dose was limited to 2 Gy to minimise radical-radical reactions, and a multipass cell of optical pathlength 7 cm was used to maximise the absorbance signal. The rate of approach to equilibrium was measured as a function of the sulfate and nitrate concentrations, to which were fitted the forward and reverse rate constants using a linear rate law. A value for the molar absorption coefficient of $NO_3\cdot$ was obtained by comparing the relative absorbances of $SO_4^{\cdot -}$ and $NO_3\cdot$, as well as confirmation of the behaviour of the equilibrium quotient, $Q_{6.1}(t)$, expected from Chapter 3 (also Ref. 7).

6.3. Formation of $NO_3\cdot$

The $NO_3\cdot$ radical was produced by the reaction of nitrate ion with $SO_4^{\cdot -}$, reaction (6.1). The absorptions due to $SO_4^{\cdot -}$ and $NO_3\cdot$ were monitored at 450 and 630 nm, respectively, taking $\varepsilon(SO_4^{\cdot -}) = 1630$ dm^3 mol^{-1} cm^{-1},[8] see Figures 6.1 and 6.2. The ·OH radical produced in reaction (1.28) was converted to a relatively unreactive radical by the addition of t-BuOH, reaction (1.32).[6] The presence of t-BuOH increased the rate of decay of $NO_3\cdot$ to the detriment of the quality of the traces and simplicity of the rate law (see below), however it was thought preferable to leaving ·OH unscavenged. It was therefore decided to use a low [t-BuOH] of 5×10^{-4} mol dm^{-3}, which was sufficient to ensure the rapid removal of ·OH but not enough to significantly affect the kinetics during the growth of the $NO_3\cdot$ radical (see Section 6.5).

Another important consideration in this reaction scheme is the reaction of the nitrate ion with e_{aq}^-, reaction (6.2).[6] At the nitrate ion concentrations used this

competes with $S_2O_8^{2-}$ for the aqueous electron, hence reducing the $SO_4^{\cdot -}$ yield and producing the unwanted $NO_3^{\cdot 2-}$ radical.

$$e^-_{aq} + NO_3^- \rightarrow NO_3^{\cdot 2-} \xrightarrow{H_2O} NO_2^{\cdot} + 2OH^- \qquad (6.2)$$

$$k_{6.2} = 9.7 \times 10^9 \text{ dm}^3 \text{ mol}^{-1} \text{ s}^{-1}$$

The $NO_3^{\cdot 2-}$ reacts with water rapidly to form $NO_2^{\cdot}$, which absorbs at 450 nm with $\varepsilon(NO_2^{\cdot}) = 150$ dm^3 mol^{-1} cm^{-1}.[9] To minimise the formation of $NO_2^{\cdot}$, solute concentrations were chosen so that $[NO_3^-] < [S_2O_8^{2-}]$, see Table 6.1. Based on the competition between NO_3^- and $S_2O_8^{2-}$ for e_{aq}^-, the absorbance at 450 nm due to $NO_2^{\cdot}$ was calculated to be $< 2 \times 10^{-4}$, which is less than the noise on the traces and therefore negligible.

Experiments were performed at an ambient temperature of 18 to 20 ºC, and constant ionic strength of 0.5 mol dm^{-3} using $S_2O_8^{2-}$ as a neutral salt. Solutions were adjusted to pH *ca*. 6 by the addition of NaOH and saturated with argon. To improve signal quality at 630 nm recorded traces were an average of six separate pulses, flushing after every three pulses. Traces at 450 nm were an average of three pulses. No variation was observed with increasing number of pulses to the same solution up to *ca*. ten pulses, ruling out any effect of a build-up of products, e.g. $NO_2^{\cdot}$, over the course of the averaging.

Table 6.1 *Solute concentrations chosen for the experiments. [$S_2O_8^{2-}$] was varied to keep the ionic strength constant at 0.5 mol dm^{-3}.*

[NO_3^-] / 10^{-2} mol dm^{-3}	**[SO_4^{2-}] / 10^{-2} mol dm^{-3}**	**[$S_2O_8^{2-}$] / 10^{-2} mol dm^{-3}**	**t-BuOH / 10^{-4} mol dm^{-3}**
2	2 to 8	14 to 8	5
2 to 8	2	14 to 12	5

Figure 6.1 *The absorbance at 450 nm (black) and 630 nm (red) following pulse radiolysis of an Ar-saturated solution containing* $[NO_3^-] = [SO_4^{2-}] = 2 \times 10^{-2}$, $[S_2O_8^{2-}] = 0.14$ *and* $[t\text{-BuOH}] = 5 \times 10^{-4}$ *mol dm*$^{-3}$ *at pH ca. 6 using a dose of ca. 2 Gy. The green line, pertaining to the right hand ordinate, is the ratio of the absorbances at 630 and 450 nm.*

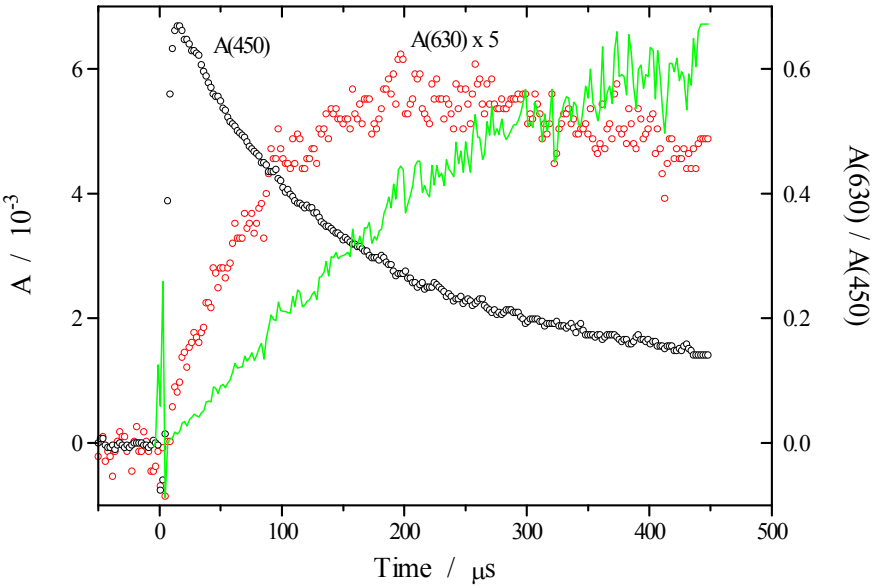

Figure 6.2 *The absorbance at 450 nm (black) and 630 nm (red) following pulse radiolysis of an Ar-saturated solution containing* $[NO_3^-] = 4 \times 10^{-2}$, $[SO_4^{2-}] = 2 \times 10^{-2}$, $[S_2O_8^{2-}] = 0.133$ *and* $[t\text{-BuOH}] = 5 \times 10^{-4}$ *mol dm*$^{-3}$ *at pH ca. 6 using a dose of ca. 2 Gy. The green line, pertaining to the right hand ordinate, is the ratio of the absorbances at 630 and 450 nm.*

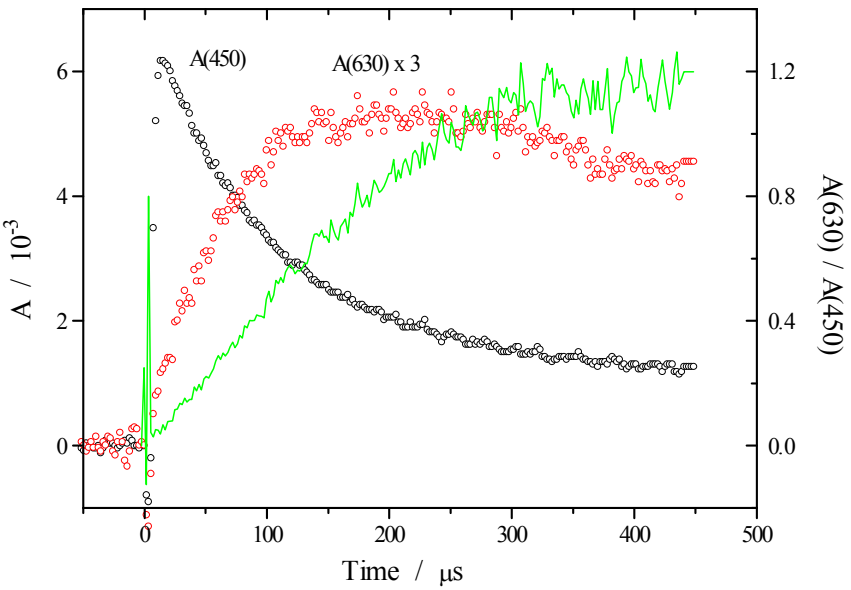

Figure 6.3 *Dependence of the first-order rate of growth of NO_3· on $[SO_4^{2-}]$, black line, and $[NO_3^-]$, red line, under the conditions of Table 6.1. Error bars are ± 1 S.D.*

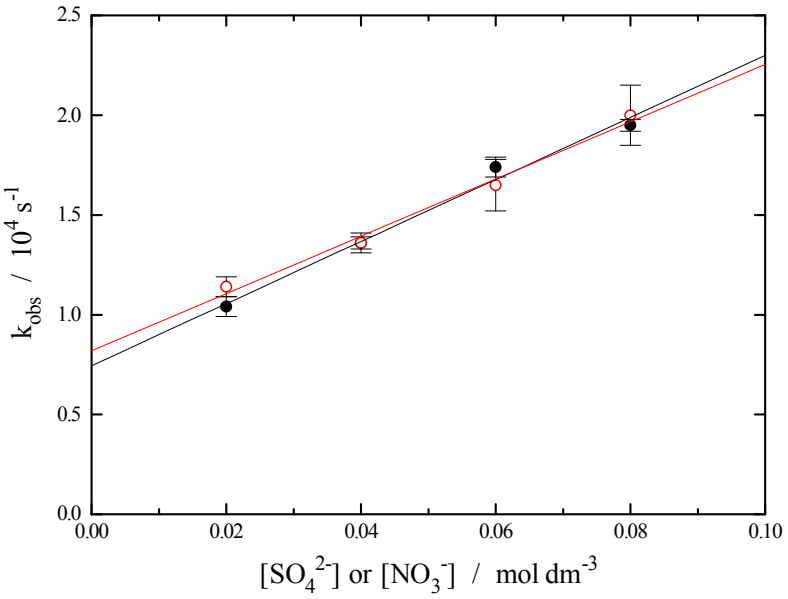

6.4. Data Analysis

Kinetic data were obtained from the growth of NO_3· rather than the decay of SO_4·$^-$ due to the difficulty in resolving biexponential components of the SO_4·$^-$ decay. The growth was fitted to a first-order mechanism, correcting for the slight first-order decay, and plotted as a function of $[SO_4^{2-}]$ and $[NO_3^-]$, see Figure 6.3. The decay of the radicals was attributed to reactions (4.2), (4.3), (6.3) and (6.4), for which rate constants were taken to be $k_{4.2} = 7.8 \times 10^5$, $k_{6.3} = 6.6 \times 10^4$ dm^3 mol^{-1} s^{-1}, $k_{4.3} \approx 690$ and $k_{6.4} \approx 300$ s^{-1}.[2,6] Other reactions, e.g. SO_4·$^-$/NO_3· + NO_2·, SO_4·$^-$/NO_3· + H·, were not easily accounted for, but it was expected that their effect would be small under the low dose conditions.

$$SO_4^{\cdot -} + \text{t-BuOH} \rightarrow SO_4^{2-} + H^+ + \text{products} \qquad (4.2)$$

$$SO_4^{\cdot -} + \text{water} \rightarrow SO_4^{2-} + \cdot OH + H^+ \qquad (4.3)$$

$$NO_3\cdot + \text{t-BuOH} \rightarrow NO_3^- + H^+ + \text{products} \qquad (6.3)$$

$$NO_3\cdot + \text{water} \rightarrow NO_3^- + \cdot OH + H^+ \qquad (6.4)$$

6.5. Rate Law for Growth of $NO_3\cdot$

The differential equations pertaining to equilibrium (6.1) and reactions (4.2), (4.3), (6.3) and (6.4) result in equation [6.3] (see Ref. 7 and Appendix 1 for similar derivation),

$$[NO_3\cdot] = C_1 e^{\lambda(1)t} + C_2 e^{\lambda(2)t} \qquad [6.3]$$

where $C_{1,2}$ are constants and $\lambda(1,2)$ are rate laws describing the growth and decay of the $NO_3\cdot$ radical. An equation for $[SO_4\cdot^-]$ may also be obtained, however in this case the $\lambda(1,2)$ terms represent two components of a biexponential decay rather than a growth and a decay. The expression for $\lambda(1)$ is given by equation [6.4].

$$-\lambda(1) \approx k_{6.1}[NO_3^-] + k_{-6.1}[SO_4^{2-}] + (k_{4.2} + k_{6.3})[\text{t-BuOH}] + k_{4.3} + k_{6.4} \qquad [6.4]$$

Equation [6.4] may be seen to be an extension of the usual rate law for the approach to equilibrium, i.e. the sum of the forward and back rate constants (k_f and k_b) given by equation [6.5],

$$k_{obs} = k_f + k_b \qquad [6.5]$$

to reaction schemes involving loss reactions (k_{loss}), equation [6.6].

$$k_{obs} = k_f + k_b + k_{loss} \qquad [6.6]$$

Under conditions where the loss reactions are significant, e.g. at high [t-BuOH], more terms must be included in the binomial expansion leading to equation [6.4] to ensure accuracy, and the simple form of equation [6.6] is lost. In order to retain the simplicity of equation [6.6], solute concentrations were chosen within the range suggested by the inequality $k_f + k_b >> k_{loss}$ or, more specifically, $k_{6.1}[NO_3^-] + k_{-6.1}[SO_4^{2-}] >> (k_{4.2} + k_{6.3})[\text{t-BuOH}] + k_{4.3} + k_{6.4}$. Using existing values for the rate constants and those of the present study, equation [6.4] holds to better than 8 % under the conditions of Table 6.1.

The decay of $NO_3\cdot$ was not investigated although it was observed to be predominantly first-order with a rate between 800 and 1200 s^{-1}, a little higher than that expected on the basis of equation [6.7] of 600 to 800 s^{-1}.

$$-\lambda(2) \approx \frac{k_{4.2}[t-BuOH] + k_{4.3} + K_{6.1}([NO_3^-]/[SO_4^{2-}])(k_{6.3}[t-BuOH] + k_{6.4})}{K_{6.1}([NO_3^-]/[SO_4^{2-}]) + 1} \quad \text{.....[6.7]}$$

6.6. Results of the Kinetic Analysis

The derivatives of equation [6.4] with respect to $[NO_3^-]$ and $[SO_4^{2-}]$ are $k_{6.1}$ and $k_{-6.1}$, respectively, and so these rate constants may be obtained from the gradients of Figure 6.3. Thus it was determined that $k_{6.1} = (1.56 \pm 0.12) \times 10^5$ and $k_{-6.1} = (1.44 \pm 0.10) \times 10^5$ dm^3 mol^{-1} s^{-1}, and hence the equilibrium constant $K_{6.1} = (1.08 \pm 0.11)$ at 0.5 mol dm^{-3} ionic strength. Reactions involving a neutral species, such as $NO_3\cdot$, are expected to be almost independent of ionic strength up to 0.5 mol dm^{-3}, and therefore an estimate can be made of the equilibrium constant at infinite dilution by substituting $k_{6.1}$ $(I\rightarrow 0) = 5 \times 10^4$ dm^3 mol^{-1} s^{-1} in place of the high ionic strength value.[10] This gives the equilibrium constant $K_{6.1}$ $(I\rightarrow 0) = 0.35$, in comparison to 0.28 reported by Logager *et al.* and 0.36 estimated from equations [6.1] and [6.2].

The intercepts of 7400 and 8200 s^{-1} in Figure 6.3 are somewhat higher than those expected on the basis of equation [6.4] of *ca*. 4500 s^{-1}. One possible explanation for this difference would be a significant reaction of $SO_4\cdot^-$ or $NO_3\cdot$ with the persulfate ion, which is present in high concentration. However, the rate constant for $SO_4\cdot^-$ with persulfate, $k_{4.4}$, has been found recently to be $< 1.5 \times 10^3$ dm^3 mol^{-1} s^{-1},[4] and, because of the similarity in reactivity of $SO_4\cdot^-$ and $NO_3\cdot$ with inorganic species, it is unlikely the $NO_3\cdot$ reaction is any faster.[6] In confirmation of this, the rate of decay of $NO_3\cdot$ has been found to remain unchanged between $[S_2O_8^{2-}] = 0.1$ and 1.0 mol dm^{-3}.[11]

The reason for the high intercepts therefore remains unclear. However since any loss reactions would show up in the k_{loss} term of equation [6.6], perhaps radical-radical reactions may account for the difference. This may also explain the slightly faster rate of decay than expected. To reduce the effect of these reactions a dose lower than 2 Gy per pulse would have to be used, however this would cause the absorbance signal from $NO_3\cdot$ to fall below the limit of our detection apparatus.

6.7. Absorption Coefficient of $NO_3\cdot$

Considering the reactions taking place in this study, the only species to absorb at 630 nm is $NO_3\cdot$, and at 450 nm are $NO_3\cdot$, $SO_4\cdot^-$ and $NO_2\cdot$. Therefore the absorbances at these wavelengths are given by A(630) and A(450),

$$A(630) = l\varepsilon_1[NO_3\cdot]$$

$$A(450) = l\varepsilon_2[NO_3\cdot] + l\varepsilon_3[SO_4\cdot^-] + l\varepsilon_4[NO_2\cdot]$$

where l is the optical pathlength and ε_{1-4} are the absorption coefficients of $NO_3\cdot$ at 630 nm, $NO_3\cdot$ at 450 nm, $SO_4\cdot^-$ at 450 nm and $NO_2\cdot$ at 450 nm, respectively. The absorbance due to $NO_2\cdot$ was calculated to be less than the noise on the traces (see Section 6.3) and was therefore neglected. Hence the ratio of the absorbances at 450 and 630 nm is given by equation [6.8].

$$\left[\frac{A(450)}{A(630)}\right]_{t\to\infty} = \frac{\varepsilon_2}{\varepsilon_1} + \frac{\varepsilon_3}{\varepsilon_1}\left(\frac{[SO_4^-]}{[NO_3^-]}\right)_{eq} = \frac{\varepsilon_2}{\varepsilon_1} + \frac{\varepsilon_3}{K_{6.1}\varepsilon_1}.\frac{[SO_4^{2-}]}{[NO_3^-]} \qquad [6.8]$$

Equation [6.8] predicts a linear relationship between $[A(450)/A(630)]_{t\to\infty}$ and $[SO_4^{2-}]/[NO_3^-]$, with gradient $\varepsilon_3/K_{6.1}\varepsilon_1$ and intercept $\varepsilon_2/\varepsilon_1$. Such a plot is shown in Figure 6.4. The ratios $[A(630)/A(450)]_{t\to\infty}$ were obtained by dividing absorbance/time traces at 630 nm by those at 450 nm as in Figures 6.1 and 6.2 (green line), and recording the long-time values. Inverting these long-time values gave $[A(450)/A(630)]_{t\to\infty}$.

Figure 6.4 *Absorbance at 450 nm divided by the absorbance at 630 nm at equilibrium, pertaining to equation [6.8]. Error bars are ± 1 S.D.*

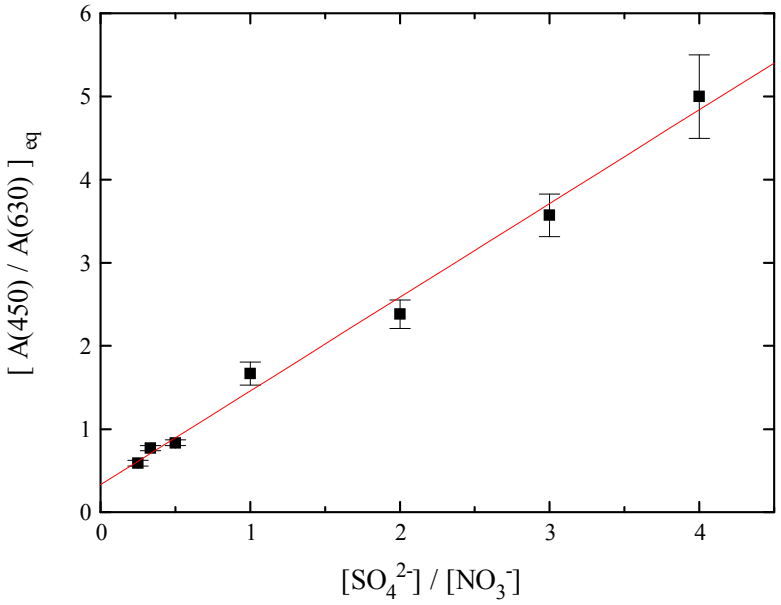

The gradient of Figure 6.4 is $\varepsilon_3/K_{6.1}\varepsilon_1 = (1.13 \pm 0.05)$. Substituting $K_{6.1} = (1.08 \pm 0.10)$ at 0.5 mol dm^{-3} ionic strength and $\varepsilon_3 = 1630$ dm^3 mol^{-1} cm^{-1} gives a value for the absorption coefficient of $NO_3\cdot$ at 630 nm, $\varepsilon_1 = (1340 \pm 150)$ dm^3 mol^{-1} cm^{-1}. The intercept is $\varepsilon_2/\varepsilon_1 = (0.33 \pm 0.10)$, giving $\varepsilon_2 = (440 \pm 140)$ dm^3 mol^{-1} cm^{-1} for the absorption coefficient of $NO_3\cdot$ at 450 nm.

Although the absorbance at 450 nm has contributions from $NO_3\cdot$ which complicate the comparison somewhat, the shape of [A(630)/A(450)], see Figures 6.1 and 6.2, is essentially the same as that expected of the equilibrium quotient, $Q_{3.1}(t)$, for the single equilibrium (3.1) investigated in Chapter 3, see Figures 3.6.

Table 6.2 *Rate constants determined at 0.5 mol dm^{-3} ionic strength.*

Reaction	Rate constant / dm^3 mol^{-1} s^{-1}	Literature / dm^3 mol^{-1} s^{-1}	Reference
$SO_4^{\cdot -} + NO_3^-$	$(1.56 \pm 0.12) \times 10^5$	$5 \times 10^{4\,a}$	10
$NO_3^{\cdot} + SO_4^{2-}$	$(1.44 \pm 0.10) \times 10^5$	1.0×10^5	5

[a] Value at zero ionic strength.

6.8. Conclusions and Discussion

The results obtained in this study at 18 to 20 ºC are listed in Table 6.2. Also determined were the values of $\varepsilon(NO_3^{\cdot}) = (1340 \pm 150)$ and (440 ± 140) dm^3 mol^{-1} cm^{-1} at 630 nm and 450 nm, respectively, which are in agreement with some previous reports.[1] The equilibrium constant, $K_{6.1} = (1.08 \pm 0.11)$, corrected to infinite dilution, $K_{6.1}$ (I→0) = 0.35, agrees with the existing literature value of 0.28.[5] It is also consistent with estimates made on the basis of other equilibrium constants, see equations [6.1] and [6.2] and see below. Using $K_{6.1}$ (I→0) = 0.35, the reduction potential of NO_3^- may be calculated from equation [4.4] to be 27 mV higher than that of SO_4^{2-} of 2.43 V,[3] so that $E^o(NO_3^{\cdot}/ NO_3^-) = 2.46$ V.

Recent work by Zuo *et al.*[12] has determined zero ionic strength values for the equilibrium constants $K(SO_4^{\cdot -} + ClO_3^- \leftrightarrow SO_4^{2-} + ClO_3^{\cdot}) = 8 \pm 7$ and $K(NO_3^{\cdot} + ClO_3^- \leftrightarrow NO_3^- + ClO_3^{\cdot}) = 11 \pm 3$, which by analogy with equations [6.1] and [6.2] predict $K_{6.1}$ (I→0) = 0.7 ± 0.6. This is consistent with the result of the present study within the large error limit. However the latter of these equilibrium constants was also found to be 42 ± 6 by a different method, based on the assumption that radical losses are not affected by solute concentrations. This is not necessarily true (*cf.* equation [6.7] for a similar reaction scheme), although the equilibrium constant also yields a value in agreement with the present study of $K_{6.1} = 0.19 \pm 0.17$. The magnitude of the equilibrium constants reported by Zuo *et al.*[12] (i.e. 10^1) suggests that the difference of 0.3 V between

the reduction potentials of SO_4^{2-} and ClO_3^-, estimated in Ref. 3, is too high. It would seem that $E^o(ClO_3\cdot/ ClO_3^-)$ is closer to the $E^o(SO_4\cdot^-/ SO_4^{2-})$ of 2.43 V. This is somewhat supported by the similar rate constants of $k(Cl\cdot + ClO_3^-)$ and $k(Cl\cdot + SO_4^{2-})$, determined in Chapter 5.

An earlier investigation[13] found that, although able to oxidise the sulfate and nitrate ions, the $ClO_3\cdot$ radical was unable to oxidise the chloride and nitrite ions. This is surprising since the reduction potentials of these species are lower than those of sulfate and nitrate.[2,3,4] We have no explanation for this result, although complications arising from the overlapping spectra of $ClO_3\cdot$, $NO_2\cdot$ and $Cl\cdot/Cl_2\cdot^-$ may have been a factor in that study.

6.9. References

1. H. Herrmann and R. Zellner, in N-Centred Radicals, Ed. Z. B. Alfassi, Wiley, New York, in press
2. G. V. Buxton, G. A. Salmon, J. Wang, *Phys. Chem. Chem. Phys.*, 1999, **1**, 3589
3. D. M. Stanbury, *Adv. Inorg. Chem.*, 1989, **33**
4. G. V. Buxton, M. Bydder and G. A. Salmon, *Phys. Chem. Chem. Phys.*, 1999, **1**, 269
5. T. Logager, K. Sehested and J. Holoman, *Radiat. Phys. Chem.*, 1993, **41**, 539
6. A. B. Ross, W. G. Mallard, W. P. Helman, G. V. Buxton, R. E. Huie and P. Neta, NDRL - NIST Solution Kinetics Database ver. 3.0, NIST Standard Ref. Data, Gaithersburg, MD 1998
7. G. V. Buxton, M. Bydder and G. A. Salmon, *J. Chem. Soc.*, *Faraday Trans.*, 1998, **94**, 653
8. G. V. Buxton, S. McGowan, G. A. Salmon, J. E. Williams and N. D. Wood, *Atmos. Environ.*, 1996, **30**, 2483
9. M. Graetzel, A. Henglein, J. Lilie and G. Beck, *Ber. Bunsenges. Phys. Chem.*, 1969, **73**, 646
10. M. Exner, H. Herrmann and R. Zellner, *Ber. Bunsenges. Phys. Chem.*, 1992, **96**, 470
11. J. Wang, PhD Thesis, University of Leeds, Leeds 1999
12. Z. Zuo, Y. Katsumura, K. Ueda and K. Ishigure, *J. Chem. Soc.*, *Faraday Trans.*, 1997, **93**, 533
13. M. Domae, Y. Katsumura, P.-Y. Jiang, R. Nagaishi, C. Hasegawa, K. Ishigure and Y. Yoshida, *J. Phys. Chem.*, 1994, **98**, 190

Suggestions for Future Work

1. The kinetic approach of Chapter 3 is applicable to the study of the equivalent bromide and iodide equilibria, the equilibrium constants of which are the subject of large variation in the literature.

2. The bromine atom and iodine atom reactions have been little studied in aqueous solution. Photolysis of the appropriate haloacetone is a simple method for producing the halogen atoms, so that rate parameters may be easily obtained. Perhaps the same method could be used to investigate the previously unstudied fluorine atom reactions.

3. The mixed dihalogen radical ions could be formed by the photolysis of a haloacetone in the presence of a different halide ion. The kinetic scheme is complicated by the occurrence of multiple equilibria, however modelling studies using the results of part 1 could be performed in order to evaluate the stability of these species.

4. The reaction of the hydroxyl radical with chloride is important from an atmospheric standpoint. The reverse of this reaction, comprising the reaction of chlorine atoms (and dichloride radical ions) with water, is similarly important. The kinetic scheme is complicated, however studies over a range of pH and chloride concentration from both sides of the equilibria should enable the full elucidation of all intermediate steps.

5. Activation energies for chlorine atom reactions seem to be largely dominated by the diffusion parameter of equation [5.2]. It would be of interest to study the reactions up to much higher temperatures so that contribution from the reaction parameter may be resolved.

6. Product analyses of the reactions of the chlorine atom would help to elucidate the mechanisms. In conjunction with part 5, relationships could then be made between the rate parameters and reaction mechanism. This approach could also be used to study the reactions of the hydroxyl, sulfate and nitrate radicals, enabling useful comparisons between these species to be made.

Appendix 1

A1.1. Kinetic Scheme for the Growth and Decay of $Cl_2\cdot^-$

For a reaction scheme involving equilibrium (3.1) and reactions (3.5) to (3.8), the differential rate equations are [A1.1] and [A1.2].

$$\frac{d[Cl\cdot]}{dt} = k_{-3.1}[Cl_2^{\cdot-}] - (k_{3.1}[Cl^-] + k_{3.5}[t-BuOH] + k_{3.7})[Cl\cdot] \qquad [A1.1]$$

$$\frac{d[Cl_2^{\cdot-}]}{dt} = k_{3.1}[Cl^-][Cl\cdot] - (k_{-3.1} + k_{3.6}[t-BuOH] + k_{3.8})[Cl_2^{\cdot-}] \qquad [A1.2]$$

Substituting the term [Cl·] from [A1.2] into [A1.1] gives equation [A1.3],

$$\frac{d^2[Cl_2^{\cdot-}]}{dt^2} + A\frac{d[Cl_2^{\cdot-}]}{dt} + B[Cl_2^{\cdot-}] = 0 \qquad [A1.3]$$

where $A = k_{3.1}[Cl^-] + k_{-3.1} + (k_{3.5} + k_{3.6})[t\text{-BuOH}] + k_{3.7} + k_{3.8}$ and $B = k_{-3.1} \times (k_{3.5}[t\text{-BuOH}] + k_{3.7}) + (k_{3.5}[t\text{-BuOH}] + k_{3.7} + k_{3.1}[Cl^-])(k_{3.6}[t\text{-BuOH}] + k_{3.8})$.

Equation [A1.3] has the general solution of equation [A1.4],

$$[Cl_2\cdot^-] = C_1 e^{\lambda(1)t} + C_2 e^{\lambda(2)t} \qquad [A1.4]$$

where $C_{1,2}$ are integration constants and $\lambda(1,2)$ are given by equation [A1.5].

$$\lambda(1,2) = \frac{-A \pm \sqrt{A^2 - 4B}}{2} \qquad [A1.5]$$

The $\lambda(1)$ and $\lambda(2)$ are expressions for the rate of approach to equilibrium and the rate of decay once equilibrium has been established, respectively. Hence equation [A1.4] describes a first-order growth and a first-order decay for the $[Cl_2\cdot^-]$. Taking values for the rate constants on the basis of a high value for $K_{3.1}$ (i.e. $K_{3.1} \geq 4700\ dm^3\ mol^{-1}$) and assuming equations [3.5] and [3.6] to be valid, it can be calculated that $A^2 >> 4B$. This permits a two term binomial expansion of the square root of equation [A1.5], which simplifies the expression and is

accurate to better than 0.7 % at the [t-BuOH] and [Cl^-] used in this study. Hence equation [A1.6].

$$\lambda(1) \approx -A \text{ and } \lambda(2) = -\frac{B}{A} \qquad [A1.6]$$

A1.2. Rate of Approach to Equilibrium

The expression λ(1) corresponds to the rate of approach to equilibrium and is typically of the order 10^7 s^{-1}. In the pulse radiolysis experiments, Cl· atoms were produced by the relatively slow (*ca*. 10^6 s^{-1}) reaction of $SO_4^{\cdot -}$ with chloride, reaction (3.4), which determines the rate of growth of $Cl_2^{\cdot -}$. However in the laser experiments Cl· was formed almost instantaneously by the nanosecond pulse, and therefore the rate of growth of $Cl_2^{\cdot -}$ directly corresponds to λ(1). Setting [t-BuOH] = 0 mol dm^{-3}, as was the case in the laser flash photolysis experiments, equation [A1.7] is obtained.

$$-\lambda(1) = k_{3.1}[Cl^-] + k_{-3.1} + k_{3.7} + k_{3.8} \qquad [A1.7]$$

This is a generalisation of the usual rate law for the approach to equilibrium, $k_{obs} = k_f + k_b$,[1] to kinetic schemes in which significant loss reactions occur, i.e. $k_{obs} = k_f + k_b + k_{loss}$.

A1.3. Rate of Decay at Equilibrium

The decay of $Cl_2^{\cdot -}$, once equilibrium had been attained, was studied by pulse radiolysis over a range of [t-BuOH]. The rate of decay is given by λ(2) from equation [A1.6]. Thus after its formation the $Cl_2^{\cdot -}$ exhibits a first-order decay of the order 10^4 s^{-1}, equation [A1.8].

$$[Cl_2^{\cdot -}] = C_2 e^{\lambda(2)t}$$

[A1.8]

$$\lambda(2) = -\frac{B}{A}$$

A1.4. Deviations from Equilibrium

The dependence of [Cl·] on time may be determined by substituting equation [A1.8] for [$Cl_2^{\cdot -}$] into [A1.1] and integrating. This gives equation [A1.9],

$$[Cl^{\cdot}] = \frac{k_{-3.1} C_2 e^{\lambda(2)\, t}}{k_{3.1}[Cl^-] + k_{3.5}[t-BuOH] + k_{3.7} + \lambda(2)} + C_3 e^{\beta t} \qquad [A1.9]$$

where C_3 is an integration constant and $\beta = -(k_{3.1}[Cl^-] + k_{3.5}[t\text{-BuOH}] + k_{3.7})$. Owing to the large negative value of β in comparison to $\lambda(2)$, the second exponential term rapidly becomes negligible and so, for $t >> 0$,

$$[Cl^{\cdot}] = C_4\, C_2 e^{\lambda(2)t} \qquad [A1.10]$$

where $C_4 = \dfrac{k_{-3.1}}{k_{3.1}[Cl^-] + k_{3.5}[t-BuOH] + k_{3.7} + \lambda(2)}$.

Now it is possible to construct an equilibrium quotient, $Q_{3.1}$, which is defined in equation [A1.11].

$$Q_{3.1} = \frac{[Cl_2^{\cdot -}]}{[Cl^-][Cl^{\cdot}]} = \frac{1}{[Cl^-]C_4} \approx K_{3.1} + \frac{k_{3.5}[t-BuOH]}{k_{-3.1}[Cl^-]} \qquad [A1.11]$$

Thus, the extent of departure from equilibrium is determined by $k_{3.5}$[t-BuOH] compared with $k_{3.1}[Cl^-]$. As the precision of the experimental data is *ca.* 10 %, the system may be considered to be in equilibrium when $k_{3.5}$[t-BuOH] is less than $k_{3.1}[Cl^-]$ by a factor of 10 which, taking $k_{3.1} = 8.5 \times 10^9$ and $k_{3.5} = 6.5 \times 10^8$ $dm^3\ mol^{-1}\ s^{-1}$, is ensured by inequality [A1.12].

$$[t\text{-BuOH}] \leq [Cl^-] \qquad [A1.12]$$

A1.5. Effect of Formation of Cl· from $SO_4^{\cdot -}$

In the pulse radiolysis experiments, Cl· was not generated instantaneously and, therefore, for a full mathematical description of the formation of $Cl_2^{\cdot -}$, a term

must be included into equation [A1.1] to account for the reaction of $SO_4^{\cdot -}$ with chloride, reaction (3.4). This results in equation [A1.13].

$$\frac{d^2[Cl_2^{\cdot -}]}{dt^2} + A\frac{d[Cl_2^{\cdot -}]}{dt} + B[Cl_2^{\cdot -}] = k_{3.1}k_{3.4}[Cl^-]^2[SO_4^{\cdot -}] \qquad [A1.13]$$

Assuming a pseudo first-order decay of $SO_4^{\cdot -}$ leads to the solutions

$$[Cl_2^{\cdot -}] = C_1 (e^{\lambda(1)t} + C_5 e^{\lambda(2)t} + C_6 e^{\alpha t}) \qquad [A1.14]$$

$$[Cl^{\cdot}] = C_4 C_1 (e^{\lambda(1)t} + C_7 e^{\lambda(2)t} + C_8 e^{\alpha t} + C_9 e^{\beta t}) \qquad [A1.15]$$

where C_{5-9} are constants and $\alpha = -k_{3.4}[Cl^-]$. Now the equilibrium quotient, taking reaction (3.4) into account, is given by equation [A1.16].

$$Q_{3.1}(t) = \frac{e^{\lambda(1)t} + C_5 e^{\lambda(2)t} + C_6 e^{\alpha t}}{[Cl^-]C_4 (e^{\lambda(1)t} + C_7 e^{\lambda(2)t} + C_8 e^{\alpha t} + C_9 e^{\beta t})} \qquad [A1.16]$$

Figure 3.6 shows how $Q_{3.1}(t)$ varies over the time-scale of the $SO_4^{\cdot -}$ decay, demonstrating that the rate of attainment of equilibrium, usually given by $\lambda(1)$, is determined by the comparatively slow reaction of $SO_4^{\cdot -}$ with chloride. After four half-lives the α, β and $\lambda(1)$ terms have become negligible and $Q_{3.1}(t)$ takes the form of equation [A1.11].

A1.6. Reference

1. R. E. Huie, C. L. Clifton and P. Neta, *Radiat. Phys. Chem.*, 1991, **38**, 477

Appendix 2

A2.1. Rate of Approach to Equilibrium

For a scheme involving equilibria (3.1) and (4.1) and the reactions of Cl· with t-BuOH and water, reactions (3.5) and (3.7),* the differential equations are given by [A2.1], [A2.2] and [A2.3],

$$\frac{d[Cl_2^{\cdot-}]}{dt} = a[Cl^{\cdot}] - b[Cl_2^{\cdot-}] \qquad [A2.1]$$

$$\frac{d[Cl^{\cdot}]}{dt} = b[Cl_2^{\cdot-}] - a[Cl^{\cdot}] + c[SO_4^{\cdot-}] - e[Cl^{\cdot}] - f[Cl^{\cdot}] \qquad [A2.2]$$

$$\frac{d[SO_4^{\cdot-}]}{dt} = e[Cl^{\cdot}] - c[SO_4^{\cdot-}] \qquad [A2.3]$$

where $a = k_{3.1}[Cl^-]$, $b = k_{-3.1}$, $c = k_{4.1}[Cl^-]$, $e = k_{-4.1}[SO_4^{2-}]$ and $f = (k_{3.5} \times [\text{t-BuOH}] + k_{3.7})$. Solving equations [A2.1], [A2.2] and [A2.3] simultaneously yields equation [A2.4],

$$\frac{d^3[Cl_2^{\cdot-}]}{dt^3} + M\frac{d^2[Cl_2^{\cdot-}]}{dt^2} + N\frac{d[Cl_2^{\cdot-}]}{dt} + P[Cl_2^{\cdot-}] = 0 \qquad [A2.4]$$

where $M = (a + b + c + e + f)$, $N = (ac + bc + be + bf + cf)$ and $P = bcf$. The general solution to equation [A2.4] is of the form [A2.5],

$$[Cl_2^{\cdot-}] = C_1 e^{\lambda(1)t} + C_2 e^{\lambda(2)t} + C_3 e^{\lambda(3)t} \qquad [A2.5]$$

where C_{1-3} are integration constants and $\lambda(1 \text{ to } 3)$ are roots of the characteristic polynomial [A2.6].

$$\lambda^3 + M\lambda^2 + N\lambda + P = 0 \qquad [A2.6]$$

The exact roots of equation [A2.6], which may be found by the method outlined in Appendix 4, are extremely complicated, see equation [A4.2]; however an approximation can be made resulting in relatively simple

* The reactions of $Cl_2^{\cdot-}$ and $SO_4^{\cdot-}$ with t-BuOH and water, reactions (3.6), (3.8), (4.2) and (4.3) are neglected at this stage, since their contribution to b and c is insignificant.

expressions for $\lambda(1,2)$. As [t-BuOH] decreases, it may be seen that P also decreases and so, for sufficiently low [t-BuOH] equation [A2.6] is approximated by equation [A2.7],

$$\lambda^3 + M\lambda^2 + N\lambda \approx 0 \qquad [A2.7]$$

and hence $$\lambda(1,2) \approx \frac{-M \pm \sqrt{M^2 - 4N}}{2}. \qquad [A2.8]$$

Equation [A2.6] may now be written as

$$[\lambda - \lambda(1)]\,[\lambda - \lambda(2)]\,[\lambda - \lambda(3)] = 0$$

which, using the approximate $\lambda(1,2)$ from equation [A2.8], expands to

$$\lambda^3 + (M - \lambda(3))\,\lambda^2 + (N - M\lambda(3))\,\lambda - N\lambda(3) \approx 0.$$

To correspond with equation [A2.6], this requires

$$M \gg |\,\lambda(3)\,| \qquad [A2.9]$$

$$N \gg |\,M\lambda(3)\,| \qquad [A2.10]$$

$$N\lambda(3) \approx -P. \qquad [A2.11]$$

An order of magnitude calculation, using existing literature values for the rate constants and typical solute concentrations used in this study, shows that $M \sim 10^7\ s^{-1}$, $N \sim 10^{13}\ s^{-2}$ and $P \sim 10^{16}\ s^{-3}$, and therefore equations [A2.9] and [A2.10] are satisfied. A two term binomial expansion of the square root in equation [A2.8] introduces no significant error and greatly simplifies $\lambda(1,2)$. Hence equations [A2.12], [A2.13] and [A2.14a].

$$\lambda(1) \approx -M \qquad [A2.12]$$

$$\lambda(2) \approx -\frac{N}{M} \qquad [A2.13]$$

$$\lambda(3) \approx -\frac{P}{N} \qquad [A2.14a]$$

Detailed comparison of equations [A2.12], [A2.13] and [A2.14a] with the numerically computed roots of equation [A2.6] indicates accuracy to better than 5 % under the conditions used in this study, within the experimental resolution of *ca*. 10 %.

A2.2. Rate of Decay Incorporating $Cl_2\cdot^-$ and $SO_4\cdot^-$ Reactions

Strictly, terms must be included in equations [A2.1] and [A2.3] for the reactions of $Cl_2\cdot^-$ and $SO_4\cdot^-$ with t-BuOH and water, reactions (3.6), (3.8), (4.2) and (4.3). In the derivation of $\lambda(2)$ above, they were neglected due to their insignificant contribution to the rate of attainment of equilibrium in comparison to other terms, which are orders of magnitude greater.

However, the rate of decay once equilibrium has been reached, $\lambda(3)$, is of the order 10^3 s^{-1} and account must be taken of these slow reactions. Therefore additional terms should appear in $\lambda(3)$. This is easy to effect by solving equations [A2.1] to [A2.3] with appropriate terms included, but the resulting equation is complicated and many of the terms are small and unnecessary due to the low [t-BuOH] used, i.e. equilibrium conditions apply.

An approximate version of $\lambda(3)$ may be found in a simple way by considering that, after the initial period required to achieve equilibrium, equilibria (3.1) and (4.1) are maintained. This can be seen from Figure 4.10 to be the case after *ca*. 25 μs.

$$K_{3.1} \approx \frac{[Cl_2^-]}{[Cl^-][Cl\cdot]} \qquad [A2.15]$$

$$K_{4.1} \approx \frac{[Cl\cdot][SO_4^{2-}]}{[SO_4^-][Cl^-]} \qquad [A2.16]$$

Adding together equations [A2.1], [A2.2] and [A2.3] and substituting [A2.15] and [A2.16] until the equation is expressed in terms of $[Cl_2\cdot^-]$ only, leads to equation [A2.17].

$$k_{obs} \approx \frac{f}{K_{3.1}[Cl^-] + 1 + ([SO_4^{2-}] / K_{4.1}[Cl^-])} \qquad [A2.17]$$

This compares with the expression for $\lambda(3)$ from equation [A2.14a], expanded to equation [A2.14b].

$$-\lambda(3) \approx \frac{f}{K_{3.1}[Cl^-] + 1 + ([SO_4^{2-}] / K_{4.1}[Cl^-]) + f(1/c + 1/b)} \qquad [A2.14b]$$

In circumstances of low [t-BuOH], and hence small f, equation [A2.17] is a close approximation to [A2.14b], the difference being terms in the denominator to account for departures from equilibrium. So under the equilibrium conditions of our experiments, $-\lambda(3) \approx k_{obs}$. The slow reactions of $Cl_2^{\cdot -}$ and $SO_4^{\cdot -}$ with water and t-BuOH may be included in equations [A2.1] and [A2.3], and following through the same procedure as above, equation [A2.18] is obtained,

$$k_{obs} = \frac{f + g K_{3.1}[Cl^-] + h([SO_4^{2-}] / K_{4.1}[Cl^-])}{K_{3.1}[Cl^-] + 1 + ([SO_4^{2-}] / K_{4.1}[Cl^-])} \qquad [A2.18]$$

where $g = (k_{3.6}[\text{t-BuOH}] + k_{3.8})$ and $h = (k_{4.2}[\text{t-BuOH}] + k_{4.3})$. Upon substituting $[SO_4^{2-}] = 0$ mol dm^{-3}, equation [A2.18] reduces to the expression for the rate of decay that would pertain in the absence of equilibrium (4.1), i.e. equation [3.1].

Appendix 3

A3.1. Reaction Mechanism

Reaction (A3.1) is described mathematically by two coupled differential equations, *cf.* equations [A1.1] and [A1.2] with $k_{3.5} = k_{3.6} = k_{3.7} = 0$.

$$A + B \underset{}{\overset{K_{A3.1}}{\leftrightarrow}} AB \overset{k_{A3.1a}}{\rightarrow} C \qquad \text{(A3.1)}$$

In the general case, a solution to these equations is not known and recourse is made to simplifying assumptions. In the steady-state-approximation (SSA), the rate of change of [AB], d[AB]/dt, is equated to zero. The resulting algebraic-differential equations are readily solved, to give equation [A3.1] for the observed rate constant, k_{obs}, for the formation of product C.[1]

$$\frac{1}{k_{obs}} = \frac{1}{k_{A3.1a}} + \frac{1}{K_{A3.1}\,k_{A3.1a}} \qquad \text{[A3.1]}$$

By associating $k_{A3.1}$ with the diffusion step, k_{diff}, and $K_{A3.1}k_{A3.1a}$ with the reaction step, k_{react}, one obtains the required expression for k_{obs}, given by equation [5.2]. Equation [A3.1] is taken to be valid when $k_{A3.1a} >> k_{-A3.1}$.[2]

A different rate law is obtained by making the assumption that equilibrium conditions apply, i.e. that $[AB] = K_{A3.1}\,[A][B]$. This yields equation [A3.2], which is used when $k_{-A3.1} >> k_{A3.1a}$.[2]

$$\frac{1}{k_{obs}} = \frac{1}{k_{A3.1a}} + \frac{1}{K_{A3.1}\,k_{A3.1a}} \qquad \text{[A3.2]}$$

However, in the special case of B >> A (i.e. under pseudo first-order conditions) the differential equations pertaining to reaction (A3.1) can be solved without resort to simplifying assumptions, to give equation [A3.3] (*cf.* equation [3.2] with $k_{3.5} = k_{3.6} = k_{3.7} = 0$).

$$\frac{1}{k_{obs}} = \frac{1}{k_{A3.1}} + \frac{1}{k_{A3.1a}} + \frac{1}{K_{A3.1}\,k_{A3.1a}} \qquad \text{[A3.3]}$$

Pseudo first-order conditions are applicable to a great number of kinetic investigations in aqueous-phase radical chemistry, and in this sense equation [A3.3] is not a special case. It can be seen that equation [A3.3] embraces both [A3.1] and [A3.2] in the appropriate limits of the approximations upon which these equations are based.

A3.2. References

1. R. D. Cannon, in Electron Transfer Reactions, Butterworths Publishers, UK 1980
2. G. V. Buxton, in General Aspects of Free Radical Chemistry, ed. Z. B. Alfassi, John Wiley and Sons, New York 1999

Appendix 4

A4.1. Exact Roots of Polynomial [A2.6]

Exact roots of polynomial [A2.6] may be found using the method outlined in Ref. 1, as follows.

$$\lambda^3 + M\lambda^2 + N\lambda + P = 0 \qquad \text{[A2.6]}$$

Let $\gamma = \lambda + \frac{M}{3}$. Then

$$\left(\gamma - \frac{M}{3}\right)^3 + M\left(\gamma - \frac{M}{3}\right)^2 + N\left(\gamma - \frac{M}{3}\right) + P = 0$$

which may be expanded to give

$$\gamma^3 + n\gamma + p = 0 \qquad \text{[A4.1]}$$

where $n = N - \frac{M^2}{3}$ and $p = P + \frac{2M^3}{27} - \frac{NM}{3}$.

Substituting $\gamma = \kappa - \frac{n}{3\kappa}$ gives a quadratic in κ^3

$$\kappa^6 + p\kappa^3 - \frac{n^3}{27} = 0$$

which has solutions

$$\kappa(1,2) = -\left(\frac{p}{2}\right)^{\frac{1}{3}}\left\{1 \pm \sqrt{\left(1 + \frac{4n^3}{27p^2}\right)}\right\}^{\frac{1}{3}}.$$

It may be calculated that $\kappa(1)\kappa(2) = -\frac{n}{3}$, and therefore $\gamma(\kappa(1)) = \gamma(\kappa(2))$. This means that there is only one solution for γ, given by

$$\gamma = \kappa(1) - \frac{n}{3\kappa(1)} = \kappa(1) + \kappa(2).$$

A4.2. Binomial Expansion of κ(1,2)

For a binomial expansion of the cube roots of κ(1,2), it is required that the magnitude of the square root term be small in comparison to 1. Assuming existing literature values for the rate constants, this can be shown to be < 0.2 for all combinations of [t-BuOH], [Cl^-] and [SO_4^{2-}] between 10^{-3} and 0.1 M.

Therefore, to an excellent approximation

$$\kappa(1,2) \approx -\left(\frac{p}{2}\right)^{\frac{1}{3}}\left\{1 \pm \frac{1}{3}\delta - \frac{1}{9}\delta^2 \pm \frac{5}{81}\delta^3 - \frac{10}{243}\delta^4 \pm \frac{22}{729}\delta^5 - \frac{154}{6561}\delta^6 \ldots\right\}$$

and therefore

$$\gamma = \kappa(1) + \kappa(2) \approx -\left(\frac{p}{2}\right)^{\frac{1}{3}}\left\{2 - \frac{2}{9}\delta^2 - \frac{20}{243}\delta^4 - \frac{308}{6561}\delta^6 - \frac{1870}{59049}\delta^8 \ldots\right\}$$

where $\delta = \sqrt{\left(1 + \frac{4n^3}{27p^2}\right)}$.

This is one of the three roots to equation [A4.1]. Let this solution be γ(1), and re-write [A4.1] as

$$\gamma^3 + n\gamma + p = \left(\gamma - \gamma(1)\right)\left(\gamma^2 + \gamma(1)\gamma - \frac{p}{\gamma(1)}\right).$$

Then the other two roots of equation [A4.1] may be found from

$$\gamma^2 + \gamma(1)\gamma - \frac{p}{\gamma(1)} = 0.$$

Solutions of this quadratic are $\gamma(2,3) = -\frac{\gamma(1)}{2} \pm \sqrt{\frac{\gamma(1)^2}{4} + \frac{p}{\gamma(1)}}$.

A4.3. Solution for λ(2)

It is now possible to obtain a solution of the original polynomial [A2.6] in λ. There are three solutions, however the expression λ(2) is used as an example.

From the earlier substitution, $\lambda = \gamma - \frac{M}{3}$, and so using $\gamma(2)$ there is the corresponding solution, $\lambda(2)$, given by equation [A4.2].

$$\lambda(2) = -\frac{\gamma(1)}{2} + \sqrt{\frac{\gamma(1)^2}{4} + \frac{p}{\gamma(1)}} - \frac{M}{3} \qquad [A4.2]$$

This is the exact rate law for the rate of approach to equilibrium and it is extremely complicated. However, it is useful insofar as it enables a test of the accuracy of the approximate rate law, equation [A2.13], to be made.

A4.4. Reference

1. R. J. B. T. Allenby, in Rings, Fields and Groups, Edward Arnold Publishers, London 1983